DISSERTATION

THE EFFECT OF RODS ON PERCEPTIVE FIELD SIZE AT 10° ECCENTRICITY IN THE FOUR RETINAL QUADRANTS

Submitted by
Cynthia L. Angel
Department of Psychology

In partial fulfillment of the requirements
for the Degree of Doctor of Philosophy
Colorado State University
Fort Collins, CO
Summer, 2003

Reproduced with permission of the copyright owner. Further reproduction prohibited without permission.

UMI Number: 3107061

UMI®

UMI Microform 3107061

Copyright 2004 by ProQuest Information and Learning Company.

All rights reserved. This microform edition is protected against unauthorized copying under Title 17, United States Code.

ProQuest Information and Learning Company
300 North Zeeb Road
P.O. Box 1346
Ann Arbor, MI 48106-1346

Reproduced with permission of the copyright owner. Further reproduction prohibited without permission.

COLORADO STATE UNIVERSITY

May 15, 2003

WE HEREBY RECOMMEND THAT THE DISSERTATION PREPARED UNDER OUR SUPERVISION BY CYNTHIA L. ANGEL ENTITLED THE EFFECT OF RODS ON PERCEPTIVE FIELD SIZE AT 10° ECCENTRICITY IN THE FOUR RETINAL QUADRANTS BE ACCEPTED AS FULFILLING IN PART REQUIREMENTS FOR THE DEGREE OF DOCTOR OF PHILOSPOHY.

Committee on Graduate Work

Co-Advisor

Advisor

Department Head

Reproduced with permission of the copyright owner. Further reproduction prohibited without permission.

ABSTRACT OF DISSERTATION

THE EFFECT OF RODS ON PERCEPTIVE FIELD SIZE AT 10° ECCENTRICITY IN THE FOUR RETINAL QUADRANTS

This research was conducted to determine the effect that rod photoreceptors have on the size of perceptive fields in the peripheral retina. Three observers used the "4+1" color-naming technique (Abramov and Gordon, 1977) to judge their perceptions of hue and saturation for test fields of varying size at 10° eccentricity in the temporal, nasal, superior, and inferior quadrants of the retina. Data were also collected in the fovea using a 1° stimulus. At each peripheral eccentricity, stimuli were judged both on the cone plateau following a rod bleach and after 30 minutes of dark adaptation to maximize cone and rod signals, respectively.

Results were analyzed for the effects of adaptation, stimulus size, and retinal location. In the no-bleach condition, with maximal rod activation, 1) colors viewed in the peripheral retina appeared less saturated at shorter wavelengths than in the fovea and rod-bleach condition, and 2) percent hue of all four basic hue terms differed from that in the fovea and the rod-bleach condition. Percent blue was lower and its spectral range was less in the no-bleach condition compared to the fovea; less red was reported at both short and long wavelengths in the no-bleach condition. Rods had their largest effects between 490 and 500 nm, increasing yellow perception and decreasing green perception as well as shifting the peak of the green function to shorter wavelengths. Several of these differences persisted under conditions where rod signals were minimized, indicating that some effects may be due to peripheral cones functioning differently from foveal cones, and not to rod signals.

Reproduced with permission of the copyright owner. Further reproduction prohibited without permission.

Decreasing stimulus size corresponded to lower percentages of hue and saturation. Blue and red were the most well-preserved hues at smaller stimulus sizes. Yellow and green were more affected by variations in stimulus size, showing both decreases in the amplitude of the response function and changes in the spectral range of the response functions. Percent hue generally grew to an asymptote as a function of increasing stimulus size under all adaptation conditions. Perceptive field sizes were calculated by fitting the Michaelis-Menten growth function to color-naming data. Rod signals increased the size of perceptive fields with the largest effect on the perceptive field for green. Not surprisingly, rod effects were most notable in the area of the visible spectrum where they are most sensitive. Under the rod-bleach condition, where rod signals were minimized, the perceptive field for blue was the smallest at all retinal locations, followed by the size of the perceptive field for red. Perceptive fields were smallest in the temporal retina under dark-adapted conditions, and perceptive field sizes were largest in the inferior retina when measured on the cone plateau. In general, results from the temporal retina were most like those of the fovea, and results from the inferior retina deviated the most from foveal results. Taken together, these results demonstrate rods differentially affect perceptive field sizes. In addition, evidence is provided that the neural processing of color in the peripheral retina differs from that in the fovea and that perceptive fields are most likely to be cortical in origin.

Cynthia Lynn Angel
Department of Psychology
Colorado State University
Fort Collins, CO 80523
Summer, 2003

Reproduced with permission of the copyright owner. Further reproduction prohibited without permission.

Acknowledgements

I would like to thank the members of my dissertation committee, Ed DeLosh, Sandy Kern, Jan Nerger, and Vicki Volbrecht for their time, support, and guidance throughout the dissertation process. The completion of this research would not have been possible without the generous contributions of Chrislyn Randell and Michael Pitts. Their countless hours spent in the lab are greatly appreciated.

I am forever gracious to my family and friends, who have supported me in innumerable and selfless ways. Mom and Dad, Chris, and Tim, your words of encouragement kept me going at times when I didn't think I could. Special thanks to Courtney, Kristin, Brandi, Mike, and Lori, my friends and co-survivors of graduate school. Brian, my solace, you have been a very welcome distraction throughout all of this. Thank you for loving me.

Reproduced with permission of the copyright owner. Further reproduction prohibited without permission.

Dedication

This is dedicated to two of the most amazing women I have ever had the honor of working with, Drs. Janice Nerger and Vicki Volbrecht. You have had an incredible impact on my life and the way I "see" the world. I have boundless gratitude for your guidance, advice, patience, and mentorship over the years. You are so much more than advisors, you are my friends.

Reproduced with permission of the copyright owner. Further reproduction prohibited without permission.

Table of Contents

Reproduced with permission of the copyright owner. Further reproduction prohibited without permission.

Reproduced with permission of the copyright owner. Further reproduction prohibited without permission.

List of Figures

Reproduced with permission of the copyright owner. Further reproduction prohibited without permission.

Reproduced with permission of the copyright owner. Further reproduction prohibited without permission.

Reproduced with permission of the copyright owner. Further reproduction prohibited without permission.

List of Tables

Reproduced with permission of the copyright owner. Further reproduction prohibited without permission.

Chapter 1

Introduction

Early investigations studying perception across the visual field noted that objects appear different when viewed directly in front as compared to off to the side. For example, the ability to see in fine detail is decreased when not looking directly at the object (Jacobs, 1979), and sensitivity to contrast diminishes with distance from the middle of the retina, called the fovea (Koenderink, Bouman, Bueno de Mesquita, & Slappendel, 1978, a,b). Colors also look different. Colors appear desaturated or "washed-out" when viewed outside the fovea and, in some cases, show a change in hue (Boynton, Schafer, & Neun, 1964; Weitzman & Kinney, 1969; Gordon & Abramov, 1977).

At first glance, one might conclude that the peripheral retina is inferior to the fovea in visual processing. However, these differences may not be due to any deficiencies of the peripheral retina, but rather, to variations in the spatial scale of visual-processing elements across the retinal surface. This changing size-scale can account for a number of perceptual differences between the fovea and periphery. For example, decreases in acuity and contrast sensitivity correspond with changes in the amount of cortical area devoted to processing information from different areas of the retina (Rovamo, Virsu, & Nasanen, 1979).

In fact, simply increasing the size of peripherally-viewed stimuli seems to alleviate many of the problems with non-central vision (e.g., Johnson, 1986). Abramov,

Reproduced with permission of the copyright owner. Further reproduction prohibited without permission.

Gordon, and Chan (1991) systematically studied how changes in stimulus size affected color perception in the periphery and found that the desaturation and hue variations that accompany peripherally-viewed stimuli diminish as field size increases. Their results showed that hue and saturation responses grow as a function of stimulus size up to an asymptotic value, as if a perceptive field (the psychological correlate to a receptive field) is being filled. Thus, it appears that the non-uniform distribution and changing density of cellular components and neural connections across the retina can be mitigated by scaling stimuli with retinal eccentricity (distance from the fovea).

Increasing stimulus size alone, however, does not necessarily lead to foveal-like color perception in all areas of the retina. The peripheral retina contains a fourth type of photoreceptor, rods, that is lacking in the central 1-1.5° of the retina. Rods are more sensitive than cones in low-light conditions and, while they are not the neural mechanisms mediating color vision, they are known to affect several aspects of color appearance (e.g., Buck, Knight, & Bechtold, 2000; Buck, Knight, Fowler, & Hunt, 1998). Consequently, under conditions where rod signals are maximal (i.e., when the eye is dark adapted), the size-scaling needed in the peripheral retina for foveal-like color perception may change.

Peripheral Color Vision

Researchers once thought that the peripheral retina could serve as a model of deficient color vision (e.g., Ferree & Rand, 1919; Moreland, 1972). The observation that colors change in hue and become increasingly desaturated with increasing eccentricity led to a model of the peripheral retina that divided it into three roughly-concentric color zones. The central region was trichromatic, with the ability to perceive all possible

Reproduced with permission of the copyright owner. Further reproduction prohibited without permission.

colors. This trichromaic region, which included the fovea, continued out to approximately 51° in the nasal retina and to 26° in the temporal retina. Moving out from the trichromatic region, color discrimination decreased and visual perception in the very outer edges of the retina was achromatic.

A number of studies corroborated the work of Ferree and Rand (1919). Using color-naming methods, both Boynton, et al. (1964) and Weitzman and Kinney (1969) demonstrated that while color vision is trichromatic in the foveal area, red and green deficiencies exist just outside of this region. Studies on color discrimination found similar results: outside the trichromatic region, red-green discrimination is compromised, and at greater retinal eccentricities, blue-yellow discrimination also deteriorates (Noorlander, Koenderink, den Ouden, and Edens, 1983; Uchikawa, Kaiser, & Uchikawa, 1982). Other studies demonstrated that the perception of the color green, in particular, diminishes at eccentricities closer to the fovea than any other hue (Connors & Kelsey, 1961; Connors & Kinney, 1962).

These findings suggest some fundamental differences between the central and peripheral retinas. One factor that can account for some of the variations in color perception across the retina is macular pigmentation, the protective yellow film that selectively absorbs short-wavelength light (Cornsweet, 1970). Macular pigment is most dense in the fovea and continually decreases in density to approximately 5° retinal eccentricity. As a result, the spectral sensitivity curves, where cone sensitivity is plotted as a function of wavelength, for all three cone types are different at 7° compared to those measured in the fovea (Wooten & Wald, 1973). When corrections are made for macular pigmentation, the shapes of these functions at 7° are very similar to the foveal functions.

Reproduced with permission of the copyright owner. Further reproduction prohibited without permission.

Another difference between the central and peripheral retina is that more cortical neurons are dedicated to processing information from the central retina than the peripheral retina. This increase in the cortical representation of the fovea is referred to as the cortical magnification factor (CMF). van Esch, Koldenhof, van Doorn, and Koenderink (1984) studied the effects of the CMF on peripheral color vision in the nasal retina by measuring wavelength discrimination and spectral sensitivity. They found that if stimulus field sizes were scaled according to the CMF specified by Rovamo and Virsu (1979), color discrimination was approximately the same for all peripheral locations out to 80° retinal eccentricity. Noorlander et al. (1983) also found that spatiotemporal color discrimination is constant with eccentricity when stimulus field sizes are scaled according to the CMF.

Similarly, Johnson (1986) investigated how increasing stimulus size accounted for differences in foveal and peripheral color vision. She reported that the color zones proposed by Ferree and Rand (1919) could not be explained by reductions in sensitivity to any specific wavelength in the peripheral retina. She concluded, however, that the increasing neural summation (the number of receptors sending information to a receiving cell) of chromatic mechanisms that occurs with eccentricity could explain the apparent dichromacy in the periphery. By measuring spatial summation functions for a series of wavelengths and eccentricities in the temporal retina, Johnson showed increases in receptive field size across the peripheral retina and how visual measurements are compromised when a constant or small stimulus size is used across the visual field.

Several other researchers have also demonstrated that increasing the size of a stimulus in the peripheral retina leads to more foveal-like color perception. Nagy and Doyal (1993) measured red-green color discrimination at 10° and 25° in the nasal retina.

Reproduced with permission of the copyright owner. Further reproduction prohibited without permission.

They found that when stimulus size was sufficiently large, peripheral color discrimination thresholds approximated those in the fovea. Kuyk (1982) measured spectral sensitivity functions in the central and peripheral retinas. The functions were markedly different unless stimulus size was increased, in which case foveal and peripheral functions appeared very similar. Likewise, unique hue loci, the equilibrium points of the chromatic-opponent mechanisms, differ from foveal loci when stimulus size is kept constant across the retina, but shift to foveal-like measurements when stimulus diameter is increased (Nerger, Volbrecht, & Ayde, 1995). Thus, contrary to earlier research supporting the "color zones" of the peripheral retina, more recent studies indicate the existence of no color deficiencies at any peripheral location when stimuli are sufficiently large.

Rod Photoreceptors

One attribute of the peripheral retina that cannot be discounted by simply increasing stimulus size is rod photoreceptors. Rods were previously assumed not to influence color vision and are thus absent from several models of color vision (e.g., Hurvich & Jameson, 1957; DeValois & DeValois, 1993). The earliest conception of the differences between cones and rods, the Duplicity Theory, suggested that rods (scotopic system) function only at low-light levels where no hue is perceived, while cones (photopic system) operate at higher-light levels where hue is perceived (e.g., Schultze, 1866; von Kries, 1905). In other words, each system is separate from the other. More recent work, however, has established that rods and cones interact significantly (e.g., Frumkes, Sekuler, & Reiss, 1972; Benimoff, Schneider, & Hood, 1982). Rods have been found to inhibit cone signals, thus decreasing cone sensitivity with dark adaptation (Lie,

Reproduced with permission of the copyright owner. Further reproduction prohibited without permission.

1963; Sugita & Tasaki, 1988a,b; Sugita, Suzuki, & Tasaki, 1989) and direct rod stimulation (Frumkes, Sekuler, Barris, Reiss, & Chalupa, 1973), as well as interfere with cone signals in flicker (MacLeod, 1972; Goldberg, Frumkes, & Nygaard, 1983). Conversely, cones have been found to affect rod sensitivity (Ingling, Lewis, & Loose, 1977; Buck, Peeples, & Makous, 1979; Buck & Makous, 1981) and even block the detection of a stimulus by rods (Makous & Boothe, 1974).

Physiological and anatomical studies have identified the neural substrates that could mediate these rod-cone interactions. The responses of ganglion cells in amphibians and non-primate mammals can be affected by stimulation of both rods and cones (Granit, 1943, 1944); when ganglion cell thresholds are measured during dark adaptation, the results show the typical two-branched function and rod-cone break after approximately 8-10 min in the dark (Donner & Rushton, 1959). Research on non-human primates has shown that rod and cone signals have different response latencies and the first signal to arrive at a ganglion cell may cancel out the effects of the signal from the other type of photoreceptor arriving later (Gouras, 1965; Gouras & Link, 1966), thus accounting for the psychophysical evidence discussed above suggesting rod-cone interference.

Further physiological evidence on humans suggests that rods and cones share common pathways to the ganglion cells. The two receptor types interact in both the inner and outer plexiform of the retina, especially along lines carrying information about low spatial frequencies that connect to ganglion cells with large receptive fields (D'Zmura & Lennie, 1986). Although mammalian bipolar cells connect exclusively to either rods or cones, rod bipolars have no direct connection to ganglion cells, and instead connect to rod amacrine cells which in turn synapse onto cone bipolars and ganglion cells (Daw, Jensen, & Brunken, 1990; Wässle, Yamashita, Greferath, Grünert, & Müller, 1991). This is not,

Reproduced with permission of the copyright owner. Further reproduction prohibited without permission.

however, the only retinal pathway for rod signals. Gap junctions exist between rods and cones in the retinas of lower vertebrates like monkeys and rabbits (Raviola & Gilula, 1973), and evidence has been found that these same connections exist in the retinas of higher primates (Schneeweis & Schnapf, 1995). Furthermore, psychophysical evidence suggests that rod signals travel along at least two separate pathways in the human retina, contingent on such factors as the temporal characteristics of the stimulus (Stockman, Sharpe, Zrenner, & Nordby, 1991).

No matter which pathway rod signals take to reach ganglion cells, they initially or eventually merge with cone pathways (Daw et al., 1990; Lee, Smith, Pokorny, & Kremmers, 1997). It therefore seems reasonable that rods could affect color appearance by the same means that they impact other aspects of cone functioning, such as flicker detection and absolute sensitivity.

Rod Effects on Color Vision

Several studies have noted an increase in the perception of blueness in peripherally-presented stimuli compared to stimuli presented to the fovea (Gordon & Abramov, 1977; Weale, 1953; Stabell & Stabell, 1980). Ambler and Proctor (1976) suggested that rods are responsible for this increase in blueness when stimuli are presented at intensities above chromatic threshold. When stimuli are below chromatic threshold, rods add an achromatic component to color perception- a finding supported by other researchers (e.g., Stabell & Stabell, 1996). It has been proposed that the enhancement of blue in the periphery may be facilitated by an interaction between rods and short-wavelength-sensitive (S) cones (Trezona, 1970). Specifically, the two cell types may share a common pathway to higher visual processing levels, thus accounting

Reproduced with permission of the copyright owner. Further reproduction prohibited without permission.

for more blue being seen in a peripheral stimulus. This explanation seems plausible given anatomical and psychophysical evidence supporting a shared neural pathway between rods and S cones (Daw et al., 1990; Naarendorp, Rice, & Sieving, 1996).

Not only have researchers supported the idea that rods specifically increase the perception of blue in peripheral stimuli (Stabell & Stabell, 1994; Ambler, 1974; Hunt; 1952; Richards & Luria, 1964; Buck, 1997), but some have claimed that rods affect hue perception across the entire visible spectrum (Buck et al., 2000). For example, using color-matching techniques, studies have found that rods differentially enhance the yellow/blue opponent mechanism relative to the red/green opponent mechanism, meaning that rods contribute a blue component to short wavelengths and a yellow component to long wavelengths (Stabell and Stabell, 1975, 1976a, 1979). Contrary to this, however, is recent anatomical evidence suggesting that rods preferentially influence the red-green opponent mechanism (Lee et al., 1997).

Another strategy that researchers have used to study rod influences on color perception is the measurement of unique hues, or the equilibrium points of the chromatic opponent mechanisms (e.g., Buck et al., 2000; Hurvich & Jameson, 1957; Nerger et al., 1995; Nerger, Volbrecht, Ayde, & Imhoff, 1998; Volbrecht, Nerger, Imhoff, & Ayde, 2000a; Angel, Volbrecht, & Nerger, submitted). Buck et al. (2000) found that rod signals produce shifts in the spectral locus of all three unique hues (blue, green, and yellow). Specifically, they found that under dark-adapted conditions, the loci of unique blue, unique green, and unique yellow shifted to longer wavelengths. Nerger et al. (1998) also reported that under certain circumstances, rods shifted the locus of unique yellow to longer wavelengths; and Angel et al. (submitted) found that the loci of unique blue and unique green shifted to longer wavelengths under dark-adapted conditions with very dim

Reproduced with permission of the copyright owner. Further reproduction prohibited without permission.

stimuli. Angel et al., however, showed no rod effects on the locus of unique yellow, nor did Nerger et al. (1995). Additionally, Nerger et al. (1995) found that rods shifted unique blue and unique green to shorter wavelengths when smaller stimuli were used. Thus, the effects rods have on color appearance seem to be highly dependent on stimulus parameters such as size and intensity.

Stimulus parameters also affected rod input in Buck et al.'s (1998) study. They employed a color-naming technique to measure hue responses on both the cone and rod plateaus using a 7° stimulus at 8° retinal eccentricity in the nasal retina. They reported that rods did not affect any one hue perception in particular, but instead, affected all four basic hue perceptions (blue, green, yellow, and red) across the visible spectrum. Specifically, they found that in the locations in the spectrum that appeared the most blue, green, and yellow, response functions shifted to longer wavelengths under conditions where rod signals were maximized (i.e., on the rod plateau). Furthermore, the perception of red at long wavelengths was reduced while the perception of red at short wavelengths was unaffected by rods. Overall, rods affected each hue function differently in different areas of the visible spectrum; and no hue perception was uniformly reduced. These rod effects on hue perception were also found to be light-level dependent: when stimuli of high retinal illuminance were used, color-naming functions measured on the cone and rod plateaus looked similar.

Retinal Topography

Not only do rods affect color perception, but they further complicate the spatial scale of the peripheral retina because their numbers, like those of other cell types in the retina, are not uniformly distributed radially or with eccentricity. Thus, the variations in

Reproduced with permission of the copyright owner. Further reproduction prohibited without permission.

the absolute and relative numbers of cell types across the retina may also affect color perception.

Cones and Rods

Cones and rods are easily distinguished anatomically. Cones have shorter outer segments that do not reach as far into the pigment epithelium and large, tapering inner segments when compared to rods (Ahnelt, Kolb, & Pflug, 1987), except in the fovea where they are long and narrow. The retina contains approximately 4.6 million cones and 92 million rods, with high levels of variability among individuals (Curcio, Sloan, Kalina, & Henrickson, 1990b). Schultze (1866) was the first to establish that the fovea contains the highest density of cones, and is nearly absent of rods. Foveal peak densities of cones vary greatly. For example, Curcio et al. estimate the peak density to be 199,000 cones / mm^2 while Ahnelt et al. indicate there are 238,000 cones / mm^2 in the fovea.

Østerberg (1935) was the first to measure photoreceptor density as a function of retinal eccentricity in the human eye. He studied several well-defined retinal locations in a single eye and described the changes in the retinal mosaic with distance from the fovea. As can be seen in figure 1.1, which is a reproduction of Østerberg's data, the density of cones falls rapidly with eccentricity, reaching a level of no change from approximately 8-10° retinal eccentricity and beyond. Again, rods are absent from the foveal center, an area of approximately 1.25°.

Østerberg's results have been confirmed by more recent anatomical work of Curcio et al. (1990b). They too found that cone densities decrease rapidly with eccentricity and that the decline is faster along the vertical meridian than along the horizontal meridian. That is, isodensitiy contours of cone densities are elliptical in shape

Reproduced with permission of the copyright owner. Further reproduction prohibited without permission.

Figure 1.1. Reproduction of Østerberg's (1935) distribution of photoreceptors as a function of eccentricity.

Reproduced with permission of the copyright owner. Further reproduction prohibited without permission.

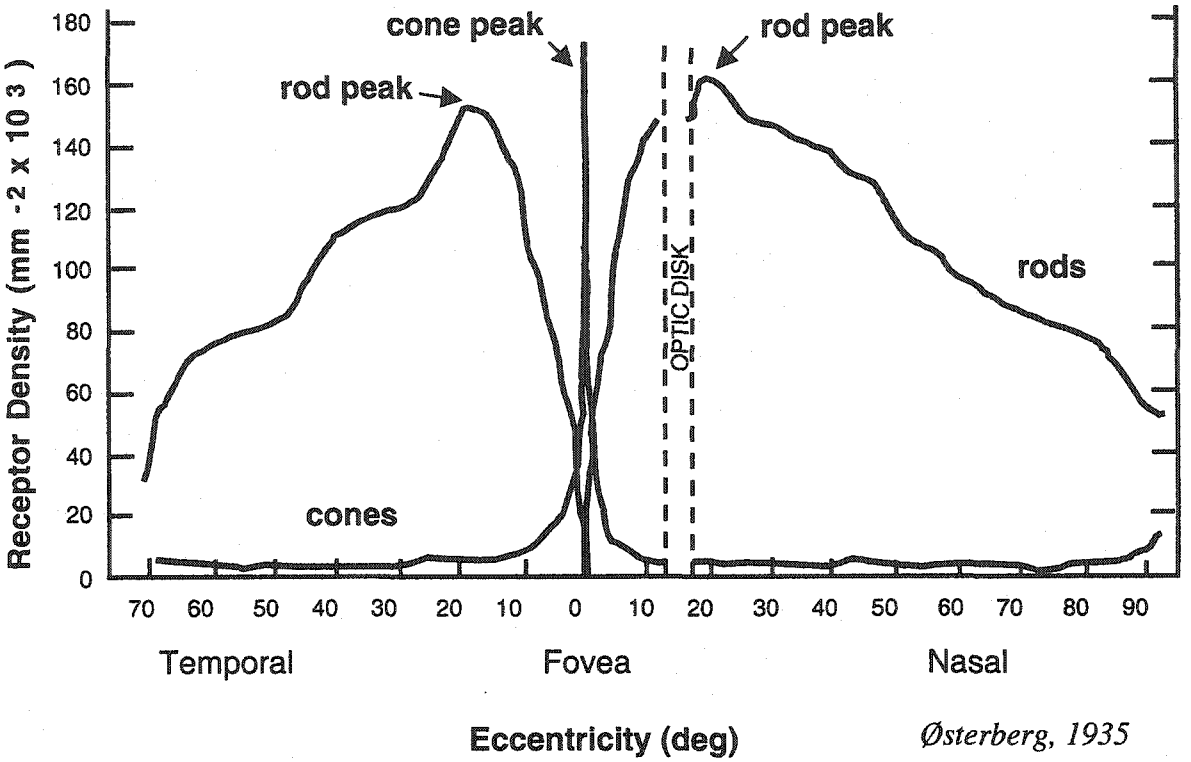

Østerberg, 1935

Reproduced with permission of the copyright owner. Further reproduction prohibited without permission.

and are aligned with the horizontal meridian (Curcio, Sloan, Packer, Hendrickson, & Kalina, 1987). Thus, there is a "cone streak" in the periphery: a zone of high cone density surrounding the fovea. Because of this streak, there are higher cone numbers in the nasal compared to the temporal retina; at corresponding eccentricities, cone packing is 40-45% higher in the nasal than in the temporal retina. Research indicates, however, that this asymmetry might not be present until eccentricities beyond the optic disk (Curcio et al., 1987). The cone streak extends slightly more in the inferior retina than the superior retina. In fact, cone density is lowest in the superior retina, near the area where rod density is highest, 15° from the fovea. The decline in cone density with eccentricity levels off at approximately 8-10° and may even increase slightly in the far periphery.

The distribution of rods is generally more symmetric than that of cones, but density among retinal quadrants does vary. For example, rods density is lower along the horizontal meridian. The highest density of rods is in the superior retina at approximately 15° retinal eccentricity where their numbers reach approximately 176,000 rods / mm^2. Regardless of retinal quadrant, rod density is highest in the "rod ring," which surrounds the fovea at an eccentricity approximately that of the optic disk. Rod density decreases 15-25% where the "rod ring" crosses the horizontal meridian in the temporal and nasal retinas and continues to decline from there.

Individual Cone Types

Anatomical data support the presence of all three cone types, short-wavelength sensitive (S), middle-wavelength sensitive (M), and long-wavelength sensitive (L) cones in the periphery (Ahnelt et al., 1987; Curcio et al., 1990b). Peripheral spectral sensitivity

Reproduced with permission of the copyright owner. Further reproduction prohibited without permission.

data indicate that all three cone types are both present and functional out to 70° (Weale, 1953) or 80° (Wooten & Wald, 1973) retinal eccentricity.

M and L cones have their peak densities in the fovea and then decrease exponentially out to approximately 7-8° in the periphery where their numbers level off at approximately 8,000 to 10,000 / mm^2 (Curcio et al., 1990b). While researchers have not yet been able to morphologically distinguish between M and L cones, psychophysical studies estimate the L:M cone ratio at approximately 2:1 out to at least 28° in the periphery (Nerger & Cicerone, 1992; Otake & Cicerone, 2000).

S cones, which are morphologically distinct from M and L cones, comprise only 8-10% of the total cone population of the human retina (Curcio et al., 1990b; Curcio, Allen, Sloan, Lerea, Hurley, Klock, & Milam, 1991; Curcio et al., 1987; Ahnelt et al., 1987; Ahnelt, Keri, & Kolb, 1990). In the fovea, S cones are rare and are spaced irregularly. Whether or not they exist at all in the very middle of the fovea is open to debate. Curcio et al. (1991) claim that the central 0.35° of the retina is completely free of S cones, while Ahnelt et al. (1987) suggest one S cone in the central fovea. The density of S cones decreases less rapidly with eccentricity than does overall cone density. Researchers agree that S cones are found in their highest density between 0.5° and 1.5° from the central fovea where estimates range from 2,000 S cones / mm^2 (Curcio et al., 1991) to 15,000 S cones / mm^2 (Ahnelt et al., 1987). Proportionally, they make up about 3-15% of the total cone population at this eccentricity, after which their numbers decline out to approximately 7-10° in the periphery (Curcio et al., 1991). Beyond 7-10° eccentricity, their absolute numbers (500 S cones / mm^2) and relative numbers (5.3%) remain approximately constant, as do the relative numbers of M and L cones.

Reproduced with permission of the copyright owner. Further reproduction prohibited without permission.

Ganglion Cells

Ganglion cell density is higher in the nasal retina compared to the temporal retina; densities of ganglion cells in the nasal retina exceed those in the temporal retina by as much as 300% at corresponding eccentricities (Curcio & Allen, 1990a). The density of ganglion cells in the superior retina exceeds the inferior by 60%. The highest density of ganglion cells occurs in the center of the retina (32,000-38,000 ganglion cells / mm^2). Their density decreases with increasing distance from the fovea. Whereas the number of cones remains relatively constant between 8-10° retinal eccentricity, ganglion cell density continues to decrease into the far periphery. Thus, the ratio of cones to ganglion cells found in the fovea (Wässle, Grunert, Rohrenbeck, & Boycott, 1989) increases in the periphery, resulting in more spatial summation (convergence of neural signals) of cone signals and larger receptive fields for ganglion cells as distance from the fovea increases.

Receptive and Perceptive Fields

A retinal receptive field is the area of the retina that, when stimulated, causes a cell to respond (Barlow, Fitzhugh, & Kuffler, 1957). How that cell fires depends on the location within the receptive field that is stimulated. For example, it is well known that retinal ganglion cell receptive fields have a circular, antagonistic spatial organization. Kuffler (1953) made single-cell recordings in the cat's retina to a small spot of light (0.2 mm in diameter) that was moved to different areas within a ganglion cell's receptive field (within 1 mm). He found that the receptive fields of retinal ganglion cells have a discharge pattern in the center that is opposite to that found in the surround. If a particular cell had an on-center and an off-surround, it increased its firing rate when

Reproduced with permission of the copyright owner. Further reproduction prohibited without permission.

stimulated in the center of its receptive field and decreased its firing rate when stimulated in the surround of its receptive field. If a cell had an off-center and an on-surround, an opposite firing pattern occurred. This same organizational pattern for receptive fields has been found in the lateral geniculate nucleus of the cat (Hubel & Wiesel, 1965) and for retinal ganglion cells in non-human primates (Hubel & Wiesel, 1960).

The size and organization of receptive fields varies with distance from the fovea (Hubel & Wiesel, 1960). In accord with the finding that spatial summation increases with eccentricity (Wilson, 1970; Scholtes & Bouman, 1977), the mean diameter of the centers of receptive fields increases continually out to approximately 40° or 50° retinal eccentricity (Hubel & Wiesel, 1960); at 10° retinal eccentricity, receptive field centers are estimated to be approximately 10' in diameter and 1° in diameter at 40-50°. Rods may also affect the sizes of receptive fields in the periphery as the adaptive state of the retina seems to impact the size and organization of receptive fields (Kuffler, 1953; Scholtes & Bouman, 1977). The borders of receptive fields are extended when the illumination of the light used to test for a response increases (Hartline, 1940; Barlow, 1953). Kuffler (1953) showed that when the eye is dark adapted or the intensity of a background light upon which a test light is superimposed decreases, the size of the receptive fields increases, and vice versa. Furthermore, Barlow et al. (1957), measuring receptive fields under conditions of light and dark adaptation using electrophysiological techniques in the cat's retina, also found that receptive field centers were larger when rods were allowed to respond. They also found that the center-surround antagonism of receptive fields measured under light-adapted conditions disappeared when measurements were made following 30 minutes of dark adaptation, i.e., in a dark-adapted

Reproduced with permission of the copyright owner. Further reproduction prohibited without permission.

state, a stimulus only elicited the response characteristic of the center of the receptive field.

Perceptive Fields for Achromatic Stimuli

Several of these same characteristics have been found to be true for perceptive fields, the psychological correlate of a physiologically-determined receptive field (Jung & Spillmann, 1970) when measured using achromatic (non-colored) stimuli. The organizational properties of perceptive fields have been studied by measuring the threshold for a spot of light as a function of the size of the background field upon which it is superimposed (Westheimer, 1965). As the background fills the excitatory center of the perceptive field and signal strength increases, threshold for the superimposed test light also increases. As the background begins to fill the perceptive field's inhibitory surround, the signal strength is reduced, and so is the intensity needed to detect the superimposed test light. When the background overfills the entire perceptive field, there is no change in signal strength and the threshold for detecting the test light no longer changes; any further increases in the background diameter do not affect threshold. Thus, it appears that perceptive fields measured in the fovea with achromatic stimuli are organized in the same manner as receptive fields, i.e., center-surround antagonism. Using the Westheimer paradigm, the peak of the threshold function is a measure of the size of the perceptive field center and the place where threshold no longer changes is a measure of the size of the entire perceptive field.

The Westheimer paradigm has been used to measure perceptive field sizes for achromatic stimuli in the periphery as a function of eccentricity (Spillmann, Ransom-Hogg, & Oehler, 1987; Ronchi & Fidanzati, 1972). By measuring perceptive field sizes

Reproduced with permission of the copyright owner. Further reproduction prohibited without permission.

from 0-70° in the nasal and temporal retinas of monkeys and humans, it was found that, as with receptive fields, perceptive fields become larger with increasing eccentricity. Mean diameters of perceptive field centers increase linearly with distance from the fovea, doubling in size between 20° and 60° retinal eccentricity (Jung & Spillmann, 1970). These measurements correspond well with measurements of receptive field centers (Oehler, 1985).

Furthermore, it has been reported that rods can affect perceptive field sizes as they do receptive field sizes. Ransom-Hogg and Spillmann (1980) measured perceptive field sizes in the fovea and the periphery under light- and dark-adapted conditions. Measurements were made at 0, 5, 10, 23, 30, 40, 50, 60, and 70° along the horizontal meridian of the nasal retina. They found, as expected, that perceptive field size centers increased with eccentricity, but also that the size of the centers of the perceptive fields were larger when measured under dark-adapted conditions and that the surrounds were almost completely ineffective. These findings have been replicated by others (Spillmann et al., 1987; Troscianko, 1982) and are in agreement with the conclusions of Barlow et al. (1957) regarding receptive field size under dark-adapted conditions.

Perceptive Fields for Chromatic Stimuli

Perceptive field sizes for chromatic stimuli have been systematically measured in the peripheral retina by Abramov et al. (1991). Using a rear-view projection system, Abramov et al. presented stimuli in the fovea and at 5, 10, 20, and 40° along the horizontal meridian of the nasal and temporal retinas. A series of stimulus sizes was shown at each retinal location at a constant intensity for 500 ms every 18 sec. Wavelengths ranged from 440-660 nm in 10 nm steps. Following 10 min of dark

Reproduced with permission of the copyright owner. Further reproduction prohibited without permission.

adaptation, observers used the "4 + 1 categories" hue-scaling technique (Gordon & Abramov, 1988; Gordon, Abramov, & Chan, 1994) to assign percentages to the four elemental hues (red, blue, green, yellow) and saturation.

As with other studies on perceptive fields, they demonstrated that perceptive field sizes increased with increasing eccentricity, that is, the minimum perceptive field size necessary to obtain foveal-like color perception increased with distance from the fovea. They also found no evidence for an inhibitory surround. In fact, their functions for hue responses across stimulus size appear very similar to Westheimer functions measured in the dark-adapted eye using achromatic stimuli (Spillmann et al., 1987).

Abramov et al. (1991), however, did not directly address the role rods might play in the organization and/or size of perceptive fields in the peripheral retina. Since they used mesopic intensity levels, where both rods and cones function, it is possible that rod signals contributed to hue perception.

Current Study

The goal of the present study was to more systematically investigate changes in chromatic perceptive field sizes as a function of rod contributions in each of the four retinal quadrants. The methodology employed was similar to that used by Abramov et al. (1991), with the addition of a bleach and a no-bleach condition that minimized and maximized rod effects, respectively. Perceptive field sizes were measured in the fovea, as a control, and at 10° retinal eccentricity in all four quadrants (superior, inferior, temporal, and nasal). Since Abramov et al. (1991) also measured perceptive fields at 10° in the temporal retina, their data were used as a comparison to that collected in the present study. Although other researchers have measured perceptive fields for chromatic

Reproduced with permission of the copyright owner. Further reproduction prohibited without permission.

stimuli in the inferior retina (Knau & Werner, 2002), there appears to be no published measurements of perceptive fields for chromatic stimuli in the superior retina, and no study measuring perceptive fields in the same observer at the same eccentricity in all four retinal quadrants using both a bleach and no-bleach condition.

Reproduced with permission of the copyright owner. Further reproduction prohibited without permission.

Chapter 2

Methods

Observers

Three females (age 28, 41, and 45) served as observers in this study. All observers had normal or corrected-to-normal visual acuity and were assessed for trichromatic color vision using anomaloscopic matches (Neitz OT-II), three panel tests (Farnsworth-Munsell 100 Hue, D-15, and Adams Desaturated D-15), and the Dvorine pseudo-isochromatic plate test including an F-2 tritan plate. All observers had previous experience with the techniques used in this study, but were naive with respect to their data.

Apparatus

A three-channel Maxwellian-view optical system was used in this study (see figure 2.1). A 300-watt xenon arc lamp (Oriel, model 66065) regulated at 290 watts by a dc power supply (Oriel, model 68811) provided the illumination for all channels. Light emitted from the xenon arc lamp (LS) exited via two ports, passed through infrared heat-absorbing filters (H1 and H2), and was collimated by lenses CL1 and CL2.

To form Channel 1, light from CL1 was reflected 90° by a beam splitter (BS1). The light was focused by lens L1 and collimated by lens L2. Pairs of lenses, such as L1 and L2, were used throughout the optical system to insure that as much light as possible was

Reproduced with permission of the copyright owner. Further reproduction prohibited without permission.

Figure 2.1. Schematic of the three-channel Maxwellian-view optical system. Components are as follows: LS = Light Source; H = Infrared Heat Absorbing Filter; CL = Initial Collimating Lens; BS = Beam Splitter; L = Lens; M = Mirror; MC = Monochromator; W = Neutral Density Wedge; FS = Field Stop; FB = Filter Box; SH = Shutter; AP = Artificial Pupil, and FL = Final Lens. The observer's position is indicated at the bottom of the figure.

Reproduced with permission of the copyright owner. Further reproduction prohibited without permission.

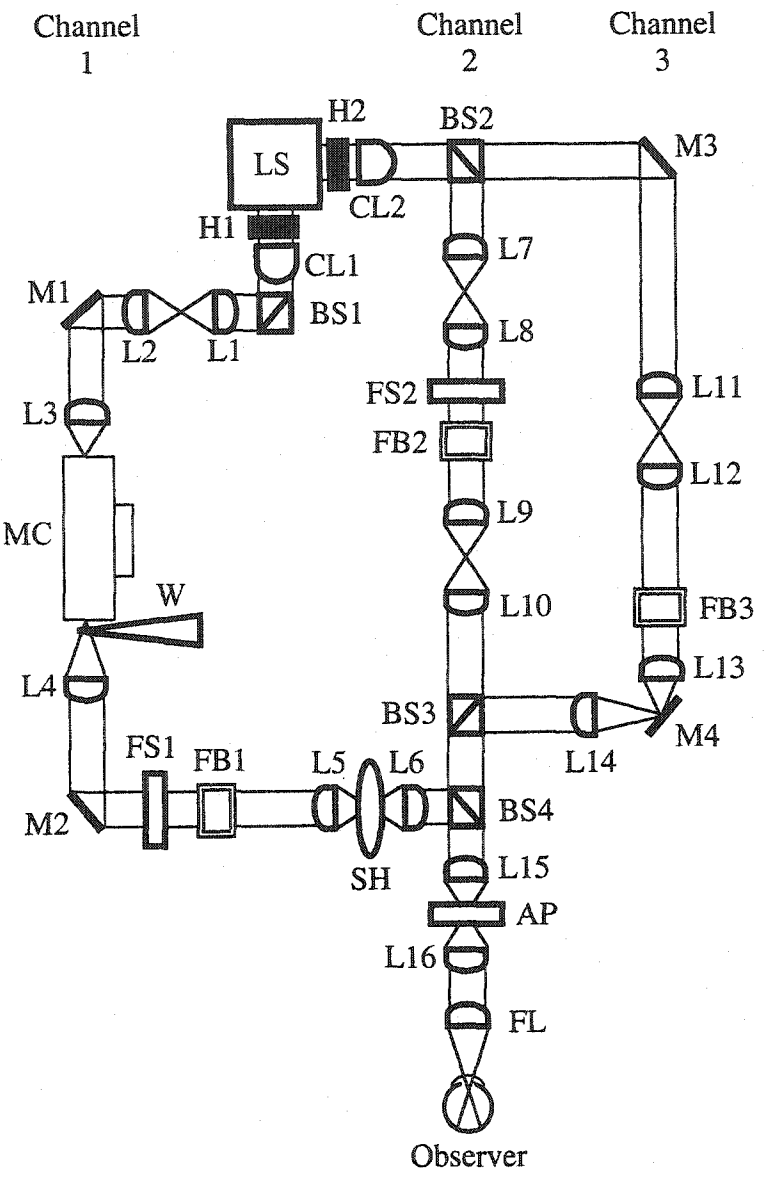

Reproduced with permission of the copyright owner. Further reproduction prohibited without permission.

being captured within the system and to provide collimated portions and focal points in which optical components could be placed.

Channel 1 controlled the wavelength, size, and intensity of the test stimulus. After being directed by a mirror (M1), L3 focused the light onto the entrance slit of a monochromator (MC; Instruments SA, Inc., Model H20, 4-nm half-amplitude bandpass). Upon exiting MC, light passed through a two log-unit neutral-density wedge (W; Ealing Electro-Optics), which was interfaced to a computer.

Upon exiting the monochromator, light was collimated by L4 and directed by M2 to a field stop (FS1), which defined the size and shape of the test stimulus. A filter box (FB1) held neutral density filters (Ealing Electro-Optics) to control the intensity of the stimulus in combination with W. The light from Channel 1 was again focused and collimated by L5 and L6. A shutter (SH), placed at the focal point of this lens pair, manipulated the exposure duration of the stimulus. SH was controlled by a driver system (Uniblitz, model T132).

BS2 created Channels 2 and 3. Light for Channel 2, which provided the fixation arrays, was projected through a pair of focusing/collimating lenses (L7 and L8). FS2 defined the size and arrangement of the fixation points and FB2 held neutral-density filters. Light was refocused and collimated (L9 and L10) and combined with light from channel 1 at BS4.

Channel 3 provided the broadband-bleaching stimulus (5500K) used to suppress rod activity. From M3, light traveled through a pair of focusing/collimating lenses (L11 and L12). The intensity of the bleaching stimulus was controlled by neutral-density filters placed in FB3. Light was then focused by L13, reflected 90° by M4, and

Reproduced with permission of the copyright owner. Further reproduction prohibited without permission.

collimated by L14. When the bleaching field was not in use, an opaque partition blocked the light coming from Channel 3.

BS3 combined light from Channels 2 and 3 and directed it to BS4 which combined the light from all three channels. Light then passed through another pair of focusing/collimating lenses (L15 and L16). An artificial pupil (AP), placed at the focal point between L15 and L16, defined the final size of the Maxwellian image (1.8 mm in diameter). This size was smaller than the smallest pupil size and thus insured that all the light from the system was entering the observer's pupil. After leaving L16, light was projected onto the final lens (FL) which focused the light from all three channels on the plane of the observer's pupil. Observers aligned their right eye with respect to the optical axis of the Maxwellian-view system by means of a dental-impression bite bar assembly which permitted adjustments for depth, height, and lateralization.

Stimuli

Stimuli were presented in the fovea and at 10° retinal eccentricity along the horizontal meridian of the temporal and nasal retinas and along the vertical meridian of the superior and inferior retinas. At each peripheral location, measurements were made on both the cone and rod plateaus ("rod-bleach" and "no-bleach" conditions, respectively). The peripheral location of 10° was chosen because 1) cone density has stabilized, and 2) the number of rods is relatively high (Curcio et al., 1990b). In addition, other researchers have measured perceptive field sizes at 10° in the temporal and nasal retinas, so their data could be compared (Abramov et al., 1991) to data from this study.

Reproduced with permission of the copyright owner. Further reproduction prohibited without permission.

All stimuli were equated to 20 td. This intensity is in the mesopic range, allowing both rods and cones to respond, and has been used by other researchers measuring perceptive fields in the peripheral retina (Abramov et al., 1991). Consistent with the methods used by Abramov and colleagues, each stimulus was presented for 500 ms on a dark background with an inter-stimulus interval (ISI) of 18 s to minimize any adaptation effects. Stimuli ranged from 440-660 nm in 10 nm steps and were presented in a pseudo-random order.

For foveal measurements, a 1° stimulus was used. At each peripheral location, a series of stimulus sizes was employed so that percent hue responses grew to an asymptotic value. The stimulus sizes required to obtain an asymptotic function differed among the observers and are shown in tables 2.1 and 2.2. The 1° stimulus was included in each stimulus set for all retinal locations to enable comparison among quadrants and between peripheral and foveal measurements.

Table 2.1. Stimulus sizes presented to observers in the rod-bleach condition.

Observer	**10° Temporal Retina**
VV	0.098°, 0.125°, 0.25°, 0.5°, 1°, 2°, 3°
JN	0.125°, 0.25°, 0.5°, 1°, 2°, 3°
CA	0.098°, 0.125°, 0.25°, 0.5°, 1°, 2°, 3°

Observer	**10° Nasal Retina**
VV	0.098°, 0.125°, 0.25°, 0.5°, 1°, 2°, 3°
JN	0.125°, 0.25°, 0.5°, 1°, 2°, 3°
CA	0.125°, 0.25°, 0.5°, 1°, 2°, 3°

Observer	**10° Superior Retina**
VV	0.098°, 0.125°, 0.25°, 0.5°, 1°, 2°, 3°
JN	0.125°, 0.25°, 0.5°, 1°, 2°, 3°
CA	0.125°, 0.25°, 0.5°, 1°, 2°, 3°

Observer	**10° Inferior Retina**
VV	0.098°, 0.125°, 0.25°, 0.5°, 1°, 2°, 3°
JN	0.25°, 0.5°, 1°, 2°, 3°
CA	0.25°, 0.5°, 1°, 2°, 3°

Reproduced with permission of the copyright owner. Further reproduction prohibited without permission.

Table 2.2. Stimulus sizes presented to observers in the no-bleach condition.

Observer	**10° Temporal Retina**
VV	0.25°, 0.5°, 1°, 2°, 3°, 5°
JN	0.25°, 0.5°, 1°, 2°, 3°
CA	0.25°, 0.5°, 1°, 2°, 3°, 5°

Observer	**10° Nasal Retina**
VV	0.25°, 0.5°, 1°, 2°, 3°, 5°
JN	0.25°, 0.5°, 1°, 2°, 3°
CA	0.5°, 1°, 2°, 3°, 5°

Observer	**10° Superior Retina**
VV	0.25°, 0.5°, 1°, 2°, 3°, 5°
JN	0.5°, 1°, 2°, 3°
CA	0.5°, 1°, 2°, 3°, 5°

Observer	**10° Inferior Retina**
VV	0.25°, 0.5°, 1°, 2°, 3°, 5°
JN	0.5°, 1°, 2°, 3°, 5°
CA	0.5°, 1°, 2°, 3°, 5°

As shown in figure 2.2, panels A and B, two vertically-displaced pinhole-size fixation points and a third, horizontally-displaced pinhole fixation point were used to control retinal positioning of the stimulus in the temporal and nasal quadrants. Observers fixated on the horizontally-displaced fixation point, and the test stimulus was centered between the two vertically-displaced fixation points. For measurements in the superior and inferior retinas, the fixation-point array was rotated 90° (figure 2.2, panels C and D). For foveal measurements, the stimulus appeared in the center of two horizontally-displaced fixation points (figure 2.2, panel E). The intensity of the fixation points was adjusted so they were just visible to the observer to minimize adaptation of the retina (Jameson & Hurvich, 1967).

For the bleach condition, a 20°, 7.32 log scot td bleaching field was centered over the eccentricity being tested. When viewed for 10 s, this field bleached approximately

Reproduced with permission of the copyright owner. Further reproduction prohibited without permission.

Figure 2.2. Schematic of the stimulus fixation arrays used for each retinal quadrant and the fovea.

Reproduced with permission of the copyright owner. Further reproduction prohibited without permission.

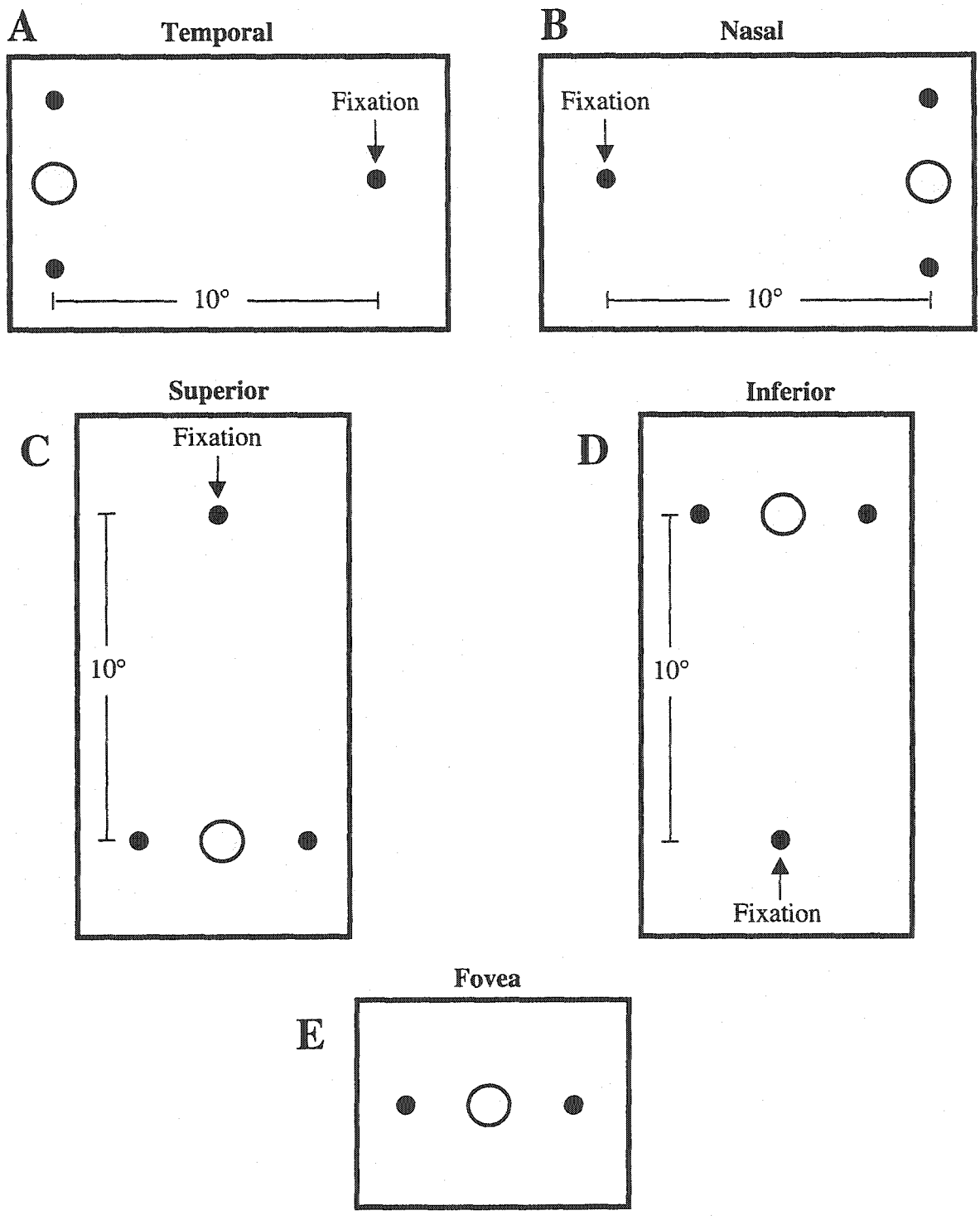

Reproduced with permission of the copyright owner. Further reproduction prohibited without permission.

99.8% of the rod photopigment (Alpern, 1971; Rushton & Powell, 1972).

Calibrations

Densities for a series of neutral density filters placed in Channel 1 (figure 2.1) were calculated by taking radiometric measurements (EG&G Gamma Scientific, Model DR-1500A) from 400-700 nm in 10 nm steps. Densities were also calculated for the neutral density wedge in Channel 1 (W, figure 2.1). The circular wedge was divided into 2000 equal increments and radiometric measurements were taken every 100 units at wavelengths ranging from 400-700 nm in 10 nm steps. Within the 100-unit wedge-position ranges, interpolations were made every 20 units. Filters used in channel 3 were calibrated for broadband light based on photometric measurements.

To calculate retinal illuminance, radiometric measurements (UDT Instruments, Model S370) were obtained from Channel 1 (figure 2.1) for wavelengths ranging from 440-660 nm in 10 nm steps. A photometric measurement (Minolta Chroma Meter, Model CS-100) was also taken in Channel 1 at a reference wavelength of 550 nm. Photopic td values were determined using Westheimer's (1966) method. Appropriate neutral density filters and wedge positions were then calculated so that test stimuli were maintained at 20 td across wavelengths based on the spectral luminosity function (Vos & Walraven, 1971). A photometric measurement was obtained from Channel 3 (figure 2.1) for the broadband light (5500k) to calculate the intensity of the bleaching field. The monochromator was calibrated so that the maximal emission of a He-Ne laser (Spectra-Physics; 632.8 nm) occurred at 633 nm.

Reproduced with permission of the copyright owner. Further reproduction prohibited without permission.

Procedure

For measurements made in the fovea (figure 2.3, panel A), observers dark adapted for 10 min prior to making color judgments. For peripheral measurements in the rod-bleach condition (figure 2.3, panel B), observers dark adapted for 10 min, viewed the bleaching field for 10 sec, then dark adapted for an additional 4.5 min. Measurements were then taken for the next 4 -5 min on the cone plateau. For the peripheral no-bleach condition (figure 2.3, panel C), observers dark adapted for 30 min prior to making color judgments.

Hue and saturation judgments were made during the 18 sec ISI following the 500 ms presentation of the test stimulus. For each stimulus presented, observers used the "4+1 categories" hue-scaling technique (Gordon & Abramov, 1988; Gordon et al., 1994). First, percentages were assigned to the four elemental hues (blue, green, yellow, and red) such that the total hue experience summed to 100%. For example, an observer might report "100% blue," or "50% green, 50% yellow." Observers were not permitted to describe a stimulus using opponent hues together (i.e. assigning percentages to both red and green or both yellow and blue for any particular stimulus). Next, observers assigned a percentage to saturation reflecting the chromatic content of the stimulus. This number ranged from 0 to 100%. A response of "0%" for saturation indicated that the stimulus contained no chromatic component (i.e. the stimulus appeared 100% achromatic). A response of "100%" for saturation indicated that the stimulus appeared entirely chromatic. For each stimulus size, the 23 wavelengths were presented in a pseudo-random order. Observers made two to five color judgments at each stimulus size for every wavelength, adaptation condition, and retinal quadrant.

Reproduced with permission of the copyright owner. Further reproduction prohibited without permission.

Figure 2.3. Schematic of the procedures used when stimuli were presented in the fovea (panel A) and at 10° in the peripheral retina for the rod-bleach (panel B) and no-bleach (panel C) conditions.

Reproduced with permission of the copyright owner. Further reproduction prohibited without permission.

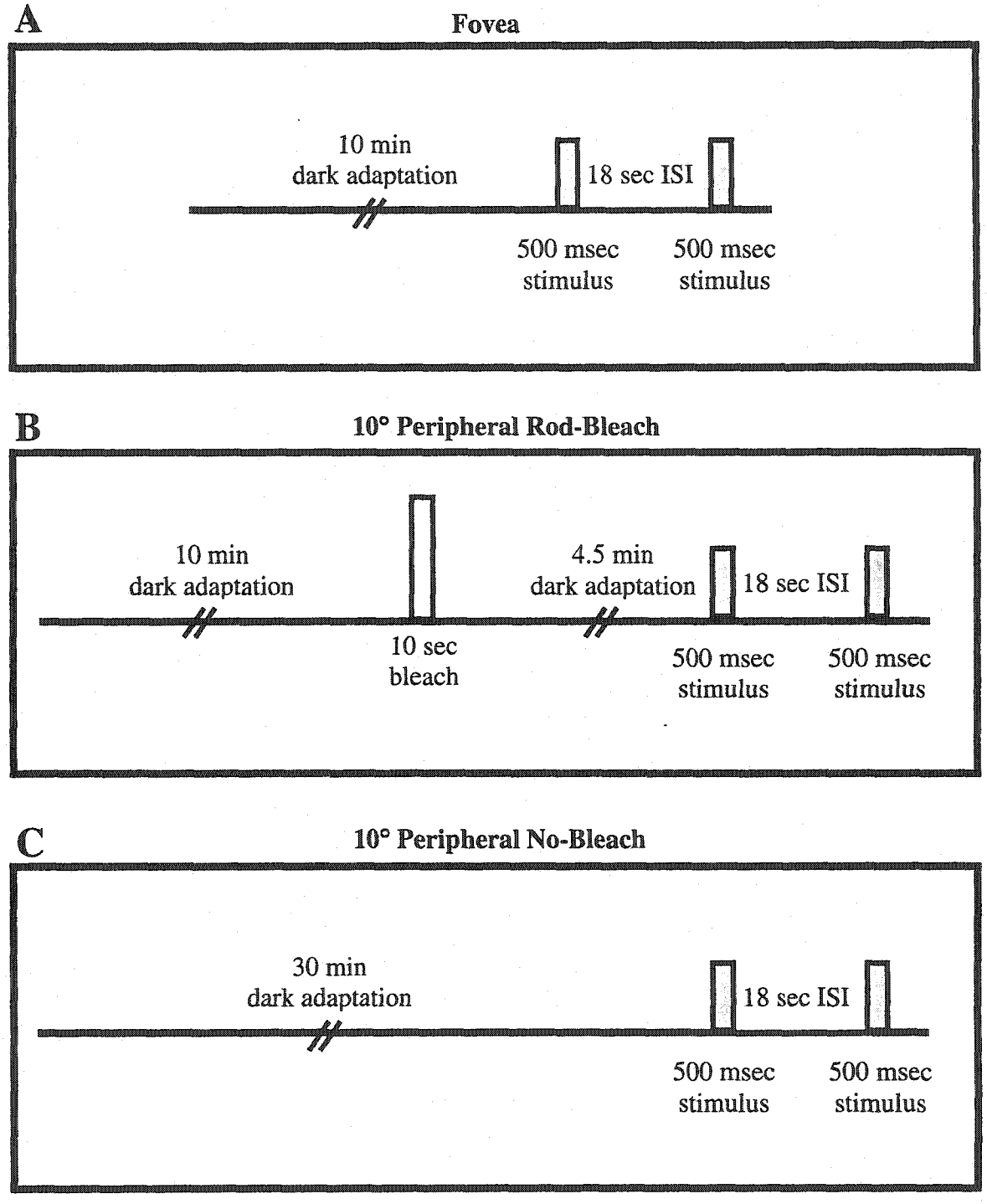

Reproduced with permission of the copyright owner. Further reproduction prohibited without permission.

Each experimental session lasted 1.5 - 2 hours. All data were collected from one retinal quadrant before moving on to another. The presentation order of the adaptation condition and retinal quadrant was pseudo-random. Stimulus sizes within an experimental session were presented randomly. Each observer completed 44 sessions, 11 for each retinal quadrant. Observers also made 2-3 responses for every wavelength in the fovea over 2-3 experimental sessions. Thus, approximately 50 2-hr sessions were required of each observer to complete data collection for this project.

Control Conditions

Two control conditions were conducted for this study. First, to ensure that the broadband bleaching (5500k) stimulus did not differentially adapt any of the three cone mechanisms, a bleach was employed in the fovea for observers VV and CA. The procedures for this condition were the same as those used in the 10° peripheral rod-bleach condition (see figure 2.3, panel B), but stimuli were presented to the fovea (figure 2.2, panel E). Observers dark adapted for 10 min, then viewed the bleaching stimulus, centered on the fovea, for 10 sec. Observers then dark adapted for an additional 4.5 min and measurements were made using a 1° stimulus for 4-5 min post bleach. These results were compared to those from the foveal condition with 10 min dark adaptation and no bleaching field.

The second control condition investigated potential differences between the fovea and 10° peripheral retina due to differences in macular pigmentation densities. Macular pigment is a protective yellow film that sits in front of the central 5° of the fovea (Cornsweet, 1970) and selectively absorbs short-wavelength light. Since monochromatic

Reproduced with permission of the copyright owner. Further reproduction prohibited without permission.

stimuli were used in this study, the macular pigment acted as a neutral density filter and would not have caused any variation in the chromatic content of the test stimulus. The lack of macular pigment at 10° would, however, cause an overall increase in the intensity of light at shorter wavelengths in the periphery compared to the fovea. To investigate the potential impact of this intensity difference, stimuli below 540 nm were increased in intensity by the density of the macular pigment in the fovea as estimated by Vos (1972) (see table 2.3).

Since estimates made by Vos (1972) were based on a 2° foveal stimulus, a 2° stimulus was used for this control condition. For each observer (CA & VV), two color judgments at each of the 23 wavelengths were made using the original intensity calculations for the fovea, and two color judgments at each of the 23 wavelengths were made using the corrections for macular pigment. The fixation array and procedures were the same as those depicted in panel E of figure 2.2 and panel A of figure 2.3.

Table 2.3. Estimated density of macular pigment in the fovea for different wavelengths of light using a 2° stimulus (Vos, 1972).

Wavelength (nm)	Macular Pigment Density
440	0.27
450	0.30
460	0.33
470	0.29
480	0.27
490	0.25
500	0.10
510	0.10
520	0.03
530	0.01

Reproduced with permission of the copyright owner. Further reproduction prohibited without permission.

Chapter 3

Results: Color Appearance

Data were analyzed for the effects of retinal location, adapted state of the retina, and stimulus size. Mean percentages of hue and saturation were included in the analysis if the following criteria were met: 1) For a given stimulus size, responses were obtained from at least two of the three observers, 2) For each wavelength presented, responses at all stimulus sizes exceeded zero by the average of the standard errors of the mean. Meeting these criteria ensured that the data being analyzed were representative across observers, and mean percentages were greater than that expected from error alone. The latter criterion was used in a previous study on perceptive fields in the peripheral retina (Abramov et al., 1991).

An arcsine transform (Winer, Brown, & Michels, 1991; Abramov et al., 1991) was applied to each percentage: Transformed % = ((2 x arcsine (square root (% hue / 100))) / pi) x 100. Since observers' responses for percent hue and percent saturation were limited by the extremes of 0% and 100%, variances may have been artificially reduced at these percent values. Applying the arcsine transform to each assigned percentage made variances more equal across wavelengths and still preserved the range of percent values from 0% to 100%.

Following transformation, for each wavelength presented, hue responses were scaled according to saturation as in the Abramov et al. study (1991),. For example, if a

Reproduced with permission of the copyright owner. Further reproduction prohibited without permission.

given wavelength was judged as 50% green and 50% yellow, with 80% saturation, the values were scaled to 40% green and 40% yellow. That is, the sum of hue percentages was equal to the assigned saturation value at each wavelength, while preserving the ratio among the hue terms. Following arcsine transformations and scaling, means were taken across observers and standard errors of the means (SEM) were calculated to reflect between-session variability.

Saturation

One of the most obvious differences in stimulus appearance when viewed in the peripheral retina under conditions where rod signals are maximized (i.e., the no-bleach condition) is a decrease in saturation of shorter wavelengths. Figure 3.1 plots the mean percentages assigned to saturation as a function of wavelength in the fovea and the four peripheral quadrants for the no-bleach condition with a 1° stimulus. Error bars specify ±1 SEM. Percent saturation in the fovea (solid, thick line) was highest in the short- and long-wavelength areas of the visible spectrum and lowest in the spectral region from approximately 550-570 nm. Percent saturation in the periphery was less at shorter wavelengths for all peripheral quadrants when compared to foveal measurements. Saturation responses at short wavelengths in the temporal retina were higher than the other three peripheral retinal quadrants. Starting at approximately 520 nm, saturation in the temporal retina was approximately the same and followed a similar pattern as in the fovea. Saturation responses for the other three quadrants also increased as wavelengths became longer, but remained overall lower than responses from the fovea and temporal retina.

Reproduced with permission of the copyright owner. Further reproduction prohibited without permission.

Figure 3.1. Mean percent saturation is plotted as a function of wavelength for the fovea and each retinal quadrant at 10° eccentricity. All functions represent mean responses across observers using a 1° stimulus in the no-bleach condition. Symbols denote different retinal locations and error bars specify ±1 SEM.

Reproduced with permission of the copyright owner. Further reproduction prohibited without permission.

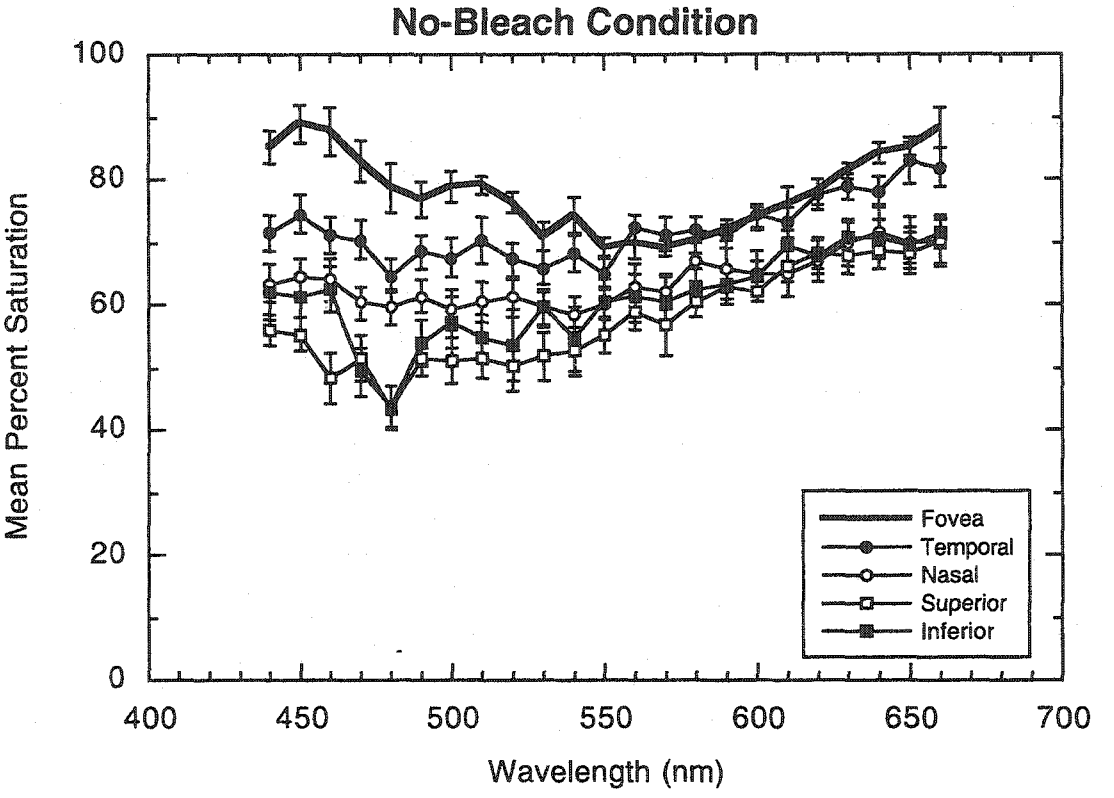

Reproduced with permission of the copyright owner. Further reproduction prohibited without permission.

Saturation also decreased as stimulus size decreased in all retinal quadrants in the no-bleach condition. Figure 3.2 plots the mean percent saturation as a function of wavelength for all of the stimulus sizes. Each panel denotes a different retinal quadrant at 10° eccentricity. As can be observed in each panel, saturation diminishes as stimulus size decreases. While some decreases in saturation are seen at longer wavelengths, the effect is most apparent at shorter wavelengths. In general, the saturation responses for the three largest stimuli (2°, 3°, and 5°) tend to cluster together and share a similar pattern, i.e., saturation is highest in the short- and long-wavelength areas of the spectrum and lowest in the spectral region from approximately 550-570 nm. This pattern for the larger stimuli is similar to the pattern in the fovea for the 1° stimulus (see figure 3.1). Percent saturation differs at the smaller stimuli compared to larger stimuli: while the U-shaped pattern remains, especially in the temporal retina (upper left panel), the spectral area of minimum saturation shifts to shorter wavelengths. An additional characteristic to note is the increase in variability with smaller stimulus sizes. A good illustration of this effect is in the nasal retina (upper right panel) where error bars are markedly larger for the two smallest stimulus sizes (0.5° and 0.25°) than for the four larger stimulus sizes.

The decrease in saturation that accompanies peripherally-viewed stimuli diminishes under conditions where rods are bleached. Figure 3.3 plots saturation for the 1° stimulus in the same manner as figure 3.1, except for the rod-bleach condition. Percent saturation is quite similar in all four retinal quadrants in contrast to the no-bleach condition (see figure 3.1). The "U-shaped" pattern found in the fovea for percent saturation is less marked in the periphery. In the spectral range where foveal saturation is

Reproduced with permission of the copyright owner. Further reproduction prohibited without permission.

Figure 3.2. Mean percent saturation is plotted as a function of wavelength for the temporal, nasal, superior, and inferior retinas at 10° eccentricity. All functions represent mean responses across observers. Symbols denote different stimulus sizes and error bars specify ±1 SEM.

Reproduced with permission of the copyright owner. Further reproduction prohibited without permission.

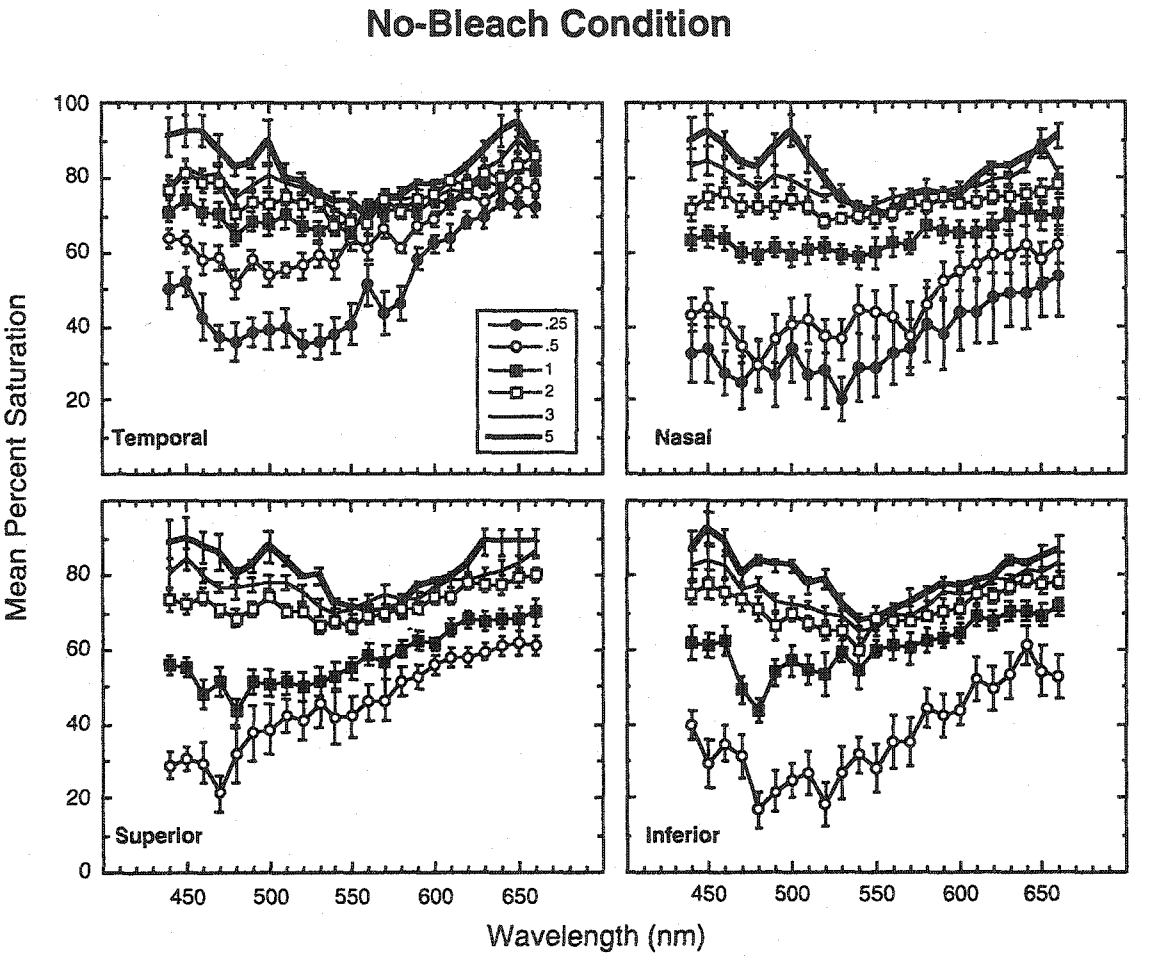

Reproduced with permission of the copyright owner. Further reproduction prohibited without permission.

Figure 3.3. Mean percent saturation is plotted as a function of wavelength for the fovea and each retinal quadrant at 10° retinal eccentricity for the rod-bleach condition. For ease of comparison, the foveal function is bolded. The functions represent data using the 1° stimulus at all retinal locations and error bars specify +1 SEM.

Reproduced with permission of the copyright owner. Further reproduction prohibited without permission.

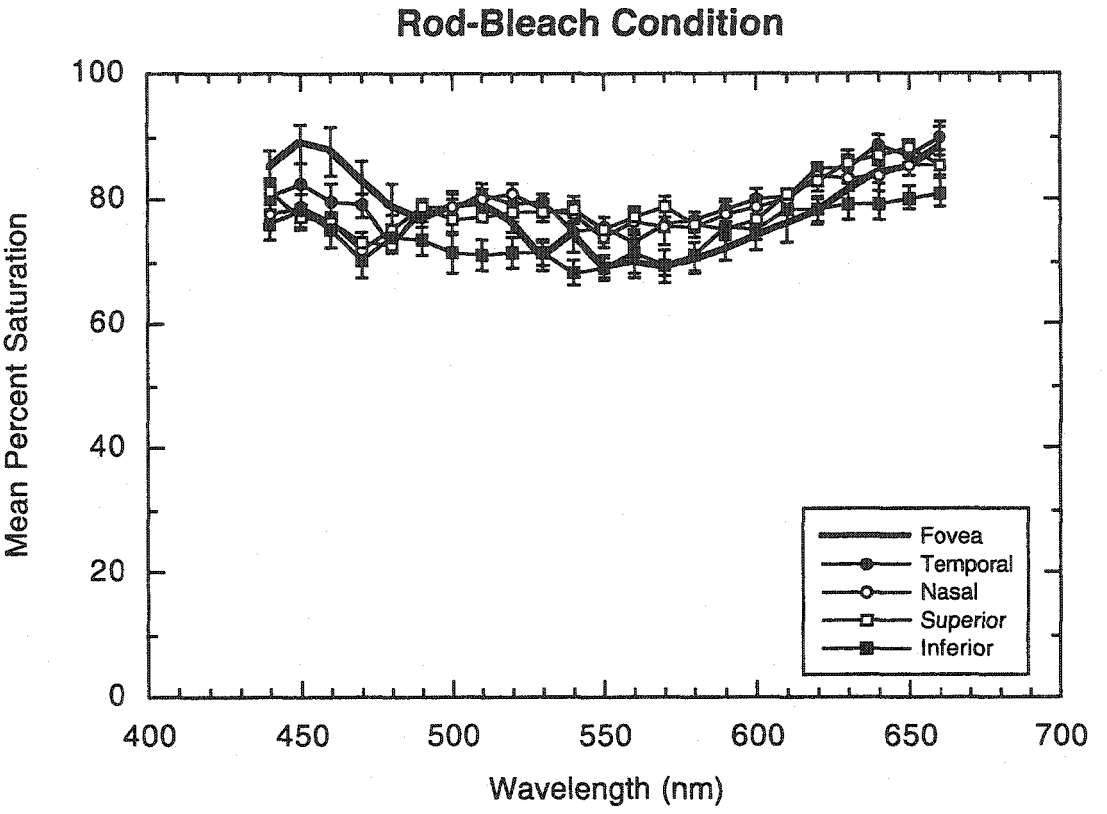

Reproduced with permission of the copyright owner. Further reproduction prohibited without permission.

at its minimum, saturation for several of the peripherally-viewed stimuli are higher than corresponding wavelengths viewed in the central retina. Furthermore, the increase in saturation at short wavelengths in the fovea is not seen for stimuli viewed in the periphery in the rod-bleach condition.

In figure 3.4, saturation responses are plotted as a function of wavelength for all of the stimulus sizes presented in each of the retinal quadrants (panels) for the rod-bleach condition. While percent saturation tends to diminish with reductions in stimulus size, as in the no-bleach condition, the decrease is much less than it was in the no-bleach condition (see figure 3.2). Also, percent saturation does not vary as much across wavelengths as in the no-bleach condition.

Hue Appearance

Effects of Retinal Location

Figure 3.5 shows the color-naming functions for the fovea and 10° peripheral locations using a 1° stimulus in the no-bleach condition. All hue values are scaled to saturation to enable comparison of the overall color experience among the different retinal locations. Several differences between the foveal and peripheral functions are apparent. While the temporal color-naming function (upper left panel) most closely resembles the foveal function (top panel), data from the other three quadrants differ from the fovea. The most notable effect is the decrease in the perception of green (open circles) and the spreading of yellow perception (closed squares) across the visible spectrum. These changes are especially noticeable in the superior and inferior retinas (bottom panels).

Reproduced with permission of the copyright owner. Further reproduction prohibited without permission.

Figure 3.4. Mean percent saturation is plotted as a function of wavelength for the temporal, nasal, superior, and inferior retinas at 10° eccentricity for the rod-bleach condition. Symbols denote different stimulus sizes, and error bars specify +1 SEM.

Reproduced with permission of the copyright owner. Further reproduction prohibited without permission.

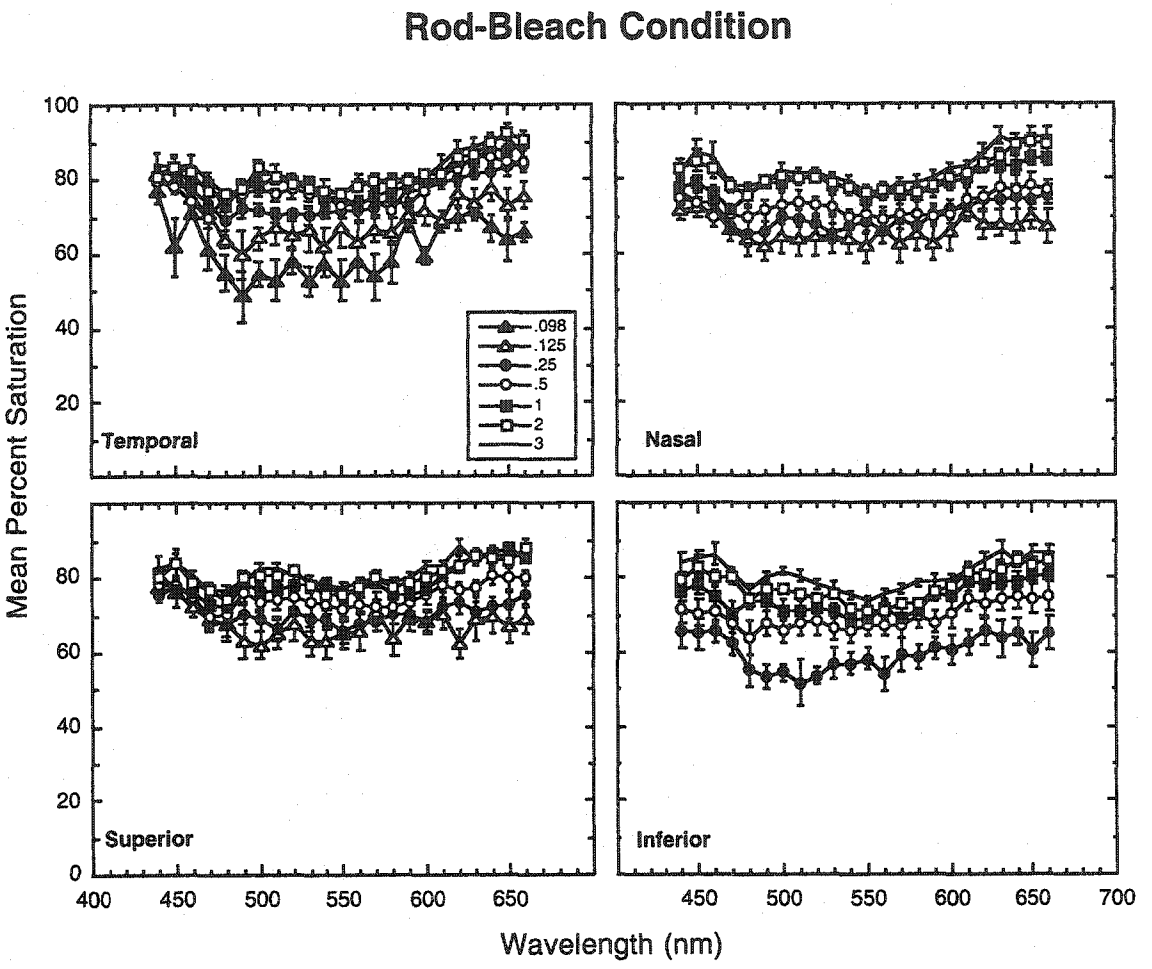

Reproduced with permission of the copyright owner. Further reproduction prohibited without permission.

Figure 3.5. Color-naming functions for the fovea and 10° peripheral locations using a 1° stimulus in the no-bleach condition. All values are scaled to saturation and functions represent mean responses across observers. Various symbols denote different hue terms and error bars specify ±1 SEM.

Reproduced with permission of the copyright owner. Further reproduction prohibited without permission.

No-Bleach Condition

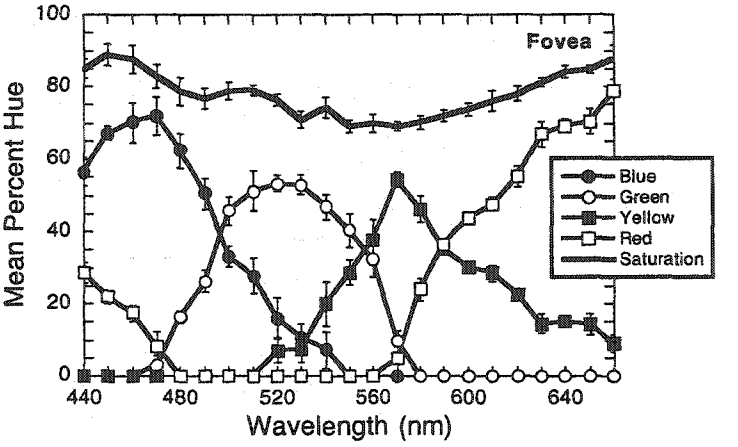

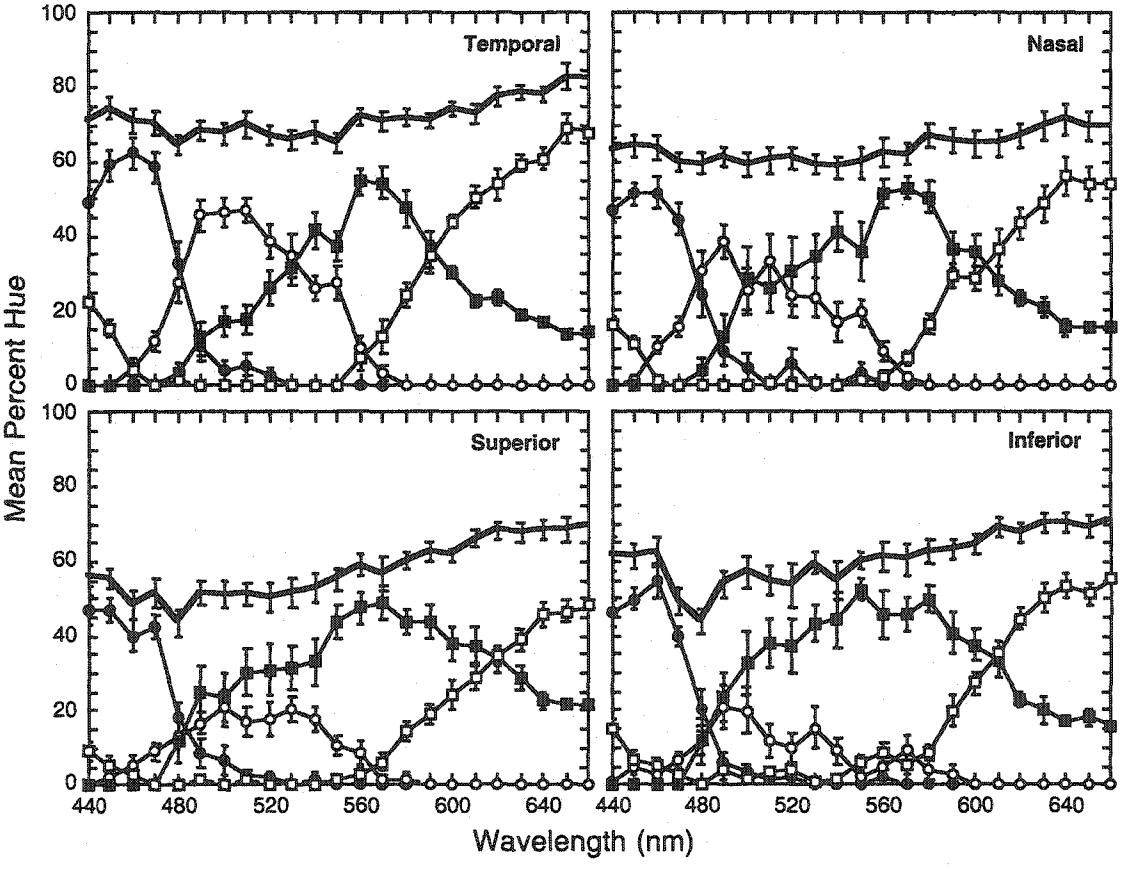

Reproduced with permission of the copyright owner. Further reproduction prohibited without permission.

These differences, and others, are more evident in figure 3.6 where mean hue response across observers is plotted as a function of wavelength for each hue term in the no-bleach condition using the 1° stimulus. In the left-hand column, all values are scaled to saturation, while the right-hand column displays unscaled hue values. Each symbol represents a different peripheral location, and the bold line represents percent hue obtained in the fovea. When stimuli are equal in size at all retinal locations, rods have the largest affect on the color green (second panel). This pattern is expected for the scaled data given that saturation values correspondingly diminish in the spectral range of green (see figure 3.2). However, this pattern persists even with the unscaled data shown in the right panel of figure 3.6. Also, for both scaled and non-scaled data, rods appear to shift the peak of the green function to shorter wavelengths; the foveal function reaches its peak at approximately 520 nm, while the functions from the temporal and nasal retinas (closed and open circles, respectively) reach their peak around 500 nm.

In the top and bottom panels of figure 3.6, it can also be seen that less blue and red were reported at all peripheral locations relative to the fovea. The differences between the foveal and peripheral perceptions are smaller for red than for blue. Again, this pattern is predicted for the scaled data since longer wavelengths were judged as more saturated overall than shorter wavelengths in the periphery (figure 3.2). Furthermore, the slight variability among retinal quadrants for blue perception, seen in the left-hand panel, seems to be an artifact of the scaling procedure.

Rods also appear to affect the spectral range of two of the four hue terms, blue and yellow (top and third panels, respectively). In the fovea, blue is reported out to

Reproduced with permission of the copyright owner. Further reproduction prohibited without permission.

Figure 3.6. Mean hue response plotted as a function of wavelength for each hue term in the no-bleach condition using the 1° stimulus. In the left-hand-column, all hue values are scaled to saturation, in the right-hand column, values are unscaled. Each panel represents a different hue term and error bars specify ±1 SEM. The foveal function is bolded and the four peripheral quadrants are denoted by different symbols.

Reproduced with permission of the copyright owner. Further reproduction prohibited without permission.

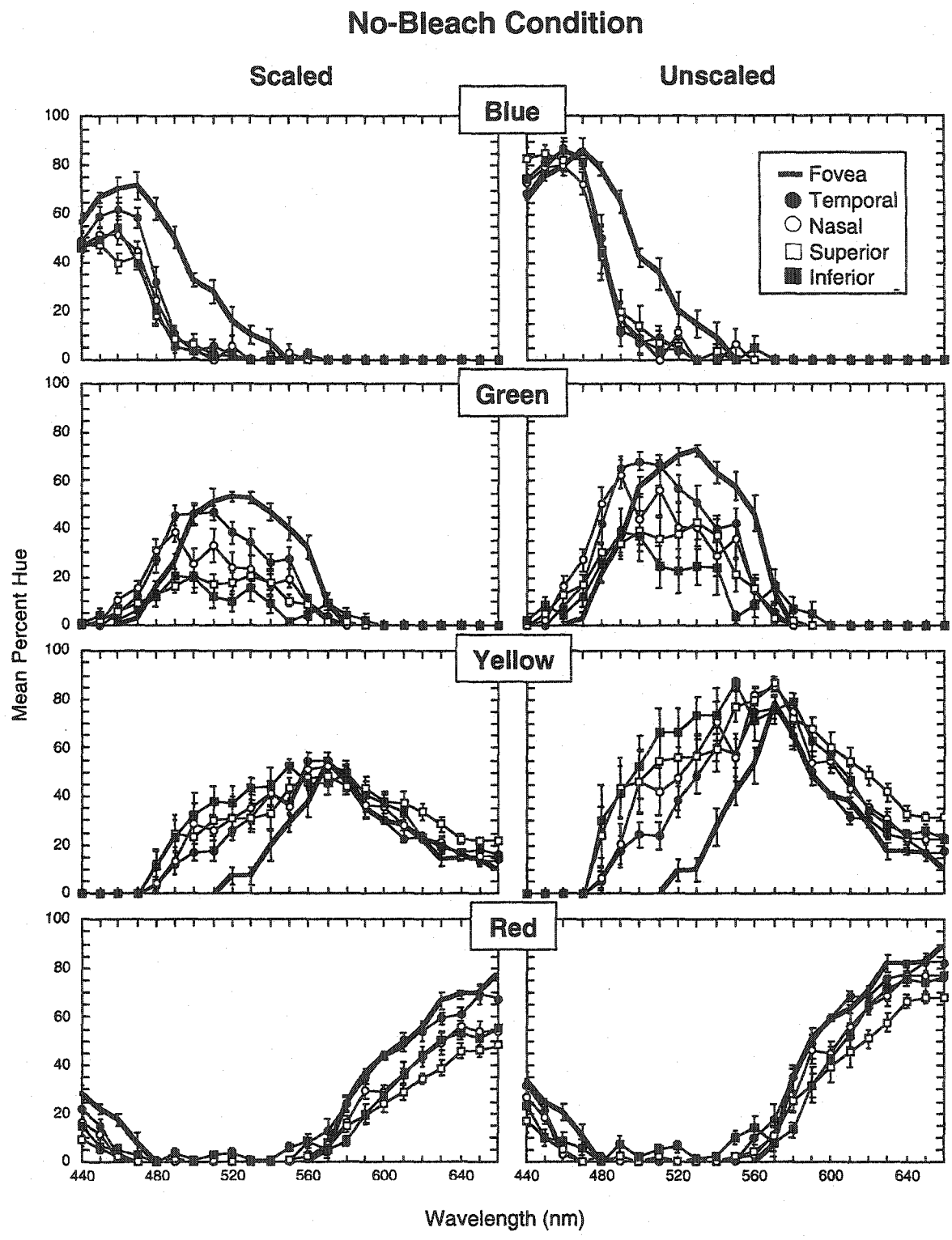

Reproduced with permission of the copyright owner. Further reproduction prohibited without permission.

approximately 540 nm, while in the periphery, the perception of blue is no longer perceived at approximately 490-500 nm. In the periphery, the spectral range of yellow extends to the left of the foveal peak to approximately 470 nm, while no yellow is perceived in the fovea at wavelengths shorter than about 520 nm. At wavelengths longer than the peak of the yellow function, more yellow is often reported in the periphery than in the fovea.

Effects of Adaptation

As shown in figure 3.7, which is plotted in the same manner as figure 3.5, color-naming functions for the 1° stimulus at all peripheral locations for the rod-bleach condition (bottom 4 panels) look more similar to the color-naming function of the fovea (top panel) than the functions in the no-bleach condition (see figure 3.5). The decrease in greenness and the spreading of yellowness associated with peripherally-viewed stimuli in the no-bleach condition are much less apparent in the rod-bleach condition. This is to be expected since the rod-bleach condition should minimize rod contributions. Some minor variations do exist, however, indicating that peripheral cones may not be operating in the same manner as foveal cones. These differences are, again, better illustrated when percent hue is plotted as a function of wavelength for each hue term at all retinal locations. In figure 3.8, unscaled data are re-plotted for the no-bleach condition in the left panels and unscaled data for the rod-bleach condition are presented in the right panels.

Reproduced with permission of the copyright owner. Further reproduction prohibited without permission.

Figure 3.7. Color-naming functions for the fovea and 10° peripheral locations using a 1° stimulus in the rod-bleach condition. All functions represent values scaled to saturation and mean responses across observers. Different symbols denote the four hue terms and error bars specify ±1 SEM.

Reproduced with permission of the copyright owner. Further reproduction prohibited without permission.

Rod-Bleach Condition

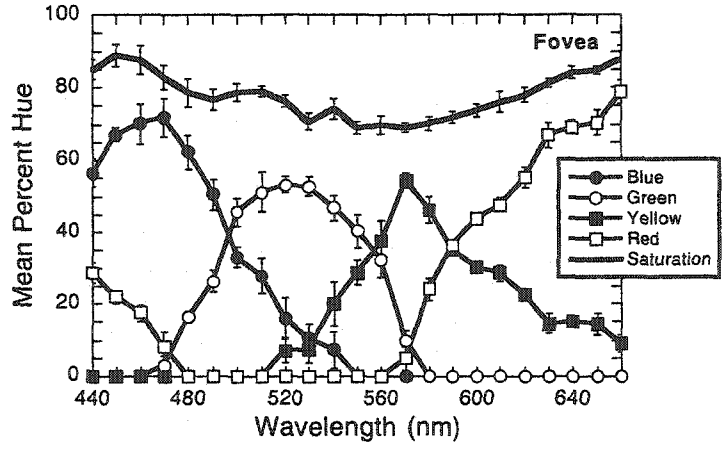

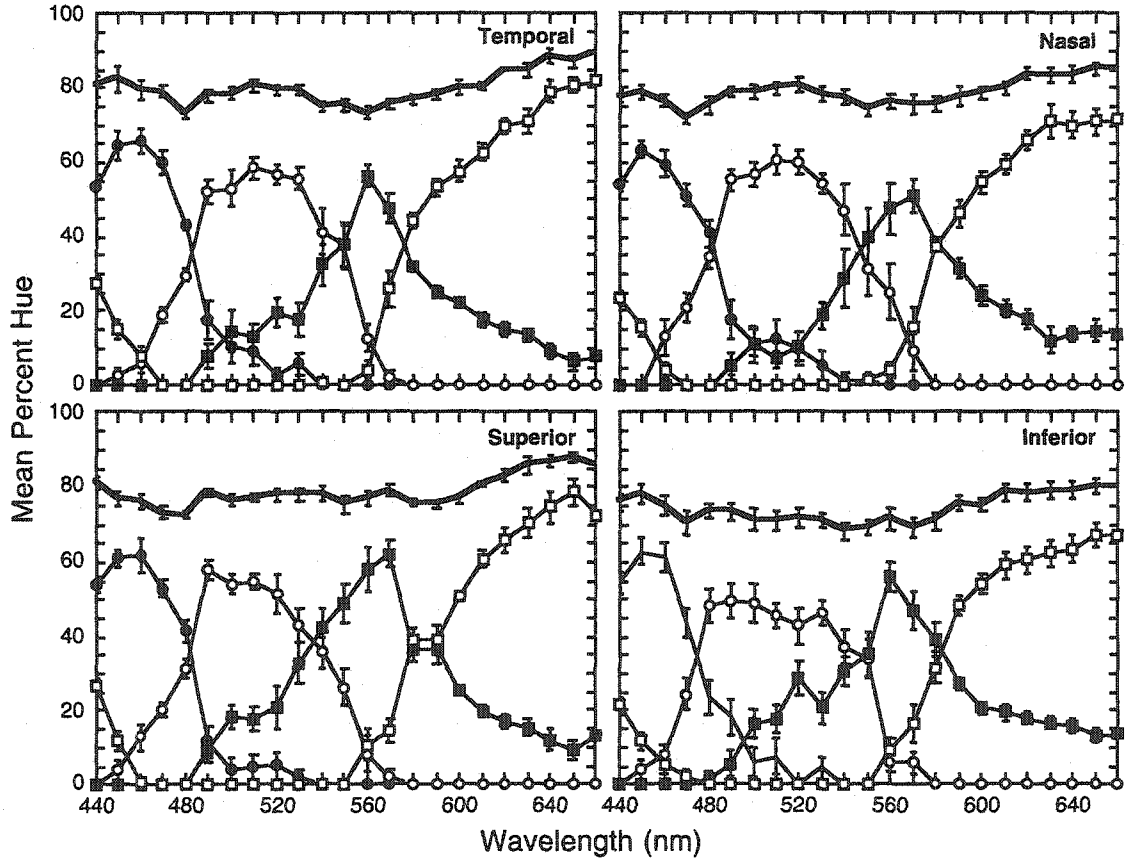

Reproduced with permission of the copyright owner. Further reproduction prohibited without permission.

Figure 3.8. Mean hue response plotted as a function of wavelength for each hue term using the 1° stimulus. In the left-hand-column, uncaled hue values are re-plotted for the no-bleach condition. In the right-hand-column, unscaled hue values are plotted for the rod-bleach condition. Each panel represents a different hue term and error bars specify ±1 SEM. The foveal function is bolded and the four peripheral quadrants are denoted by different symbols.

Reproduced with permission of the copyright owner. Further reproduction prohibited without permission.

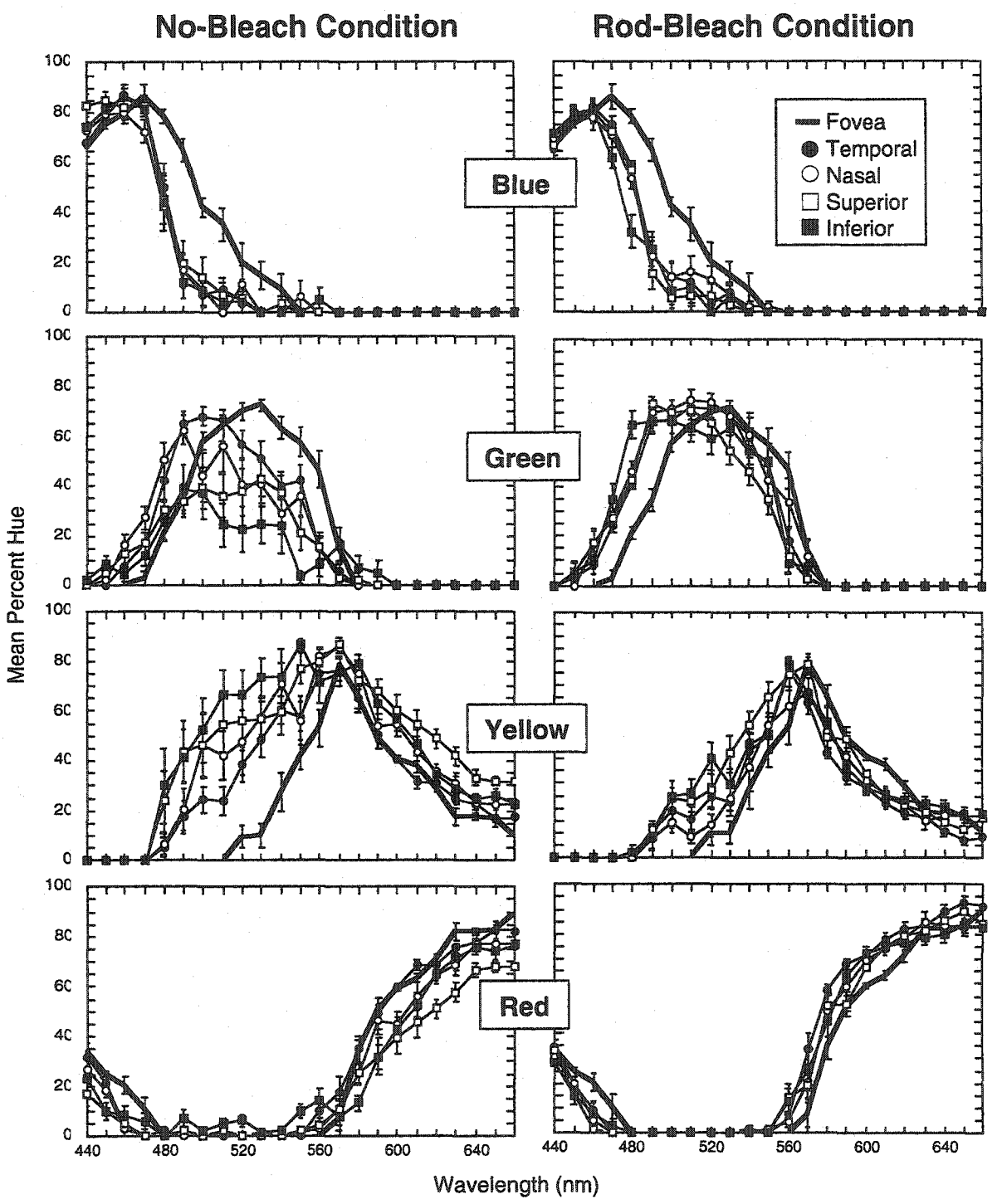

Reproduced with permission of the copyright owner. Further reproduction prohibited without permission.

Overall, functions for the rod-bleach condition are more similar to the foveal function; there is less variability among the four quadrants, particularly for the green and yellow response functions (middle panels). The decrease in blue perception (top panels) and the shifting of the green peak to shorter wavelengths (second panels) is seen in both adaptation conditions.

For the rod-bleach data, the spectral range of percent blue is narrower while the spectral range of percent yellow is broader than in the fovea, as was the case for the no-bleach condition. The broadening of the yellow function, however, is much less pronounced in the rod-bleach condition; the increase in percent yellow for the peripheral retina at wavelengths longer than the foveal peak disappears in the rod-bleach condition.

Lastly, the decrease in the perception of red seen in the no-bleach condition is not found under conditions where rods are minimized (bottom row). In fact, between approximately 600 and 620 nm, slightly more red was reported at the peripheral locations than in the fovea fro the rod-bleach condition.

Effects of Stimulus Size

In figure 3.9, scaled hue responses are plotted as a function of wavelength for each hue term (rows) and for each retinal quadrant (columns) from the no-bleach condition. Different stimulus sizes are denoted by different symbols. In each panel, data from the smallest stimulus size used in that quadrant (0.25° for the temporal and nasal quadrants, and 0.5° for the superior and inferior quadrants) is plotted along with data from the 1° and 5° stimuli (largest stimulus in all quadrants).

Reproduced with permission of the copyright owner. Further reproduction prohibited without permission.

Figure 3.9. Scaled mean hue responses are plotted as a function of wavelength for various stimulus sizes in the unbleach condition. Each column represents a different retinal location, each row a different hue term. In each panel, the smallest and largest stimuli sizes are plotted along with data from the 1° stimulus. For the temporal and nasal retinas, different symbols denote the 0.25°, 1°, and 5° stimulus sizes. For the superior and inferior retinas, different symbols denote the 0.5°, 1°, and 5° stimulus sizes. Error bars specify ±1 SEM.

Reproduced with permission of the copyright owner. Further reproduction prohibited without permission.

No-Bleach Condition: Scaled Data

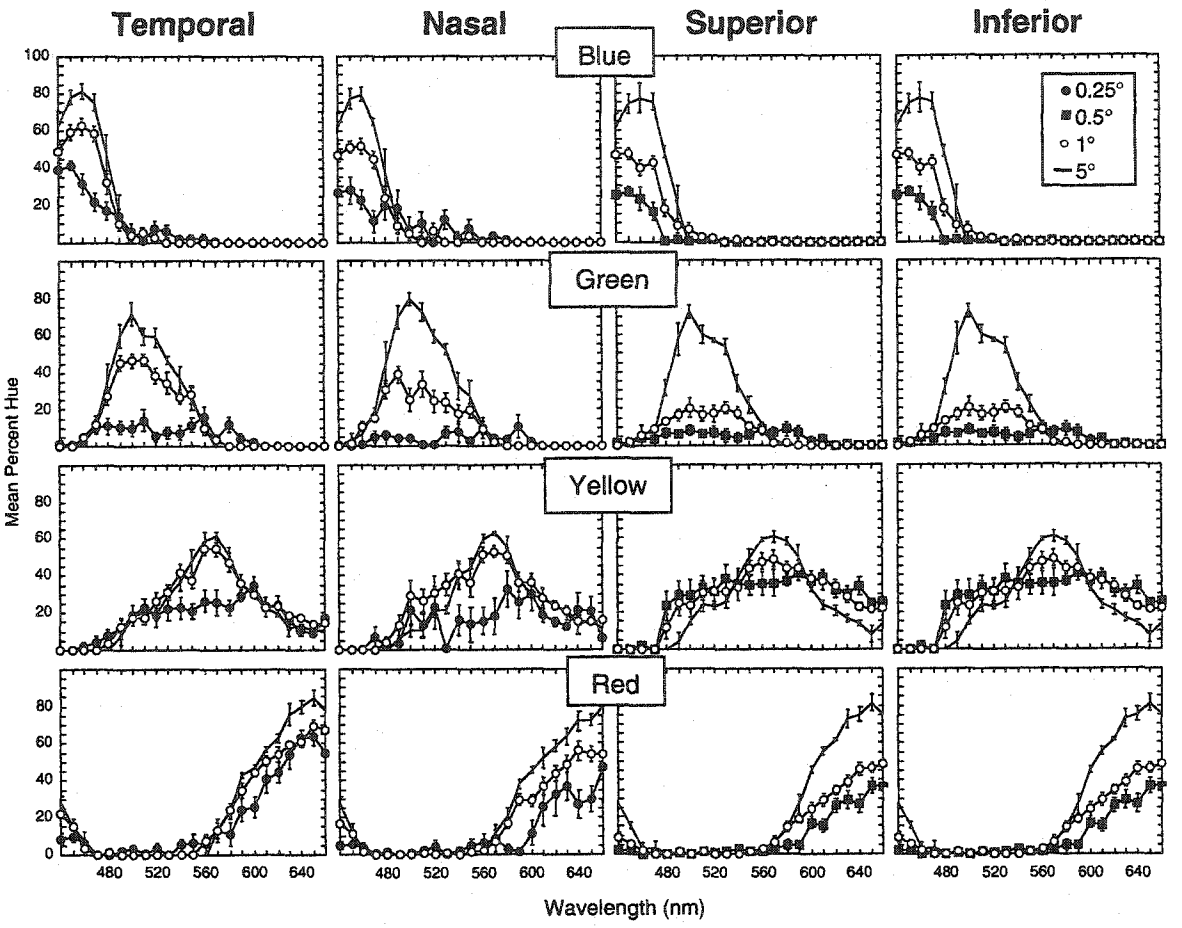

Reproduced with permission of the copyright owner. Further reproduction prohibited without permission.

As predicted from reductions in saturation accompanying smaller field sizes in the no-bleach condition (see figure 3.2), the overall perception of hue decreased as a function of stimulus size in all retinal quadrants. This is especially true for green (second row) where responses to the smallest stimulus size (closed circles) are markedly reduced compared to the largest stimulus size shown (solid line).

The changes in the ratio of assigned hue percentages as a function of decreasing stimulus size are illustrated in figure 3.10, where unscaled hue responses are plotted in the same manner as figure 3.9. Some variations in percent hue with changes in stimulus size are apparent for all hue terms in each of the four retinal quadrants, most notably for green and yellow.

Blue and red (first and last rows) show only slight changes in hue percentages with decreasing stimulus size. Some changes in the spectral range of the perception of blue are apparent. With diminishing field size, the spectral range of blue ends at longer wavelengths than with larger stimuli. The increase in the spectral range of blue with decreasing stimulus size is seen in all retinal quadrants except the superior retina (third column).

Changes in percent hue with decreasing stimulus size were more pronounced for yellow and especially for green (second and third rows). The green response functions for the 0.25° stimulus in the temporal and nasal retinas and the 0.5° stimulus in the superior and inferior retinas elucidate the change in percent green. This effect is especially pronounced in the superior and inferior retinas (third and fourth columns). It also appears that the spectral range of percent green extends to longer wavelengths with smaller field sizes. The yellow functions vary less with stimulus size than the green

Reproduced with permission of the copyright owner. Further reproduction prohibited without permission.

Figure 3.10. Unscaled hue responses plotted as a function of wavelength for various stimulus sizes in the no-bleach condition. Data are plotted as in Figure 3.9.

Reproduced with permission of the copyright owner. Further reproduction prohibited without permission.

No-Bleach Condition: Unscaled Data

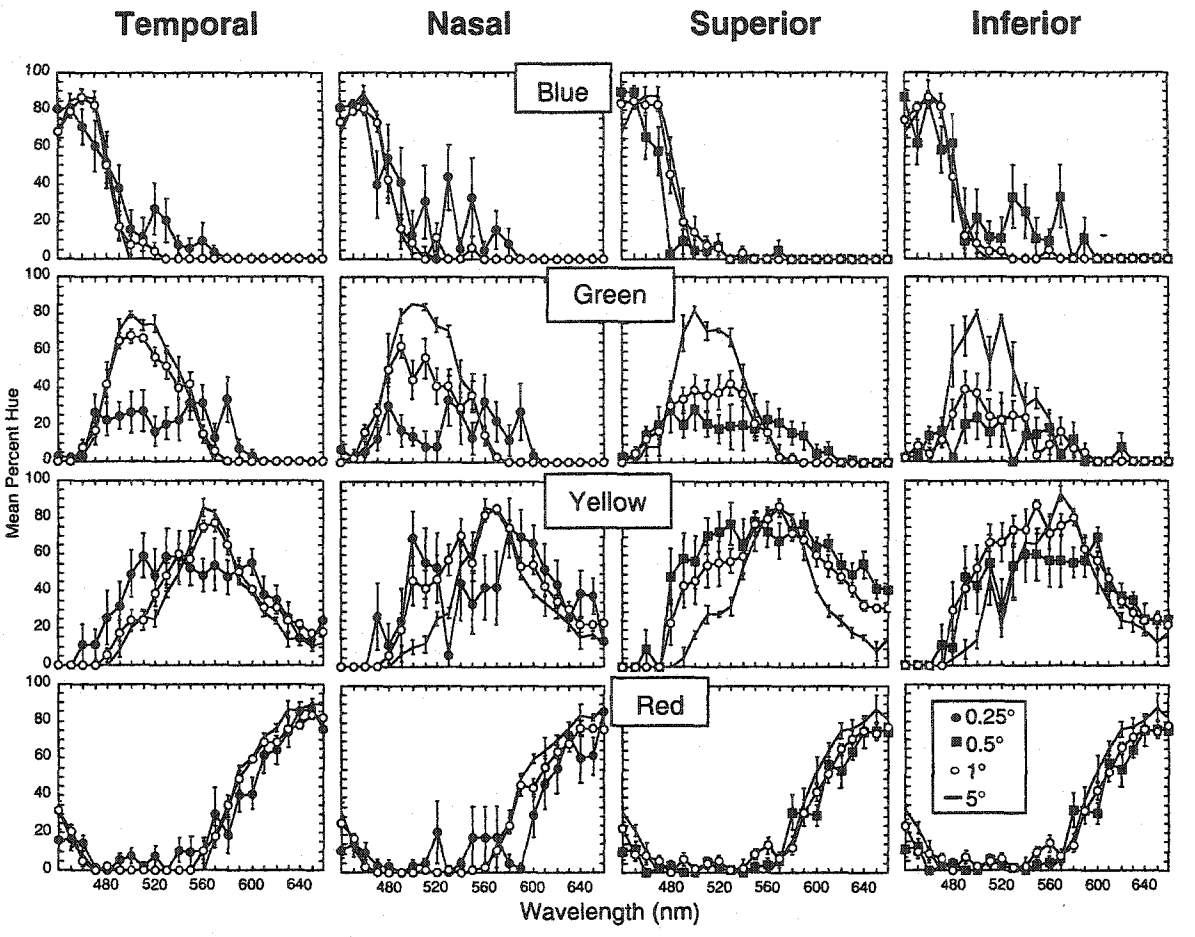

Reproduced with permission of the copyright owner. Further reproduction prohibited without permission.

functions. More yellow was reported at wavelengths above and below the peak of the yellow function at smaller stimulus sizes.

Figure 3.11 is plotted in the same manner as figure 3.9 except for scaled data from the rod-bleach condition. Again, each panel plots data from the smallest stimulus size used in that quadrant (0.098° for the temporal retina, 0.125° for the nasal and superior quadrants, and 0.25° for the inferior quadrant) along with data from the 1° and 3° stimuli (largest stimulus size shown in all quadrants). Several of the same patterns are observed for the scaled rod-bleach data as for the scaled no-bleach data. Decreases in hue perception with reductions in stimulus size are apparent for all four hue terms, most notably for green, yellow, and red.

Any changes in the ratio of assigned hue percentages as a function of decreasing stimulus size are illustrated with unscaled values for the rod-bleach condition in figure 3.12. By far, the most well-preserved hue term with decreases in stimulus size is blue (top row). Consequently, at shorter wavelengths, where both red and blue are used to describe an observer's hue perception, the ratio of the hue perception does not change. While the spectral range of the perception of blue extends to longer wavelengths with decreasing field size, there is little to no reduction in percent blue at the smaller stimulus sizes. Surprisingly, the hue term red is less preserved at smaller stimulus sizes than in the no-bleach condition, but this is most notable for the longer wavelengths and not the shorter wavelengths. Hue percentages at the smallest stimulus size for red are markedly reduced compared to data from the 3° field size, indicating a related increase in the percent yellow.

Reproduced with permission of the copyright owner. Further reproduction prohibited without permission.

Figure 3.11. Scaled hue responses are plotted as a function of wavelength for various stimulus sizes in the rod-bleach condition. Each column represents a different retinal location, each row a different hue term. In each panel, the smallest and largest stimulus sizes are plotted along with data from the 1° stimulus. For the temporal retina, different symbols denote the 0.098°, 1°, and 3° stimulus sizes. For the nasal and superior retinas, different symbols denote the 0.125°, 1°, and 3° stimulus sizes. For the inferior retina, different symbols denote the 0.25°, 1°, and 3° stimulus sizes. Error bars specify ±1 SEM.

Reproduced with permission of the copyright owner. Further reproduction prohibited without permission.

Rod-Bleach Condition: Scaled Data

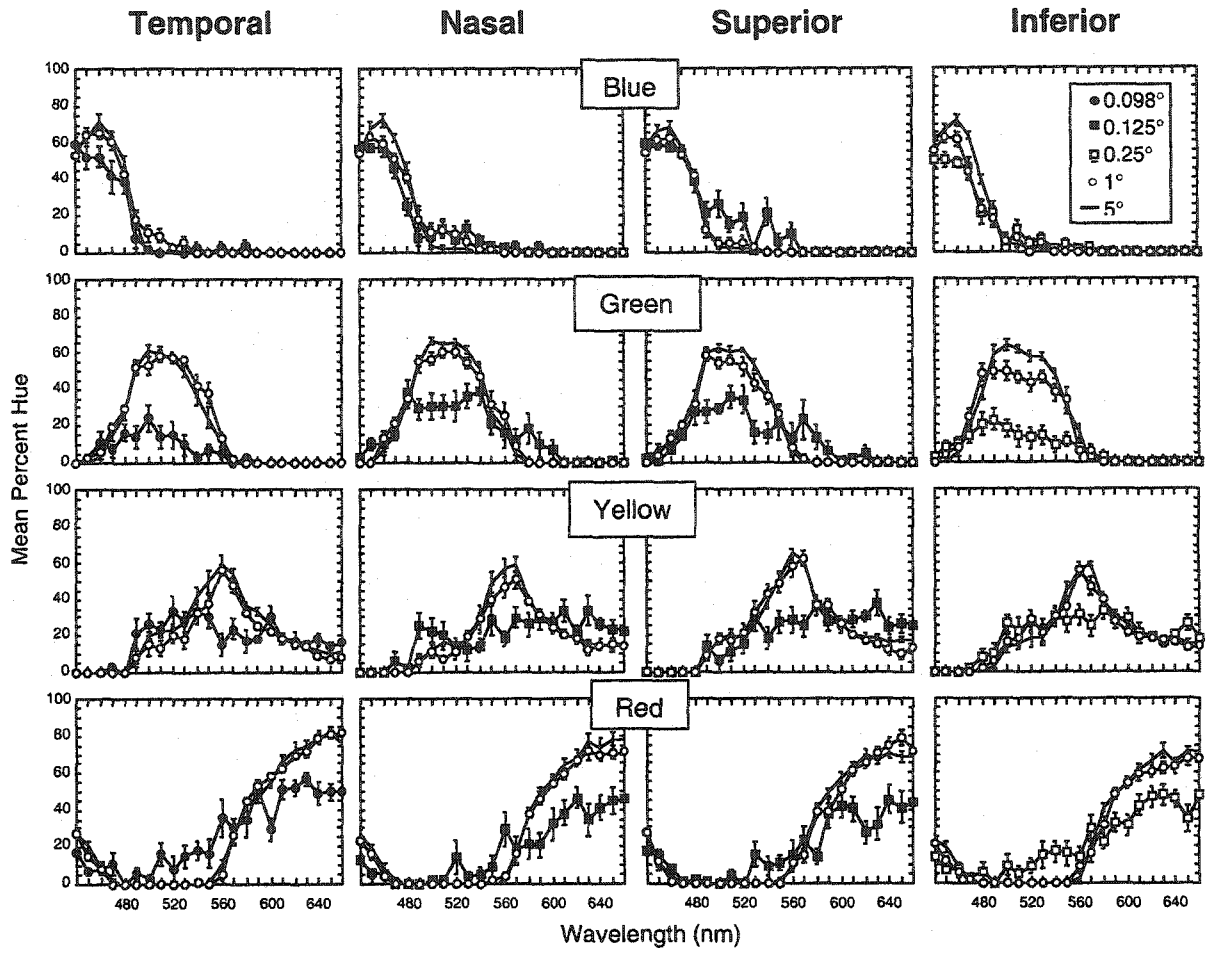

Reproduced with permission of the copyright owner. Further reproduction prohibited without permission.

Figure 3.12. Unscaled hue responses plotted as a function of wavelength for various stimulus sizes in the rod-bleach condition. Data are plotted as in Figure 3.11.

Reproduced with permission of the copyright owner. Further reproduction prohibited without permission.

Rod-Bleach Condition: Unscaled Data

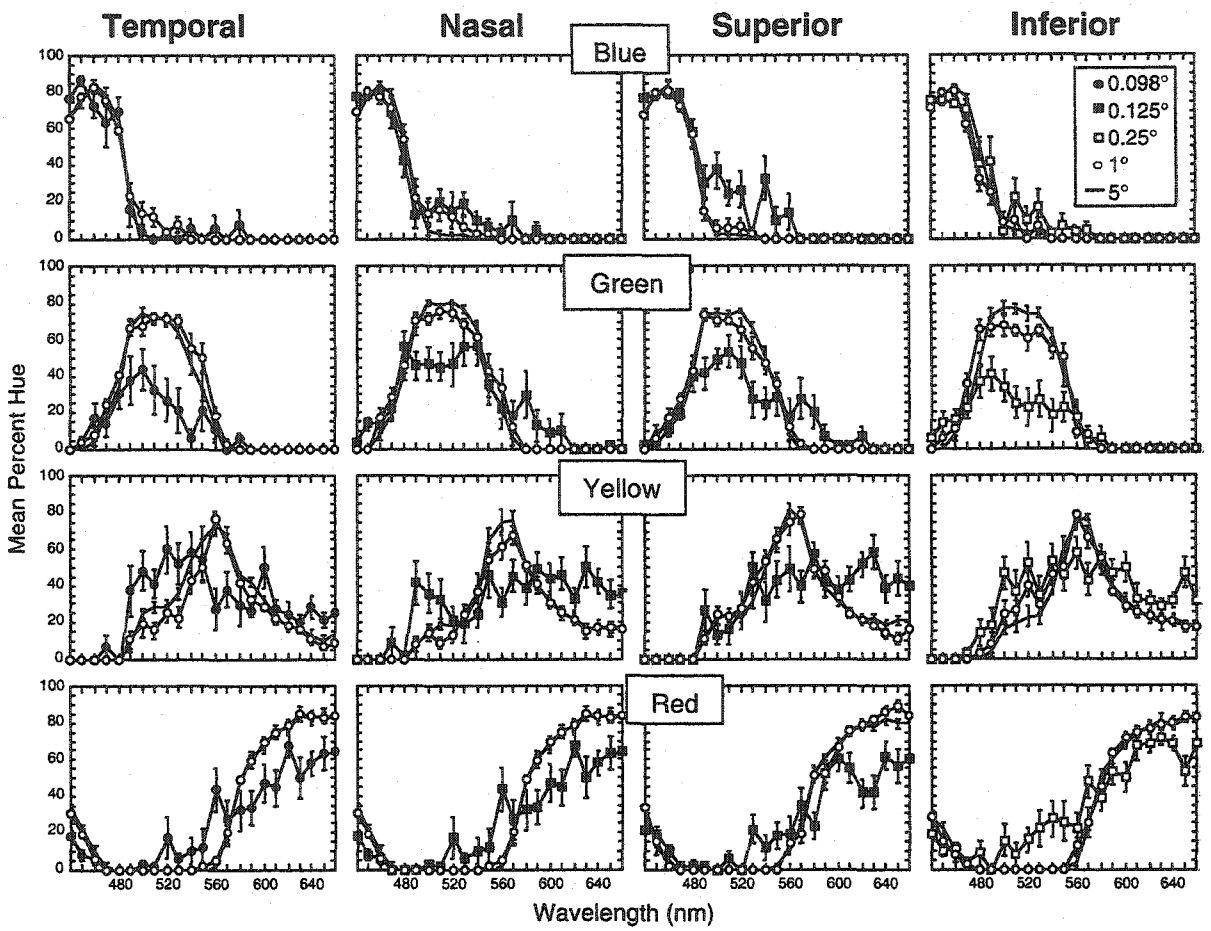

Reproduced with permission of the copyright owner. Further reproduction prohibited without permission.

As was the case in the no-bleach condition, decreasing stimulus size has a large effect on green (second row). Hue responses to the smallest stimulus size are reduced, but to a lesser extent as compared to the no-bleach condition (figure 3.9). Whereas green was, by far, the most affected hue in the no-bleach condition, data for green from the rod-bleach condition show reductions. Thus, there is a change in the ratio of hue percents assigned to green and yellow with decreasing stimulus size.

Reproduced with permission of the copyright owner. Further reproduction prohibited without permission.

Chapter 4

Results: Perceptive Field Sizes

The field size required to elicit maximal hue responding was calculated for each color term at each wavelength for both the rod-bleach and no-bleach conditions using group mean scaled data. Perceptive fields were calculated for conditions that met three criteria: 1) non-zero responses were available at all stimulus sizes, 2) percentages assigned for each stimulus size exceeded the value of the average SEM across stimulus sizes, and 3) data were obtained from at least two of the three observers. The first two criteria were also used by Abramov et al. (1991).

Effects of Stimulus Size

To quantify the growth in hue responses with changes in stimulus size, the Michaelis-Menton function (%hue = (g*diam)/(k+diam) was fitted to the data (Abramov et al., 1991). This is a mathematically-convenient function that has two parameters, k and g, which are shown for a sample function in figure 4.1. The function's asymptotic value is defined by g (%) and any further increases in stimulus size will not affect this value. k is the stimulus size where the function reaches half of its asymptote, or 0.5g, and 3k is the stimulus size where the function reaches 75% of its asymptotic value, i.e., 0.75g. As in Abramov et al. (1991), 3k is operationally defined as the critical size for a

Reproduced with permission of the copyright owner. Further reproduction prohibited without permission.

Figure 4.1. Parameters of a sample Michaelis-Menten function used to quantify the growth in hue responses with changes in stimulus size. g(%) is the function's asymptotic value, k is the stimulus size where the function reaches half of its asymptote, and 3k (the stimulus size where the function reaches 75% of its asymptotic value) is defined as the critical size or where the perceptive field is effectively filled (Abramov et al., 1991).

Reproduced with permission of the copyright owner. Further reproduction prohibited without permission.

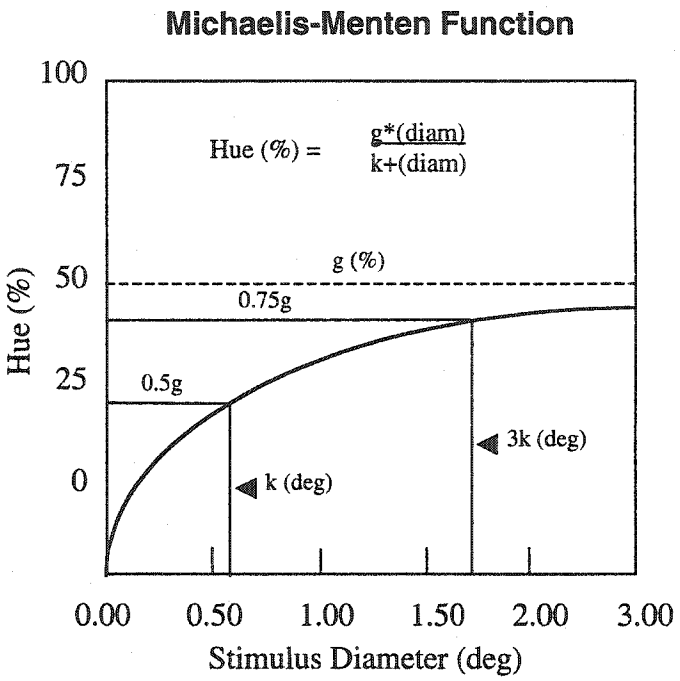

Reproduced with permission of the copyright owner. Further reproduction prohibited without permission.

particular hue mechanism or where the perceptive field is effectively filled. A Michaelis-Menten function was fitted to mean group data meeting the criteria outlined above.

Figure 4.2 shows the effect stimulus size had on hue responses in the no-bleach condition from this study. Mean percent hue is plotted against stimulus size, and all plots are fitted with the Michaelis-Menten growth function for each of the retinal quadrants (columns). Individual panels represent the growth function that had the best fit (highest R value) for each hue term (rows) in each quadrant. In most panels, as stimulus size increases, hue responses correspondingly increase up to an asymptotic value. R-values are indicated in the upper-right-hand corner of each panel and only functions that had positive k-values are displayed.

Similarly, as shown in figure 4.3, hue responses grew to an asymptotic value for all hue terms in all quadrants for the rod-bleach condition. Some notable differences exist between the figures from the rod-bleach and no-bleach conditions. For percent blue (top rows, figures 4.2 & 4.3), functions are flatter in the rod-bleach condition, indicating that the asymptote of the function is reached sooner than in the no-bleach condition. For percent green, the functions for the nasal, superior, and inferior retinas do not reach an asymptote in the no-bleach condition (second row). Only subtle differences between the rod-bleach and no-bleach conditions exist for the fit of the Michaelis-Menten function to the hue responses of yellow and red.

The range and mean of all R-values across wavelength are shown in table 4.1 for all hue terms in the four retinal quadrants for both the no-bleach and rod-bleach conditions. This table includes functions that had a negative k value.

Reproduced with permission of the copyright owner. Further reproduction prohibited without permission.

Figure 4.2. Mean percent hue plotted as a function of stimulus size for each retinal quadrant (columns) and each hue term (rows) in the no-bleach condition. Each plot has been fitted with the Michaelis-Menten growth function that had the highest R-value (best fit) in its hue category. Only functions with positive k-values were included.

Reproduced with permission of the copyright owner. Further reproduction prohibited without permission.

No-Bleach Condition

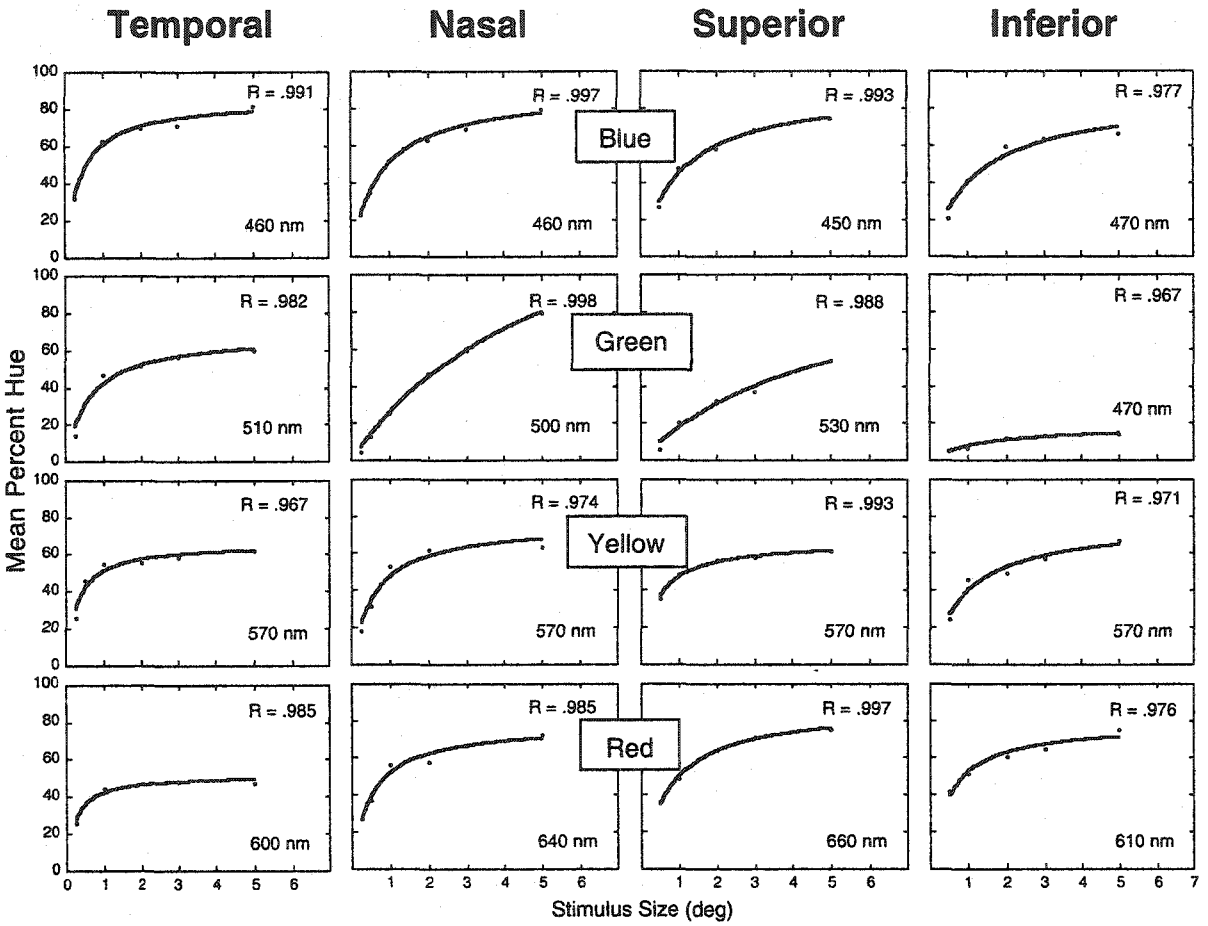

Reproduced with permission of the copyright owner. Further reproduction prohibited without permission.

Figure 4.3. Mean percent hue plotted as a function of stimulus size for each retinal quadrant (columns) and each hue term (rows) in the rod-bleach condition. Each plot has been fitted with the Michaelis-Menten growth function that had the highest R-value (best fit) in its hue category. Only functions with positive k-values were included.

Reproduced with permission of the copyright owner. Further reproduction prohibited without permission.

Rod-Bleach Condition

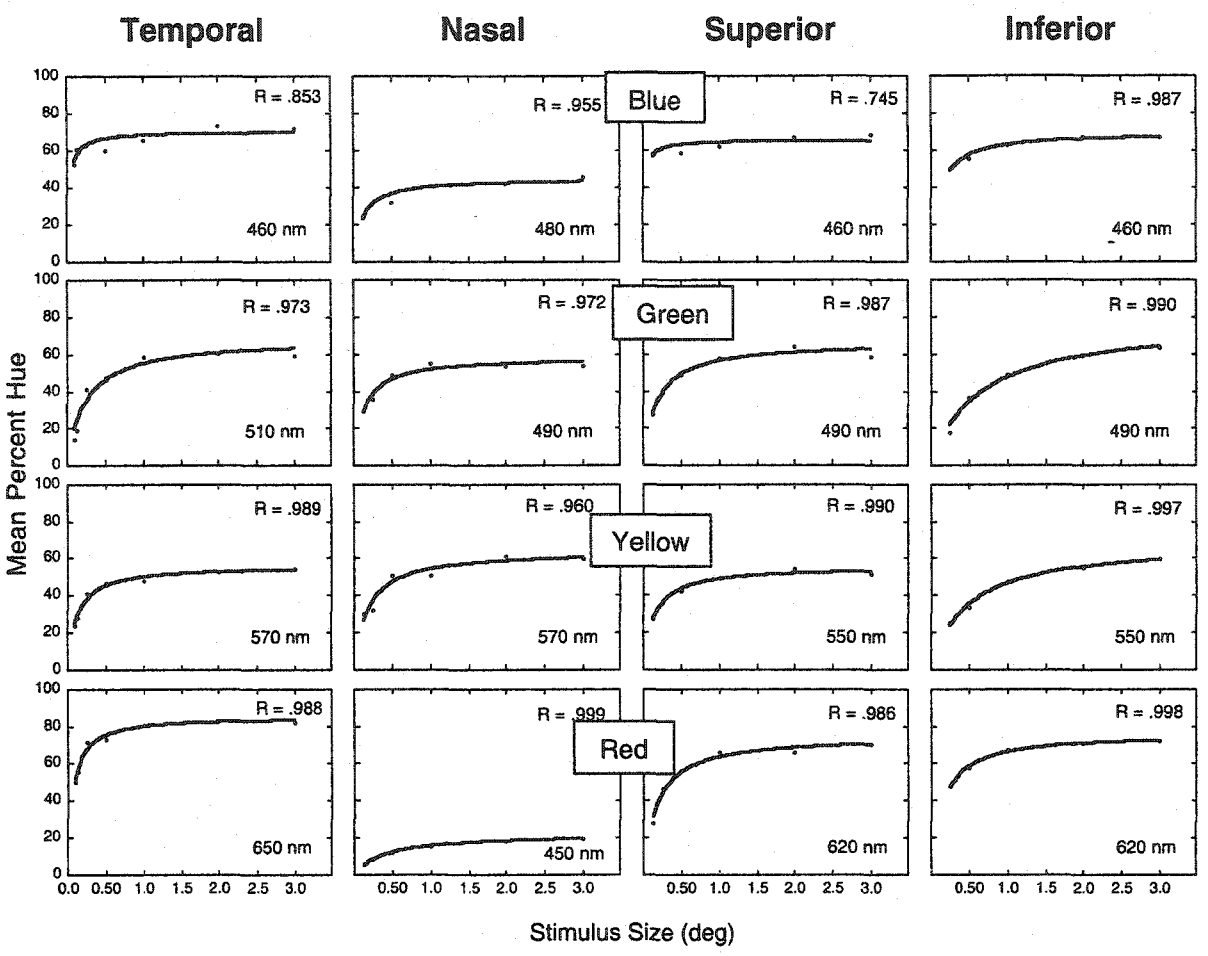

Reproduced with permission of the copyright owner. Further reproduction prohibited without permission.

Table 4.1 Range and mean R values across wavelength.

No-Bleach Condition

Temporal	Blue	Green	Yellow	Red
Range	0.54-0.99	0.23-0.98	0.08-0.97	0.19-0.99
Mean	0.892	0.805	0.530	0.736
Nasal				
Range	0.89-1.00	0.94-1.00	0.14-0.97	0.38-0.99
Mean	0.972	0.971	0.679	0.887
Superior				
Range	0.97-0.99	0.14-0.99	0.25-0.99	0.59-1.00
Mean	0.983	0.815	0.830	0.919
Inferior				
Range	0.87-0.98	0.96-0.97	0.02-0.97	0.43-0.99
Mean	0.953	0.966	0.512	0.911

Rod-Bleach Condition

Temporal	Blue	Green	Yellow	Red
Range	0.33-0.85	0.43-0.97	0.04-0.99	0.02-0.99
Mean	0.673	0.747	0.649	0.784
Nasal				
Range	0.44-0.96	0.09-0.97	0.02-0.98	0.53-1.00
Mean	0.689	0.644	0.686	0.924
Superior				
Range	0.26-0.75	0.32-0.99	0.00-0.99	0.28-0.99
Mean	0.556	0.756	0.581	0.801
Inferior				
Range	0.59-0.99	0.39-0.99	0.22-1.00	0.03-1.00
Mean	0.834	0.855	0.637	0.866

Effects of Adapted State of the Retina

Values of k were obtained for all data fitted with the Michaelis-Menten function that met the criteria outlined above. For most wavelengths, percent hue increased with stimulus size, while for a minority of test wavalengths, percent hue decreased with stimulus size. This was particularly true for the perception of yellow. This pattern produced a negative value for k and can be seen for certain wavelengths in table 4.2. Positive values in table 4.2 should be multiplied by 3 to obtain perceptive field sizes.

Reproduced with permission of the copyright owner. Further reproduction prohibited without permission.

In figure 4.4, mean k values are plotted as a function of wavelength for the no-bleach condition. Each column indicates a different retinal quadrant and each row a different hue term. k values vary with wavelength for all hue mechanisms and quadrants, most notably for green (second row). Among the four retinal locations, the least amount of variability across wavelength is seen in the temporal quadrant (left column).

Mean k values for the rod-bleach condition are illustrated in figure 4.5. A very different trend is observed from the experimental conditions chosen to minimize rod signals; the variability in k values observed with the no-bleach condition disappears, leaving relatively flat functions across wavelength for all hue terms and retinal locations in figure 4.5. The only exception to this is for the perception of green in the inferior retina.

Effects of Retinal Location

In figure 4.6, perceptive field sizes (3k) are shown for the four peripheral locations: 10° temporal, 10° nasal, 10° superior, and 10° inferior. In the left-hand column, data from the no-bleach condition are plotted; in the right-hand column, data from the rod-bleach condition are plotted. Note that the two columns have different scales on the ordinate; and within each column, a different ordinate scale is used for green. In each panel, perceptive field sizes are shown for either blue, green, yellow, or red according to the wavelength that had the approximate maxima for the respective hue term (i.e., the highest g value, bolded in table 4.3).

Reproduced with permission of the copyright owner. Further reproduction prohibited without permission.

Table 4.2. Mean k values for all locations in the no-bleach and rod-bleach conditions.

	No-Bleach Condition				Rod-Bleach Condition			
10° Temporal								
λ	Blue	Green	Yellow	Red	Blue	Green	Yellow	Red
440	0.126			0.486	-0.010			0.057
450	0.234			0.170	-0.007			0.117
460	0.401			0.086	0.029	0.035		
470	0.513	-0.038			0.036	0.059		
480	0.551	0.354			0.080	0.038		
490	0.433	0.708			0.124	0.138	-0.059	
500		1.098	-0.021			0.145	-0.039	
510		0.642	0.051			0.239	-0.025	
520		0.922	0.021			0.187	-0.029	
530		1.136	0.012			0.181	-0.002	
540		0.758	0.099				0.013	
550		0.413	0.175			0.093	0.090	
560		-0.036	0.223				0.237	
570			0.287	0.030			0.118	0.001
580			0.225	0.405			0.064	0.030
590			0.029	0.306			0.033	0.004
600			-0.047	0.219			-0.006	0.043
610			0.003	0.090			-0.019	0.046
620			-0.031	0.078			-0.024	0.041
630			-0.016	0.096			-0.020	0.037
640			0.068	0.048			-0.039	0.056
650			0.014	0.089			-0.040	0.065
660			-0.088	0.111			-0.045	0.052
10° Nasal								
440	0.414			1.616	-0.005			0.275
450	0.587			0.280	0.023			0.421
460	0.770				0.028	-0.009		0.182
470	0.932	0.893			0.043	0.039		
480	0.562	1.262			0.118	-0.010		
490		2.557			0.090	0.130	-0.099	
500		5.496	-0.068			0.198	-0.058	
510			-0.030			0.115	-0.033	
520			-0.039			0.163	-0.001	
530		1.915				0.193	0.008	
540		1.567	0.178			0.061	0.099	
550			0.336			0.055	0.109	
560			0.507			0.023	0.270	
570			0.600	0.170			0.179	
580			0.213				0.048	0.180
590			0.130				0.006	0.184
600			0.038	0.643			-0.006	0.091
610			0.097	0.374			-0.052	0.083
620			0.097	0.323			-0.022	0.071
630			0.111	0.244			-0.074	0.153
640			-0.076	0.490			-0.062	0.104
650			-0.074	0.506			-0.051	0.091
660			0.112	0.234			-0.050	0.089

Reproduced with permission of the copyright owner. Further reproduction prohibited without permission.

	No-Bleach Condition				Rod-Bleach Condition			
			10° Superior					
440	0.713			4.244	-0.009			0.116
450	1.039			4.851	0.010			-0.028
460	1.477	0.598			0.020	0.039		
470	1.780	0.632			0.005	0.050		
480		1.876			0.025	0.027		
490		3.302				0.172	-0.033	
500		4.030	-0.250			0.176	0.062	
510		4.412	-0.139			0.155	0.057	
520		3.815	-0.175			0.188	0.013	
530		5.093	-0.122			0.174	-0.004	
540			0.082			0.098	0.148	
550		1.803	0.252			0.010	0.132	
560		0.057	0.399			-0.047	0.187	-0.064
570			0.396	0.824			0.160	-0.019
580			0.320	0.679			0.003	0.271
590			0.047	1.444			0.011	0.080
600			-0.054	1.199			-0.011	0.090
610			-0.179	1.575			-0.041	0.093
620			-0.159	1.003			-0.052	0.171
630			-0.198	1.112			-0.226	0.168
640			-0.280	1.062			-0.053	0.112
650			-0.245	0.856			-0.057	0.104
660			-0.209	0.742			-0.050	0.087
			10° Inferior					
440	0.443			2.410	0.048			0.211
450	1.023			3.101	0.104			0.333
460	0.821				0.143	-0.078		-0.053
470	1.188	1.342			0.131	0.066		
480	1.128				0.340	0.174		
490			-0.223		-0.046	0.364		
500		3.973	-0.070			0.641	-0.129	
510			0.064			0.591	-0.092	
520			0.172			0.746	-0.049	
530			0.098			1.200	-0.035	
540			0.224			1.357	-0.033	
550			0.359			0.510	0.127	
560		9.837	0.526			0.877	0.240	
570			0.941				0.473	-0.114
580			0.573	0.269			0.046	0.166
590			0.367	0.777			0.018	0.142
600			0.036	1.148			-0.052	0.179
610			0.080	0.495			-0.009	0.135
620			0.079	0.588			-0.029	0.131
630			0.044	0.457			0.016	0.120
640			0.105	0.246			-0.045	0.127
650			0.006	0.488			-0.129	0.210
660			0.062	0.463			-0.055	0.151

Reproduced with permission of the copyright owner. Further reproduction prohibited without permission.

Figure 4.4. Mean k (deg) values plotted as a function of wavelength for the no-bleach condition. Each column indicates a different retinal quadrant and each row a different hue term.

Reproduced with permission of the copyright owner. Further reproduction prohibited without permission.

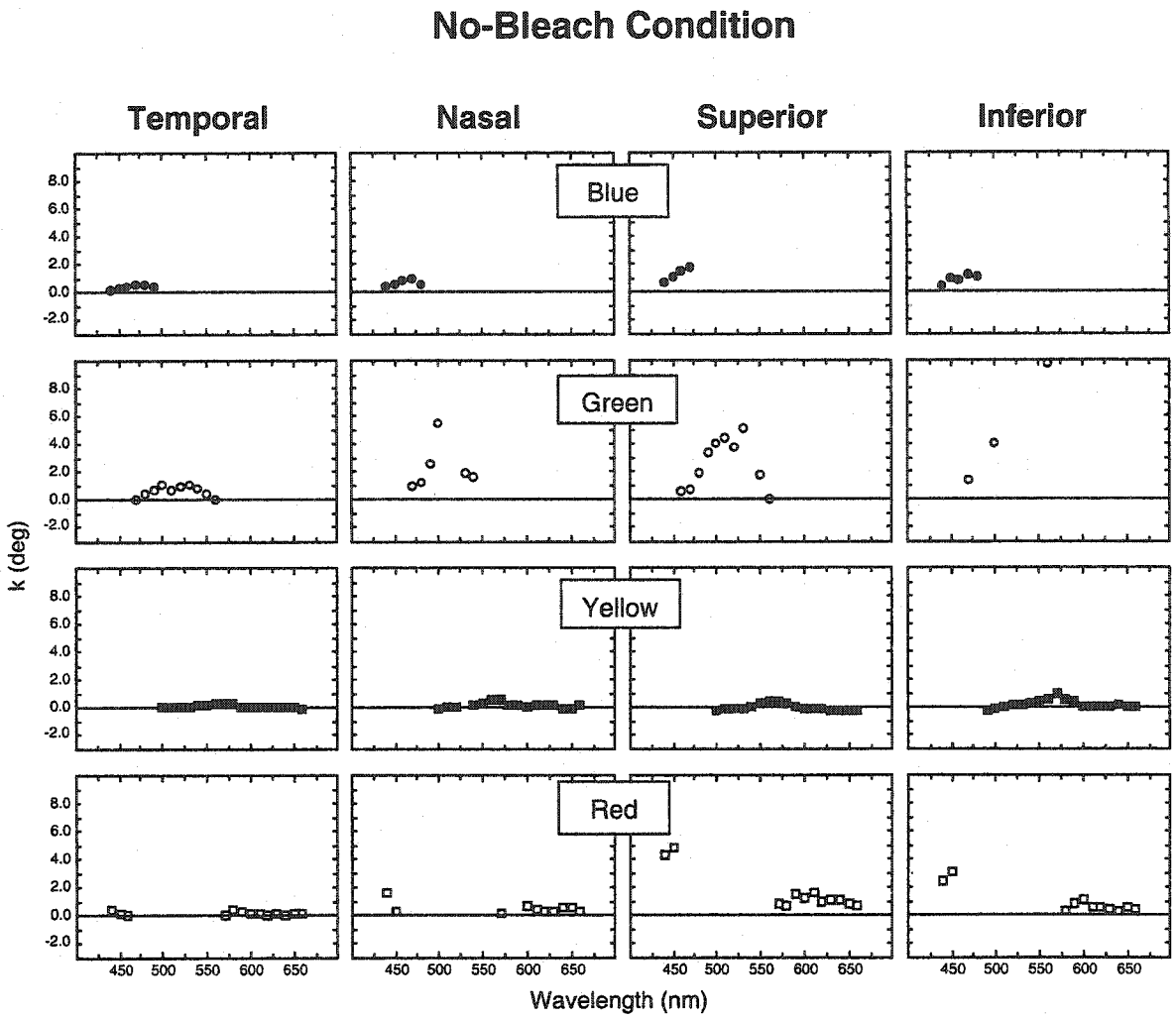

Reproduced with permission of the copyright owner. Further reproduction prohibited without permission.

Figure 4.5. Mean k (deg) values plotted as a function of wavelength for the rod-bleach condition. Each column indicates a different retinal quadrant and each row a different hue term.

Reproduced with permission of the copyright owner. Further reproduction prohibited without permission.

Rod-Bleach Condition

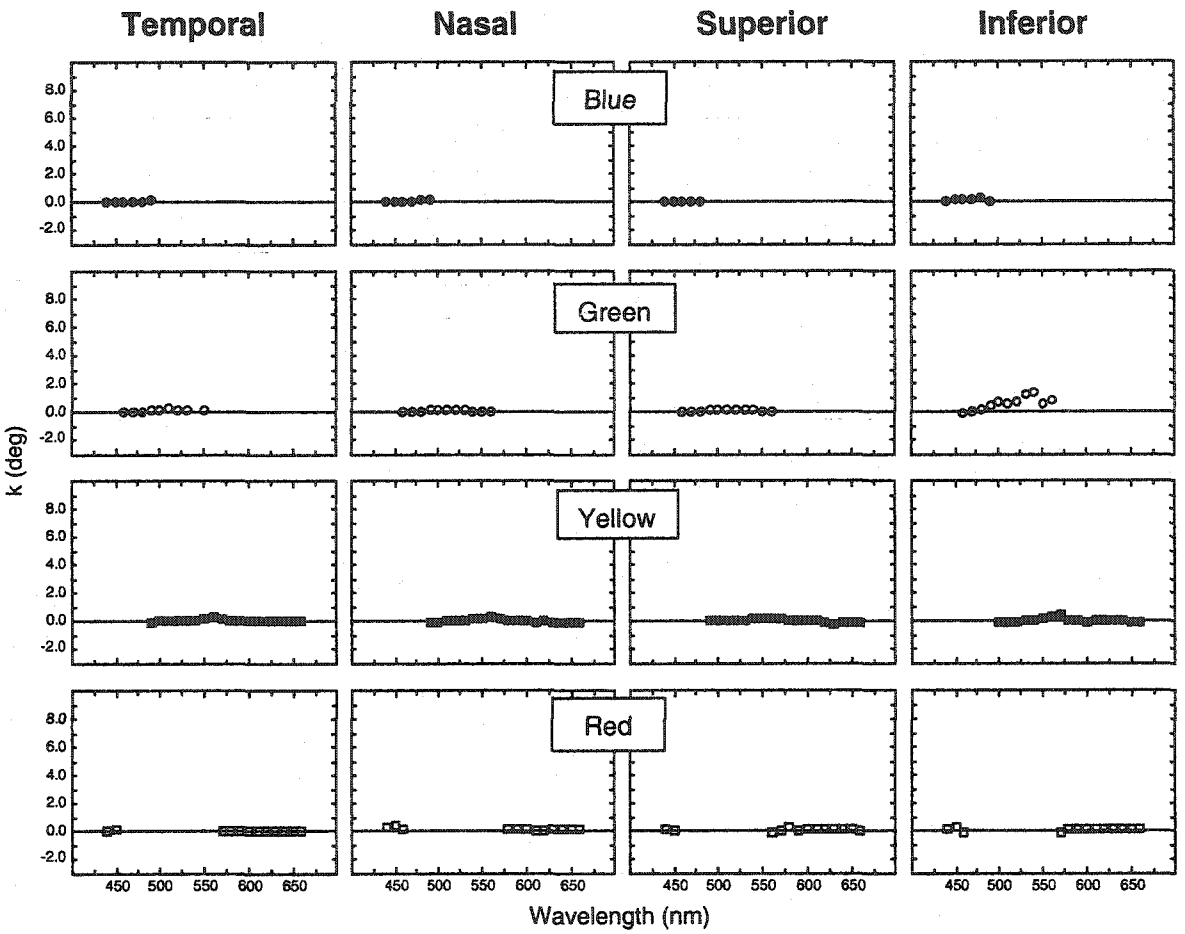

Reproduced with permission of the copyright owner. Further reproduction prohibited without permission.

Figure 4.6. Perceptive field sizes (3k) plotted as a function of the four peripheral locations: temporal, nasal, superior, and inferior. In the left-hand column, data from the no-bleach condition are shown, in the right-hand column, data from the rod-bleach condition are displayed. Note that the two columns have different scales on the ordinate and within each column; a different scale is used for green. Each row represents data for a different hue term.

Reproduced with permission of the copyright owner. Further reproduction prohibited without permission.

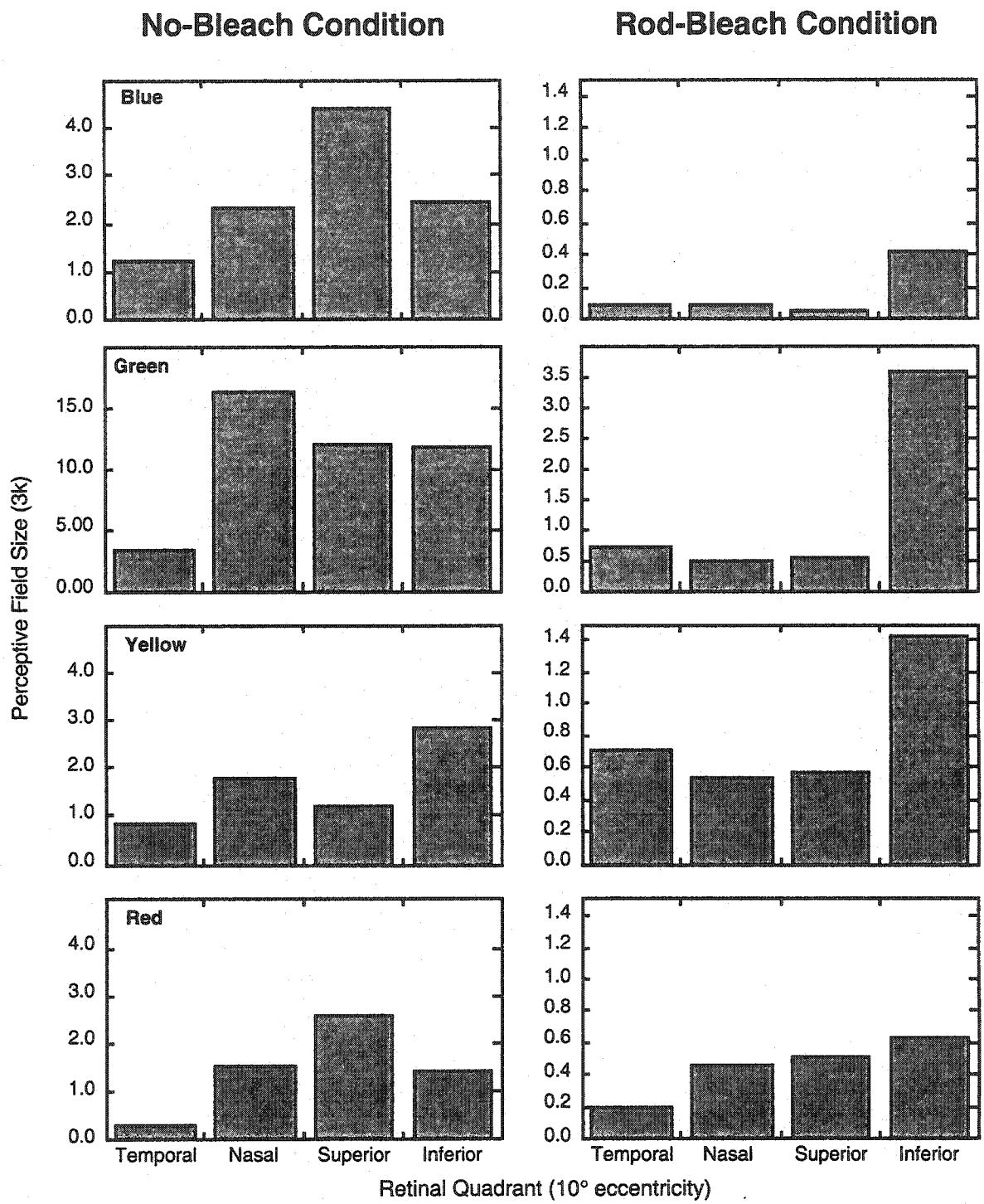

Reproduced with permission of the copyright owner. Further reproduction prohibited without permission.

Table 4.3. Mean g values for all locations in the no-bleach and rod-bleach conditions.

No-Bleach Condition — **10° Temporal**

λ	Blue	Green	Yellow	Red
440	58.259			30.625
450	74.720			16.380
460	**84.699**			6.024
470	83.312	9.819		
480	53.739	34.754		
490	20.713	66.103		
500		**82.640**	19.462	
510		68.727	18.818	
520		70.044	23.433	
530		64.127	29.919	
540		46.169	37.558	
550		30.616	47.608	
560		13.006	59.441	
570			**65.533**	15.836
580			51.968	30.254
590			36.212	44.902
600			29.692	51.400
610			23.532	56.381
620			20.921	59.786
630			16.352	69.409
640			16.118	70.507
650			12.289	**79.313**
660			11.641	77.364

Rod-Bleach Condition — **10° Temporal**

λ	Blue	Green	Yellow	Red
440	54.73			27.83
450	63.54			19.70
460	**70.09**	7.10		
470	62.43	16.20		
480	45.77	33.50		
490	17.90	59.68	8.76	
500		65.49	16.21	
510		**68.21**	18.65	
520		63.60	22.08	
530		57.14	25.22	
540			34.39	
550		30.41	47.78	
560			**67.85**	
570			55.78	25.42
580			36.83	44.26
590			31.05	48.31
600			23.67	58.48
610			18.24	66.79
620			15.00	73.03
630			13.93	75.85
640			11.57	81.50
650			9.77	**84.83**
660			9.10	82.87

10° Nasal

440	66.996			36.170
450	82.782			12.255
460	**89.142**			
470	80.112	23.376		
480	44.125	56.164		
490		105.650		
500		**168.100**	18.266	
510			16.506	
520			20.515	
530		78.749		
540		49.961	39.736	
550			47.923	
560			68.294	
570			**75.618**	9.424
580			57.422	
590			43.704	
600			33.500	51.464
610			28.395	55.738
620			25.439	60.408
630			22.066	62.808
640			16.356	77.175
650			14.922	**81.525**
660			15.280	74.196

54.79			30.40
64.94			22.15
66.70	9.08		6.43
57.38	19.48		
44.81	33.26		
20.74	58.46	5.16	
	67.20	12.74	
	66.10	12.77	
	67.34	14.31	
	63.93	20.14	
	43.44	35.90	
	30.69	46.63	
	22.41	61.66	
		63.79	
		42.41	40.62
		33.40	51.52
		25.65	57.43
		19.29	64.04
		18.40	68.36
		13.87	**80.20**
		13.08	78.06
		13.51	78.11
		12.91	78.42

Reproduced with permission of the copyright owner. Further reproduction prohibited without permission.

	No-Bleach Condition				Rod-Bleach Condition			
	10° Superior							
440	72.574			51.589	55.44			27.23
450	90.212			31.301	64.58			10.97
460	**101.220**	10.672			**65.49**	11.21		
470	99.610	16.261			54.37	20.61		
480		49.512			40.61	33.39		
490		105.120				**66.24**	12.52	
500		**135.210**	15.030			65.19	20.79	
510		119.920	24.343			62.05	21.26	
520		107.110	21.266			62.98	23.81	
530		107.340	28.787			54.93	27.86	
540			39.529			38.49	45.48	
550		31.824	53.272			24.87	55.13	
560		9.401	**66.412**			9.37	**69.95**	7.27
570			65.960	13.487			65.25	16.28
580			58.947	22.660			41.48	43.99
590			44.743	43.401			33.75	45.48
600			33.512	58.740			27.36	56.34
610			26.005	76.654			20.23	65.74
620			23.068	75.208			18.49	74.23
630			18.544	87.156			2.76	**76.89**
640			15.094	90.280			15.30	76.57
650			13.232	**91.087**			14.70	75.64
660			15.131	87.012			15.38	74.49
	10° Inferior							
440	67.347			40.832	58.44			26.02
450	91.481			29.360	69.23			17.17
460	**92.503**				**73.24**	7.07		5.64
470	86.325	18.324			62.63	19.71		
480	48.679				41.55	43.99		
490			8.760		16.61	66.22		
500		**124.560**	15.284			77.94	12.91	
510			26.973			74.25	14.04	
520			26.853			71.62	22.07	
530			31.389			**83.42**	22.28	
540			39.965			73.40	28.52	
550			52.094			41.37	41.06	
560		47.553	64.372			22.92	60.24	
570			**76.356**				**68.31**	16.63
580			66.254	17.821			39.43	40.05
590			50.888	36.692			30.26	50.56
600			35.110	55.111			22.73	59.27
610			30.295	55.395			20.59	65.24
620			23.814	65.651			17.79	68.40
630			20.236	69.806			16.69	71.44
640			17.814	68.886			15.42	71.89
650			14.907	77.913			12.14	**77.76**
660			16.183	**77.957**			14.00	76.00

Reproduced with permission of the copyright owner. Further reproduction prohibited without permission.

In the no-bleach condition (left-hand column), perceptive field sizes were smallest in the temporal retina for all four hue terms. This pattern was not found in the rod-bleach condition (right-hand panel). While perceptive fields were largest in the inferior retina for all four hue terms in the rod-bleach condition, there was no consistency among the other three quadrants as to which had the largest and smallest perceptive field size for any particular hue term.

Effects of Hue Term

In figure 4.7, data are replotted from figure 4.6 to better illustrate variation in perceptive field sizes among hue terms. 3k values are plotted as a function of the four hue terms: blue, green, yellow, and red. The left-hand column presents the no-bleach condition and the right-hand column the rod-bleach condition. Note that the two columns have different scales on the ordinate. Each row is data from a different retinal quadrant. In each panel, perceptive field sizes are plotted for either the temporal, nasal, superior, or inferior retina according to the wavelength that had the approximate maximum for the respective hue category (bolded values in table 4.3).

At all retinal locations in the no-bleach condition, green had the largest perceptive field, i.e., stimulus sizes were much larger when the green function reached its asymptote compared to the other three hue terms within the no-bleach condition. Red had the smallest perceptive field in all but the superior retina, where yellow was the smallest. In the rod-bleach condition (right-hand column), the size of the perceptive field was smallest for blue in all four retinal quadrants. The perceptive field size for green was largest in the inferior retina by a factor of four compared to the other retinal locations.

Reproduced with permission of the copyright owner. Further reproduction prohibited without permission.

Figure 4.7. Perceptive field sizes (3k) plotted as a function of the four hue terms: blue, green, yellow, and red. In the left-hand column, data from the no-bleach condition are shown, in the right-hand column, data from the rod-bleach condition are displayed. Note that the two columns have different scales on the ordinate. Each row represents data from a different retinal quadrant.

Reproduced with permission of the copyright owner. Further reproduction prohibited without permission.

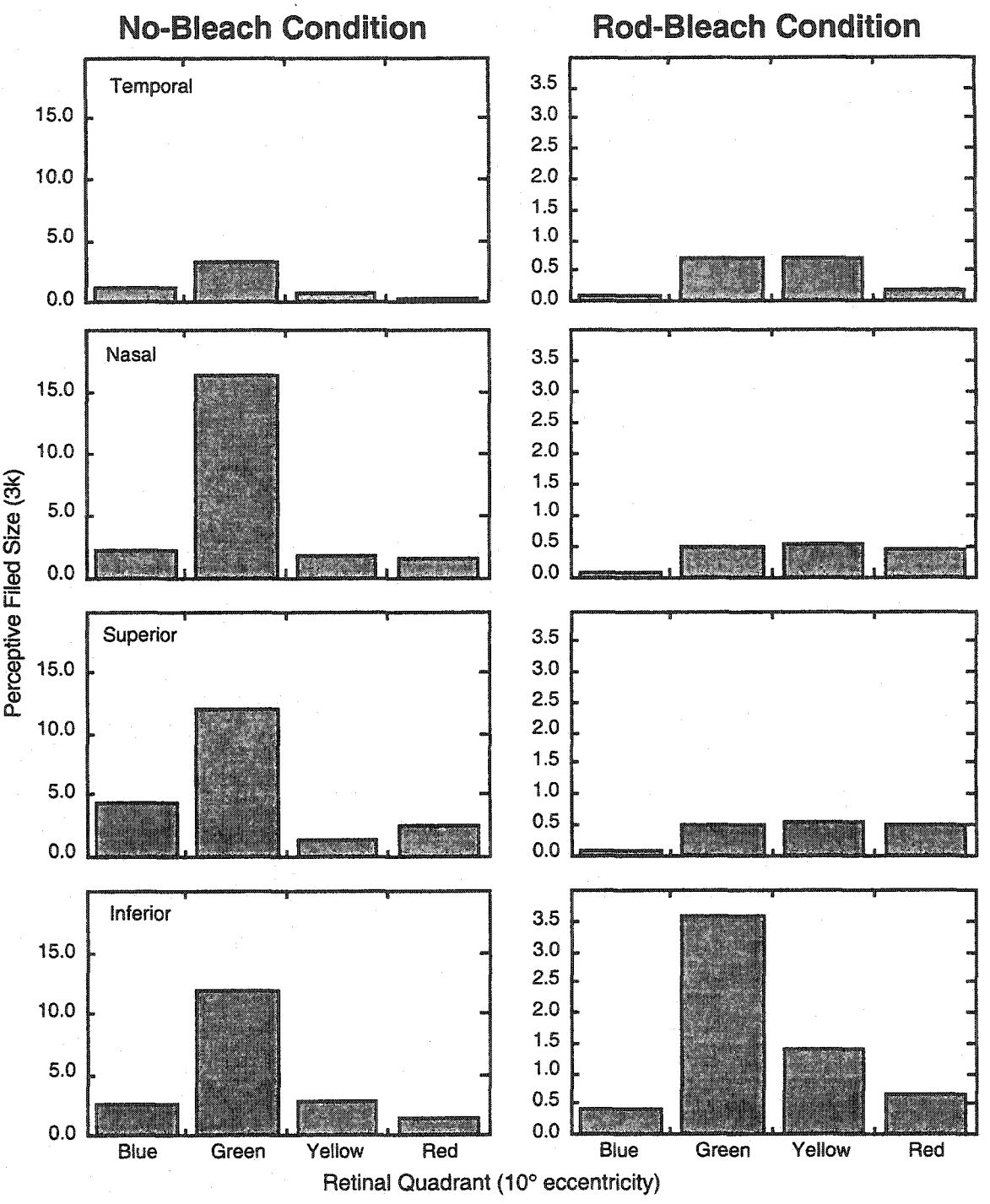

Reproduced with permission of the copyright owner. Further reproduction prohibited without permission.

Chapter 5

Discussion

The goal of the current study was to assess the effects of rod photoreceptors on the sizes of perceptive fields in the peripheral retina. Measurements were made in the fovea and in the four retinal quadrants (temporal, nasal, superior, and inferior) at 10° eccentricity. At these locations, hue and saturation responses were recorded for a series of wavelengths ranging from 440-660 nm in 10 nm steps. At the peripheral locations, various stimulus sizes were tested under conditions of light and dark adaptation, the rod-bleach and no-bleach conditions, respectively. Perceptive fields were calculated by fitting the Michaelis-Menten growth function to plots of hue percentage across stimulus size. Results were analyzed for the effects of rods, stimulus size, and retinal location.

Rod Effects on Color Appearance

Saturation

One of the most profound effects that rods had on color appearance was a decrease in saturation. For three of the four retinal quadrants, colors measured following 30 min of dark adaptation were less saturated across the entire spectrum, with the greatest effect in the short-wavelength region of the spectrum (see figure 3.1). This short-wavelength effect was absent in the rod-bleach condition (figure 3.3). Thus, it appears

Reproduced with permission of the copyright owner. Further reproduction prohibited without permission.

that rods contribute an achromatic percept to color appearance; and the effect is largest at short wavelengths.

These findings are consistent with previously-conducted studies in the peripheral retina. Boynton et al. (1964), who measured color-naming and saturation functions at 0°, 20°, and 40° in the temporal retina, found that saturation decreased in the periphery; and the effect was greatest at shorter wavelengths for at least one of their observers (MN). Hunt (1952) investigated color appearance of a 20° test field under conditions of light and dark adaptation, or where cone and rod signals are maximized, respectively. He used a dichoptic color-matching technique where the right and left eyes were under different states of adaptation. He found that as the illuminance of the adapting field decreased, so did the saturation of the superimposed test field. While Hunt identified "spilling over" of responses between nerve fibers as a possible source of the desaturation, he also mentioned rods as a potential desaturating factor in the retina.

Studies by Stabell and Stabell, using asymmetric color-matching and absolute threshold techniques (1975, 1976a), demonstrated that rods add an achromatic component to color perception. They reported that the saturation of colors was greatly reduced following 30 min of dark adaptation at 6° and 7.5° in the temporal retina compared to the fovea and that the amount of desaturation increased from 2.5° to 7.5°, as the number of rod receptors increased.

Gordon and Abramov (1977) and Abramov et al.'s (1991) findings also support those of the present study. Using similar methodologies to this study, they found that color perception at 45° eccentricity in the nasal retina and at 10° eccentricity in the temporal and nasal retinas was less saturated than in the fovea. They also reported that

Reproduced with permission of the copyright owner. Further reproduction prohibited without permission.

saturation continued to decrease as distance from the fovea increased. It is quite possible that the desaturation seen in Abramov et al.'s study is due to rod influences since their stimuli were presented at mesopic intensities (where both rods and cones are responding). The same reasoning cannot be applied to Gordon and Abramov's data since their intensity level was above the saturation level of rods (Stabell & Stabell, 1977; Nagy & Doyal, 1993). Although not discussed specifically by Abramov et al. and Gordon and Abramov, their results show that the desaturation effect at 10° was more substantial at shorter than at longer wavelengths.

Why rods should have a larger effect on wavelengths at the shorter end of the spectrum cannot be explained by spectral sensitivity alone. Rod photoreceptors are most sensitive to wavelengths around 510 nm. This is illustrated in figure 5.1 where rod spectral efficiency is plotted as a function of wavelength (Wyszecki & Stiles, 1982). One might conclude that any desaturation effect attributed to rods should be maximal around 510 nm since this is where the luminous efficiency function peaks. In fact, colors at 510 nm did appear less saturated than longer wavelengths (see figure 3.1); however, wavelengths shorter than 510 nm, where the sensitivity of rod photoreceptors is decreasing, appeared even less saturated.

Another possible explanation for the decrease in saturation with short-wavelength stimuli is that signals from rods might differentially effect the three cone types. As discussed previously, rods have no direct connection to ganglion cells and have been shown to share pathways with cones by converging onto cells higher in the visual pathway and through gap junctions in the outer nuclear layer of the retina (Daw, et al.,

Reproduced with permission of the copyright owner. Further reproduction prohibited without permission.

Figure 5.1. Rod spectral luminous efficiency function (V'λ) defining the standard scotopic observer (Wyszecki & Stiles, 1982).

Reproduced with permission of the copyright owner. Further reproduction prohibited without permission.

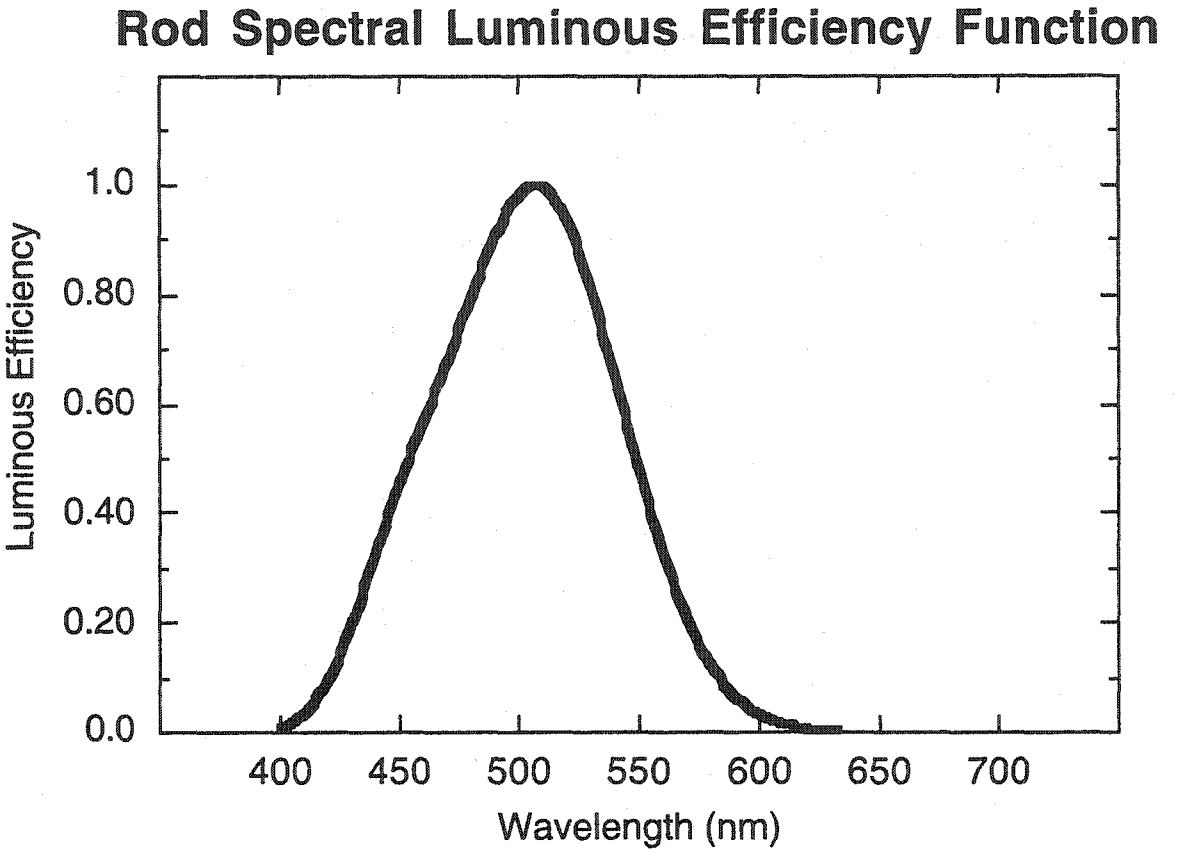

Reproduced with permission of the copyright owner. Further reproduction prohibited without permission.

1990; Wässle et al., 1991; Raviola & Gilula, 1973). Considering the area of the spectrum that is most affected, the decrease in saturation at the shorter wavelengths might be explained by rods interacting preferentially with the signals from the S cones. While anatomical evidence does support the idea that rods and S cones share a common neural pathway (Daw et al., 1990), more recent studies show that rods preferentially impact the red-green opponent channel (Lee et al., 1991).

Results of the current project indicate that rods might actually decrease the S-cone signal, or at least interfere with it to the point that rods add more of an achromatic component at shorter wavelengths. This idea is supported by Stabell and Stabell (1990) who psychophysically found that rod activity suppresses cone signals, raising chromatic thresholds as time in the dark increases. This occurred, however, for all wavelengths across the visible spectrum, not just the shorter wavelengths.

Other psychophysical studies have noted that peripherally-viewed stimuli appear bluish both within the photochromatic interval (Ambler, 1974) and under dark-adapted conditions (Richards & Luria, 1964; Hunt, 1952). Trezona (1970) specifically proposed that the enhancement in blue perception away from the fovea might be explained by the shared neural pathway of S cones and rods. If, however, rods are boosting the S-cone signal, then colors in the short-wavelength portion of the spectrum may be expected to be more saturated than longer wavelengths. In fact, the opposite was the case here. Other researchers have suggested, however, that increases in blueness exist in the periphery even in the absence of rod signaling (Abramov & Gordon, 1977), so perhaps the two effects can be modeled independently.

Reproduced with permission of the copyright owner. Further reproduction prohibited without permission.

Hue Appearance

When hue responses from the 1° stimulus are compared across retinal locations, rods influence the perception of all four basic hues, and do not preferentially increase blueness (see figure 3.6). In fact, less blue was reported in the four retinal quadrants at wavelengths longer than the peak of the unscaled blue function when compared to the fovea. Furthermore, the spectral range of the perception of blue decreased in the peripheral retina; in the fovea, percent blue was reported out to approximately 540 nm, while in the periphery, blueness was no longer seen beyond approximately 490-500 nm. Rods had their largest effect in the spectral range of approximately 480-540 nm. In this region, stimuli appeared less green and more yellow than foveally-presented stimuli (figure 3.6). The peak of the green function was also shifted to shorter wavelengths, which is expected since the color green has a spectral sensitivity that is most like that of rods, and rod spectral sensitivity is shifted to shorter wavelengths relative to that of cones. In addition, very short and very long wavelengths appeared less red when rods contributed to hue judgments. These results are consistent with findings indicating that rods influence color perception in addition to contributing an achromatic component in the periphery (Ambler & Proctor, 1976). Additionally, rods impact all hues across the spectrum, not just blue (Stabell & Stabell, 1975, 1976a, 1979; Buck et al., 1998, 2000).

Stabell and Stabell's (1975, 1976a, 1979) results suggest that rods may enhance the signaling of the yellow/blue opponent mechanism relative to the red/green opponent mechanism. With their asymmetric color-matching technique, these researchers showed that rods contributed a blue component to short wavelengths and a yellow component to long wavelengths using stimuli ranging from 1 to 1000 photopic td. The finding that rods

Reproduced with permission of the copyright owner. Further reproduction prohibited without permission.

may enhance the perception of yellowness is consistent with the present results; however, the conclusion that rods enhance blueness is not. This explanation may still be plausible, however, considering that slight increases in blue perception were observed at the shortest wavelengths for the unscaled data (figure 3.6, top right-hand panel).

Buck et al. (1998), using a color-naming technique, also showed that rods affect the perception of all four basic hues across most of the visible spectrum. In Buck et al.'s study, under dark-adapted conditions, the peaks of the blue, yellow, and green functions shifted to longer wavelengths compared to conditions where rod influences were minimized, opposite to the results of this study. Consistent with the present study, Buck et al. report that rods decrease the perception of long-wavelength red, but they did not find a rod-induced decrease in short-wavelength redness. Again, this is similar to the results of this study.

Similarly, Buck et al. (2000) found results consistent with those from their earlier color-naming study when they measured the loci of unique hues at different intensity levels in the peripheral retina. They found that under conditions where rod contributions were maximized, unique yellow shifted to longer wavelengths, consistent with the idea that rods decrease the perception of redness. This decrease in redness is consistent with the results of the present study (figure 3.6, bottom panels). Furthermore, Buck et al. found that at low intensities, where rod signals should be greater, unique blue shifted to longer wavelengths, supporting a decrease in greenness due to rods, a result that is also consistent with those of the present study. The locus of unique green also shifted to longer wavelengths when rod signals were maximized in Buck et al.'s experiment indicating that rods either enhanced blue or diminished yellow. Although unique green

Reproduced with permission of the copyright owner. Further reproduction prohibited without permission.

was not directly measured in this study, the results in figure 3.6 suggest that unique green should shift to shorter wavelengths with rod contributions due to percent blue describing a smaller range of short wavelengths, the opposite of that reported by Buck and colleagues.

A possible explanation for the few discrepancies between Buck and colleague's findings and those of the present study is that Buck et al. equated stimuli for scotopic tds, whereas stimuli in the current experiment were equated for photopic tds. In equating for scotopic trolands, the rod activity was equated across wavelength but cone activity varied. As cone activity varied, the observers' perceptions of hue may also have varied. The strategy used in the present study was to equate stimuli photopically. In this manner, cone activity was held constant and rod activity varied; thus any differences in hue perception could more directly be attributed to differences in rod contribution.

Other researchers have measured rod effects on unique hue loci using different stimulus parameters and equating stimuli photopically. Nerger et al. (1995) measured the loci of unique hues in the fovea and at 20° temporal retinal eccentricity using 2.4 log td stimuli of varying sizes. They found that under dark-adapted conditions, rods had no effect on the locus of unique yellow but the loci of unique blue and unique green shifted to shorter wavelengths when small stimuli were used (generally less than 4 degrees of visual angle). The shifting of unique blue to shorter wavelengths would be consistent with either an enhancement of greenness or a reduction in short-wavelength red. Since unique yellow was unaffected, however, the reduction in short-wavelength red is the most parsimonious explanation. The shifting of unique green to shorter wavelengths is consistent with an enhancement of yellow, which was found in this study, or a decrease

Reproduced with permission of the copyright owner. Further reproduction prohibited without permission.

in blueness, which was also found in this study, due to rod signals. Thus, the present findings and those of Nerger et al. are consistent with a model whereby rods inhibit S-cone signaling.

Angel et al. (submitted) measured unique hues using very dim stimuli and also reported that rods did not affect the locus of unique yellow, but found that the loci of unique blue and unique green shifted to longer wavelengths under dark-adapted conditions at 8° superior retinal eccentricity. These results were found using stimuli of lower intensity (0.0-2.0 log td), but of comparable size (1.5°) to those used by Nerger et al. (1995). It is possible that with very dim stimuli, the inhibitory effect of rods on S cones diminishes. Subsequently, the perceptual effect is an apparent increase in blueness. If this is the case, then the loci of unique blue and unique green would be expected to shift to longer wavelengths.

Additional results from the same laboratory demonstrate other rod effects on color perception. Nerger et al. (1998), measuring red-green equilibria at 1° and 8° nasal and superior retinal eccentricities, found that rods shifted the locus of unique yellow to longer wavelengths. Volbrecht, et al. (2000a) found no rod effects on the locus of unique green when measuring at the same eccentricities and using the same stimulus parameters (intensity of 2.4 log td; sizes ranging from 0.25° to 2.0°) as Nerger et al. The former finding is consistent with rods affecting the signal of either M or L cones feeding into the red-green opponent mechanism. Buck and colleagues (1994, 1997) have discussed the possibility that rods affect M- and L-cone signaling, which would explain several of their results; and others have claimed that rods specifically interact with L cones (McCann & Benton, 1969). Any changes in M- or L-cone signaling due to rods should also impact

Reproduced with permission of the copyright owner. Further reproduction prohibited without permission.

the locus of unique green. The results of these studies may be internally consistent, if rods influence the red-green opponent mechanism to a greater extent than the yellow-blue. This idea is supported by current physiological findings (Lee et al., 1997).

A simple model that explains all the research findings regarding the influence that rods have on color perception remains elusive. It appears that rod contributions can vary depending on whether stimuli are above or below chromatic threshold (Ambler & Proctor, 1976). Rod signals can either add an achromatic/desaturating effect, usually at mesopic intensities where both rods and cones are responding, or an enhancement of blueness when only rods are being stimulated, as is the case for scotopic color contrast (Stabell & Stabell, 1994; Buck, 1997). Rods can also cause shifts in the perception of hue at mesopic intensities, and the specific effects that occur seem to be contingent on the particular region of the visible spectrum that is being tested (Stabell & Stabell, 1975, 1976a, 1979; Buck et al., 1997, 1998, 2000) as well as stimulus intensity and size (Nerger et al., 1995, 1998; Volbrecht et al., 2000a; Angel et al., submitted).

Peripheral Cone Functioning

Caution should be used when interpreting the effects that rods have on hue perception since several of the trends seen in the no-bleach condition are also apparent in the rod-bleach condition (figure 3.8). This was an unexpected result since it was assumed that the bleach employed in the periphery should have minimized rod contributions. Presuming that only cones were contributing to the perception of stimuli at 10° eccentricity in the rod-bleach condition, color-naming functions should have approximated those of the fovea. While color-naming functions from the rod-bleach condition certainly looked more foveal-like (figure 3.7) than color-naming functions from

Reproduced with permission of the copyright owner. Further reproduction prohibited without permission.

the no-bleach condition (figure 3.5), some differences still existed between the rod-bleach and foveal conditions. These differences could be due to 1) the bleach employed in the periphery not effectively minimizing rod signals, or 2) peripheral cone mechanisms not functioning in the same manner as in the fovea.

The differences in the perception of blue, green, and yellow between the no-bleach and foveal conditions are attenuated in the rod-bleach condition but are still evident (see figure 3.8). Percent blue is lower relative to the fovea in the rod-bleach condition, but the slight increase in percent blue at the shortest wavelengths seen in the no-bleach condition is absent. While the perception of yellow is still slightly greater in the rod-bleach condition, and its spectral range is expanded, the enhancement is not nearly the same magnitude as it is in the no-bleach condition. Perception of greenness is not diminished in the rod-bleach condition compared to the fovea, but the shift in the peak to shorter wavelengths of the peripheral functions remains. Furthermore, the decrease in the perception of long-wavelength red for the peripheral functions in the no-bleach condition are absent in the rod-bleach condition. One explanation of these results is that rod signals may not have been eliminated by the bleaching stimulus and thus, rods may still have contributed to hue perception in the rod-bleach condition.

An alternative explanation is that peripheral cones may be functioning differently than foveal cones. There are at least two possible substrates for differential cone functioning in the periphery: (1) the spectral sensitivity functions of the cones could be altered in the periphery, or (2) the relative contributions of the three cone types into the visual pathway could vary with eccentricity. The literature suggests that option (1) is unlikely. Peripheral spectral sensitivity curves are found to be very similar to foveal

Reproduced with permission of the copyright owner. Further reproduction prohibited without permission.

functions if stimulus size in sufficiently increased (Kuyk, 1982; c.f., Abramov & Gordon, 1977), and the photopic spectral luminosity function does not vary with eccentricity (Stabell and Stabell, 1976b). Option (2) appears to depend on what is being measured. Unique hue loci, which reflect the equilibrium points of the chromatic opponent mechanisms, will shift if the relative contributions of the three cone types into the opponent processes change with retinal eccentricity. Researchers have shown that the loci of some unique hues do shift in the peripheral retina relative to measurements made in the fovea even when rod signals are minimized and stimuli sizes are large (Nerger et al., 1995). Others, however, have shown that the L:M cone ratio is constant out to at least 28° retinal eccentricity (Nerger & Cicerone, 1992; Otake & Cicerone, 2000) indicating that the relative contributions of at least M and L cones remains constant with distance from the fovea.

Thus, in the periphery, the variation in cone functioning seems to result in a decrease in blueness and a shortening of its spectral range. There is also an increase in yellowness, a decrease in short-wavelength red, and a shifting of the green function to shorter wavelengths. These results for blue and yellow are consistent with those of Nerger et al. (1995) who found that even with the largest stimuli employed in the periphery, the locus of unique green was at shorter wavelengths than in the fovea, consistent with decreases in blueness and increases in yellowness.

Stimulus Size Effects

Decreasing stimulus size affected the perception of all four basic hues in the no-bleach (see figure 3.10) and rod-bleach (see figure 3.12) conditions. The effects were

Reproduced with permission of the copyright owner. Further reproduction prohibited without permission.

greatest for the percent of yellow and green. As stimulus size decreased, the spectral ranges of blue and green extended to longer wavelengths and more yellow was seen at wavelengths above and below the peak of its response function. The percents assigned to yellow and green diminished with decreasing stimulus size while red and blue were more well-preserved with stimulus size reductions.

It is well established that stimulus size has a large affect on the perception of color in the peripheral retina (Johnson, 1986). Kuyk (1982) measured spectral sensitivity functions in the fovea at several peripheral locations out to 45° temporal retinal eccentricity. He found that when a constant stimulus size was used, the peripheral functions looked markedly different from the foveal functions. By either increasing the size of peripheral stimuli or decreasing the size of foveal stimuli, the spectral sensitivity functions became more alike. Similarly, Noorlander et al. (1983) found no evidence for either a red-green or a yellow-blue loss at any peripheral location as long as stimulus size was sufficiently increased with increases in retinal eccentricity.

More recently, Abramov et al. (1991) studied the effects of stimulus size on color appearance in the peripheral retina. They found decreases in hue perception when a stimulus of a constant size was moved away from the fovea. At the most eccentric location studied, 40° in the temporal and nasal retinas, the perception of all hues was reduced and within-observer variability (standard errors of the mean) was high. As in the present study, Abramov et al.'s data show that blue and red were the most well-preserved hues in the periphery and that the spectral range of blue was extended, while yellow and green were the least preserved when a 1° stimulus was shown to the peripheral retina.

Reproduced with permission of the copyright owner. Further reproduction prohibited without permission.

It stands to reason that as stimulus size decreases, the number of cones responding correspondingly decreases. This may not, however, be the only factor responsible for the compromised hue perception with small test stimuli. The results of Abramov et al. and those of the present study indicate that percentages for most hues increased with stimulus size up to an asymptotic value (see figure 4.2). That is, as stimuli become larger, the percent hue grew to a point where any further increases in field size did not change the response. This pattern indicates that some sort of neural summation area is being progressively filled. Thus, small stimuli in the periphery do not adequately fill this summation area and hue perception suffers.

Growth Functions

Perceptive fields sizes for each of the four hue terms were obtained by fitting the color-naming data with the Michaelis-Menten growth function. The function's asymptotic value is indicated by g (%) and k is the stimulus size where the function reaches half of its asymptote (see figure 4.1). The values of k varied with wavelength for blue, green and short-wavelength red in the no-bleach condition (see figure 4.4). Interestingly, this variability in k values across wavelength somewhat follows the shape of the rod spectral luminous efficiency function shown in figure 5.1. The peak of the rod function is at approximately 510 nm. Not surprisingly, the greatest amounts of variability in k values were seen for green.

The variability in k values is absent at longer wavelengths in the no-bleach condition (for yellow and long-wavelength red) and is not observed for any hue terms in the rod-bleach condition (see figure 4.5). Thus, in the region of the visible spectrum

Reproduced with permission of the copyright owner. Further reproduction prohibited without permission.

where rods are not very sensitive or under conditions where they have been effectively eliminated (i.e. in the rod-bleach condition), k values are constant across wavelength.

Abramov et al. (1991) also found variability in k values across wavelengths though the pattern they report differs from the present study. They showed that the k values for red and green were approximately constant as a function of wavelength, and that the greatest amount of variability across wavelength occurred for blue and yellow. Abramov et al. claimed that the pattern found for their blue k values indicates the presence of two sub-mechanisms with different spatial properties. Up to approximately 480 nm, k values for blue were positive, meaning that hue responses grew as stimulus size increased. Beyond 480 nm, k values for blue became negative, indicating that hue responses decreased with increasing stimulus size. No evidence for any blue sub-mechanisms were found in the present study. It should be noted that some k values in the present study were negative (see table 4.2). The negative values were predominantly associated with the color yellow, possibly corresponding to the decreases in saturation for smaller stimuli, but some were found for the color blue in the rod-bleach condition only. The negative blue and yellow k values do not, however, correspond to the same areas of the spectrum where Abramov et al. reported negative values.

Perceptive Field Sizes

The growth of percent hue up to an asymptotic value with increases in stimulus size indicates that a perceptive field is being filled (Abramov et al., 1991; Knau & Werner, 2002). The shapes of these functions both in the current study and in Abramov et al.'s study do not fall after their asymptote is reached, indicating the absence of the

Reproduced with permission of the copyright owner. Further reproduction prohibited without permission.

inhibitory surround that exists when achromatic stimuli are used (Westheimer, 1965). This finding is expected since the spatial organization of receptive fields has been found to differ when using achromatic versus chromatic stimuli (DeValois & DeValois, 1975). From the values of k in table 4.2, perceptive field sizes were obtained by multiplying the values by 3. As in Abramov et al. (1991), 3k was operationally defined as the critical size for a particular hue mechanism, i.e., where the perceptive field is effectively filled.

Rod Effects

In the present study, perceptive field sizes varied with adaptation, hue mechanisms, and retinal location. Perhaps the largest effect on the sizes of perceptive fields was whether they were measured on the cone or rod plateau. Perceptive field sizes with rod contributions are larger than those in the rod-bleach condition. This is in agreement with researchers who have studied perceptive fields as a function of adaptation level of the retina and have found that perceptive field sizes are approximately 25% larger when measured under dark-adapted conditions (Ransom-Hogg & Spillmann, 1980). This increase can be attributed to the ineffectiveness of the inhibitory surround and expansion of center-size that occurs with dark adaptation.

Another explanation for the increases in perceptive field size with rod contributions may be the increase in spatial summation that occurs with dark adaptation. Researchers have shown that the receptive fields in the retina undergo a spatial reorganization with dark adaptation (Barlow, 1953; Barlow et al., 1957; Hartline, 1940), and psychophysical studies have shown that decreasing the intensity of a background

Reproduced with permission of the copyright owner. Further reproduction prohibited without permission.

increases the spatial summation that occurs when a test field is superimposed on it (Barlow, 1957).

These factors considered, the interpretation of rod influences on color-naming functions may need to be reassessed. Many color-naming functions in chapter 3 were based on data obtained with a 1° stimulus at all retinal locations. While a field size of 1° fills the perceptive fields for all colors in the rod-bleach condition, except those of green and yellow in the inferior retina (see figure 4.7), in the no-bleach condition, the 1° stimulus does not fill the perceptive field for most of the hue terms and quadrants. Thus, the influence of rods on hue perception may be different once perceptive field sizes are filled.

In figure 5.2, unscaled mean percent hue responses are plotted as a function of wavelength for each hue term and retinal location using the 5° stimulus. A 5° stimulus fills all perceptive field sizes at all retinal locations in the no-bleach condition except those of green in the nasal, superior, and inferior quadrants. Several differences are seen from the figure with the 1° stimulus (left-hand panel of figure 3.8). First, variability and differences among retinal quadrants are reduced with the 5° stimulus when compared to the color-naming functions obtained with the 1° stimulus. Furthermore, the peripheral green functions, while maintaining their shift to shorter wavelengths, show higher percents than those in the fovea for some wavelengths, not lower, as in figure 3.8. Not many changes are seen for percent blue when perceptive field sizes are filled, but the enhancement of yellow at wavelengths above its peak and the reductions in long-wavelength red are not seen in figure 5.2 as they are in figure 3.8.

Reproduced with permission of the copyright owner. Further reproduction prohibited without permission.

Figure 5.2. Unscaled mean percent hue response plotted as a function of wavelength for each hue term using the 5° stimulus in the no-bleach condition. Each panel represents a different hue term and error bars specify ±1 SEM. The foveal function is bolded and the four peripheral quadrants are denoted by different symbols.

Reproduced with permission of the copyright owner. Further reproduction prohibited without permission.

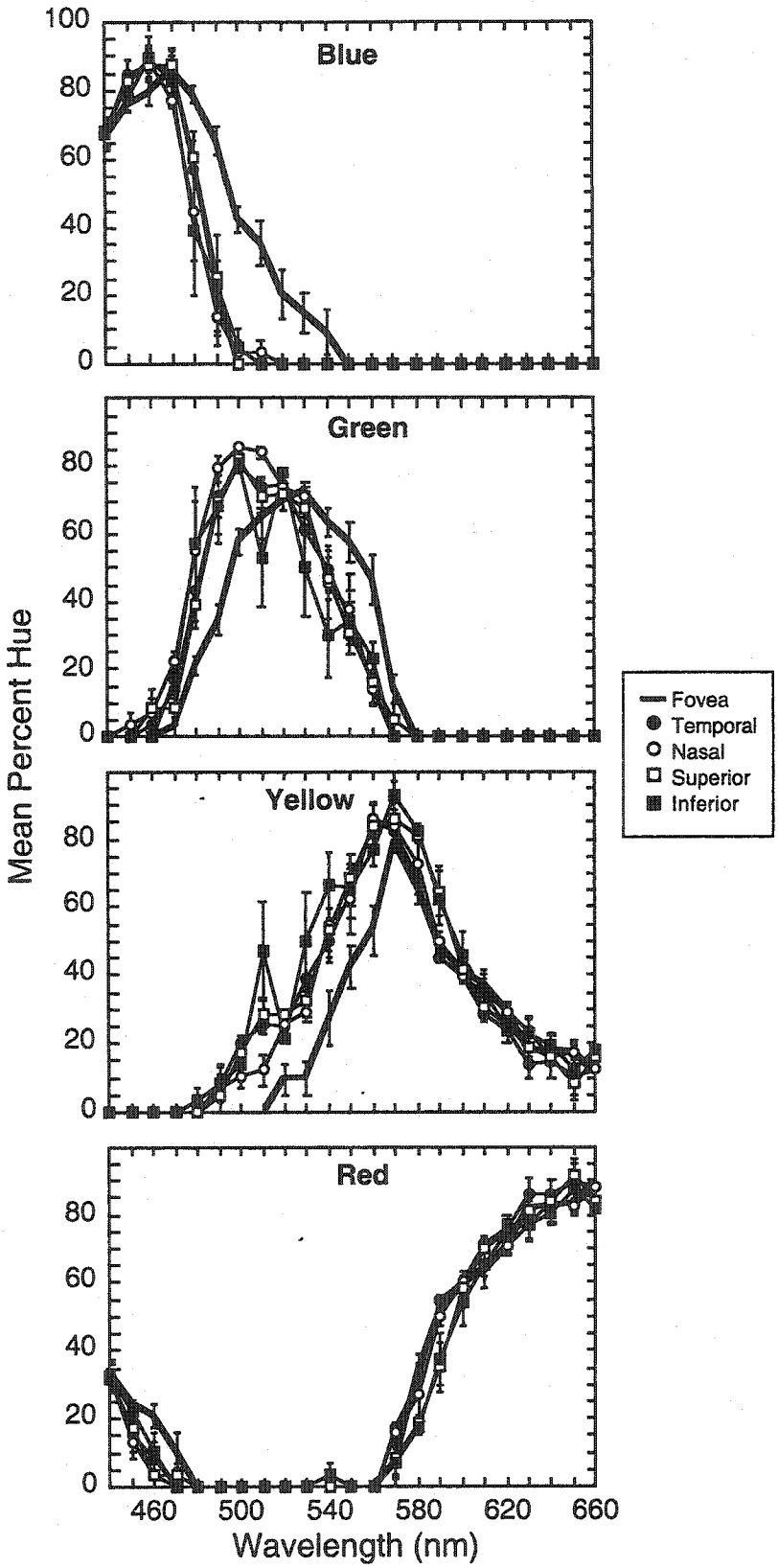

Reproduced with permission of the copyright owner. Further reproduction prohibited without permission.

Considering this data in figure 5.2, where perceptive fields are filled for most hue terms and retinal locations, the idea that rods enhance blue perception in the periphery (e.g., Ambler & Proctor, 1976; Trezona, 1970) or increase the responding of the yellow-blue opponent mechanism (Stabell & Stabell, 1975, 1976a) seem less plausible. While a small increase in blue perception still exists at the shortest wavelengths, it is not as noticeable as it was with the 1° stimulus. The yellow function with the 5° stimulus appears similar to the functions from the rod-bleach condition (right-hand panel, figure 3.9). Also, the decreases in percent red with the 1° stimulus is absent with the 5° stimulus. The only rod effect that remains is an enhancement of greenness when stimuli are closer to filling the perceptive field for green. This result is consistent with findings that unique yellow shifts to longer wavelengths (Buck et al., 2000; Nerger et al., 1998) and unique blue to shorter wavelengths (Nerger et al., 1995) under dark-adapted conditions, but contradicts findings that unique blue actually shifts to longer wavelengths when rod signals are maximized by making measurements on the rod plateau and using very dim stimuli (Angel et al., submitted).

Retinal Topography

If rods are enhancing greenness in the periphery, it might be expected that perceptive field sizes for green in the no-bleach condition might be the smallest at retinal locations where rod numbers are highest. The density of rods is highest in the superior retina (Curcio et al., 1990b). The perceptive field sizes are not, however, the smallest in the superior retina for any of the hues (see figure 4.6).

Reproduced with permission of the copyright owner. Further reproduction prohibited without permission.

Furthermore, if perceptive field sizes are determined by the density of cones, the density of ganglion cells, or the convergence of rods and cones onto ganglion cells, then perceptive fields should be smallest where these cell types are most dense and/or where convergence values are lowest. Cone numbers are highest in the temporal retina, closely followed by the nasal retina (Curcio et al., 1990b). Perceptive field sizes were smallest for all four hue terms in the temporal retina for the no-bleach condition (see figure 4.7). Abramov et al. (1991) also found that perceptive field sizes in the temporal retina were consistently smaller than those at corresponding eccentricities in the nasal retina. While this pattern was not found for the rod-bleach condition, perceptive fields were consistently larger in the inferior retina compared to the other three retinal locations for the rod-bleach condition; cone densities are lowest in this quadrant. Because ganglion cell densities are also highest in the temporal retina and lowest in the inferior retina (Curcio and Allen, 1990a), leading to convergence factors being highest and lowest in these same areas, results from this study cannot differentiate between perceptive field sizes being correlated with cone density, ganglion cell density, or spatial summation. Ganglion cell density is more likely to be the case, however, given recent findings that ganglion cell density correlates well with spatial summation measured psychophysically in the S- and L-cone pathways (Volbrecht, Shrago, Schefrin, & Werner, 2000b). However, as discussed later, perceptive fields may not be retinal in origin.

Comparisons to Abramov, Gordon, and Chan (1991)

Figure 5.3 plots perceptive field sizes from the present study (open symbols) and from Abramov et al. (1991) (filled symbols) for the 10° temporal and nasal retinas. In

Reproduced with permission of the copyright owner. Further reproduction prohibited without permission.

Figure 5.3. Perceptive field sizes plotted for the 10° temporal and nasal retinas. Symbols denote different hue terms. Open symbols represent data from the present study and filled symbols, data from Abramov et al. (1991). The dotted lines represent the widths of dendritic trees of ganglion cells in non-human primate projecting to parvocellular (P) and magnocellular (M) layers of the lateral geniculate nucleus, and the cortical magnification of striate cortex (V1). In the top panel, perceptive field sizes for the rod-bleach condition are plotted from the present study along with data from Abramov et al. In the bottom panel, Abramov et al.'s data are re-plotted along with perceptive field sizes for the no-bleach condition of the present study.

Reproduced with permission of the copyright owner. Further reproduction prohibited without permission.

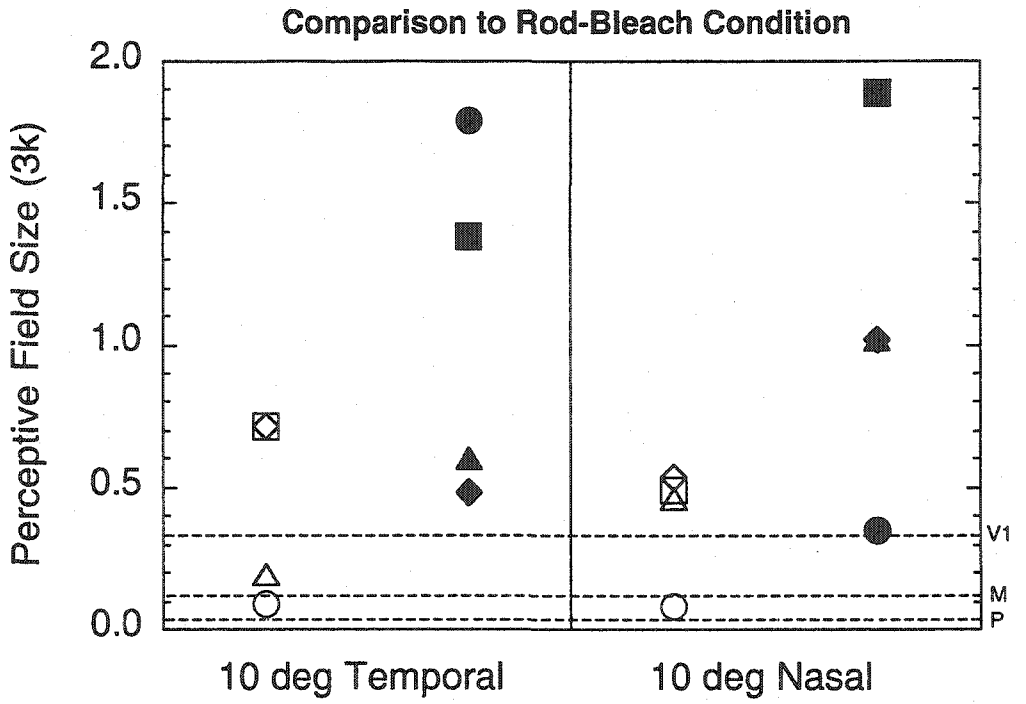

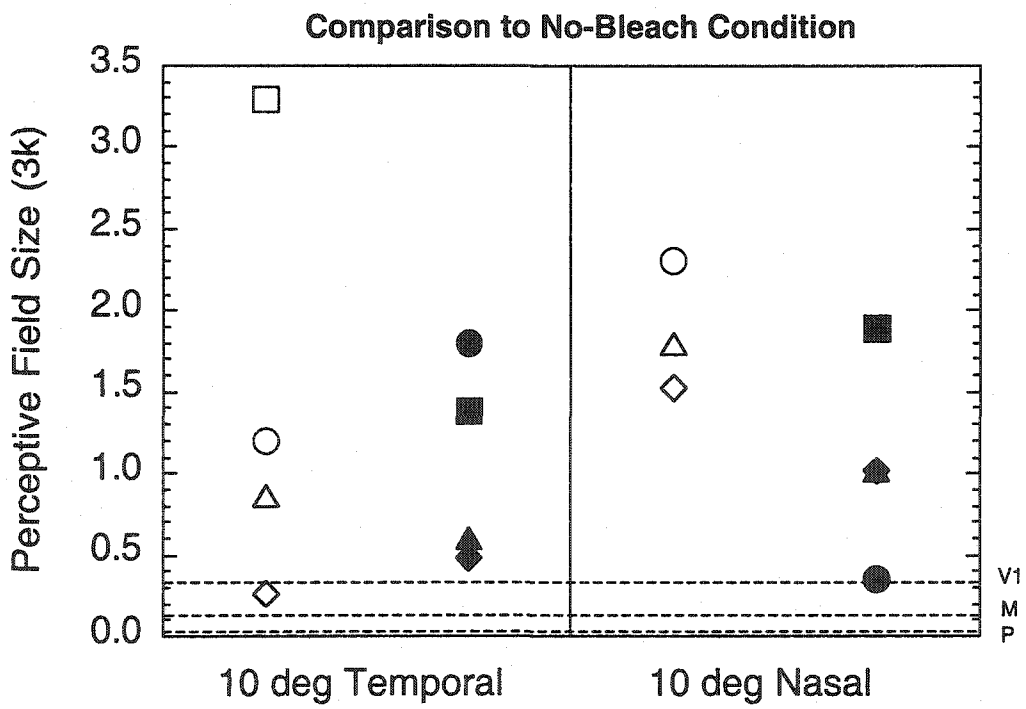

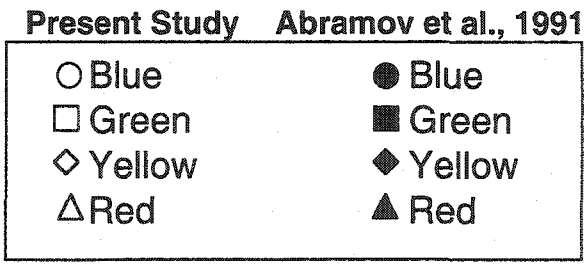

Reproduced with permission of the copyright owner. Further reproduction prohibited without permission.

the top panel, perceptive field sizes for the rod-bleach condition are compared to those from Abramov et al.; the bottom panel compares perceptive field sizes from the no-bleach condition to those of Abramov et al. The dotted lines represent the diameter of dendritic trees of ganglion cells in non-human primates projecting to parvocellular (P) and magnocellular (M) layers of the lateral geniculate nucleus (Shapley & Perry, 1986), and the cortical magnification of striate cortex (V1) (Tootell, Switkes, Silverman, & Hamilton, 1988). Since Abramov et al. calculated two perceptive field sizes for blue (one for each of their sub-mechanisms), the average of the values is shown in figure 5.3. The perceptive field size for green in the nasal retina for the no-bleach condition in the present study was exceptionally large (16.49) and is not plotted in the figure.

As seen in figure 5.3, the sizes of perceptive fields from the present study in the rod-bleach condition (top panel) were generally smaller than those from Abramov et al.'s (1991) study. In fact, Abramov et al.'s measurements are closer to the size scale of perceptive fields in the no-bleach condition from this study (bottom panel; note the different scale on the ordinate). This indicates that the perceptive field measurements from Abramov et al. may reflect rod influences. In addition, this figure provides some insight into the location within the visual system where perceptive fields might originate. Abramov et al. (1991) claimed that perceptive field sizes exceed the diameters of the dendritic trees of retinal ganglion cells measured in non-human primates and in most cases were closer in size to receptive fields measured for cortical area V4. Other evidence suggests perceptive field sizes fall mostly between receptive field sizes of retinal ganglion cells and striate cortical cells (Knau & Werner, 2002).

Reproduced with permission of the copyright owner. Further reproduction prohibited without permission.

As can be seen in figure 5.3, only a few perceptive field sizes from the present study fall within the bounds of retinal (M and P) receptive fields. It can be concluded that perceptive fields are unlikely mediated by a retinal mechanism. It should be noted, however, that certain assumptions were made when determining perceptive field sizes. The perceptive fields plotted in figure 5.3 from the present study represent wavelengths for which g values were highest, or where a hue mechanism had maximal responding. A better representation of perceptive field size may have been obtained from taking an average of 3k values across wavelength. However, since perceptive field sizes in the no-bleach condition varied so much across the visible spectrum, this may not be appropriate. Similarly, these comparisons are dependent upon how the critical size for perceptive fields is operationally defined. Consistent with Abramov and colleagues, perceptive fields in the present study were defined as 3k. If a smaller or a larger criterion had been chosen, speculations as to the neural level represented by perceptive fields may have differed.

Further Considerations

Differential Bleaching of Cone Mechanisms

To ensure that the broadband (5500k) bleaching stimulus did not differentially adapt any of the three cone mechanisms in the peripheral retina, a bleach was employed in the fovea for two of the three observers. This is an important consideration since differential adaptation could impact hue perception. Figure 5.4 shows scaled mean hue and saturation responses as a function of wavelength for each hue term and saturation. In this figure, results are compared to those from the foveal condition where no bleach was

Reproduced with permission of the copyright owner. Further reproduction prohibited without permission.

Figure 5.4. Scaled mean percent hue and saturation responses as a function of wavelength for each hue term and saturation. Open symbols represent data from the foveal-bleach condition and filled symbols, data from the foveal no-bleach condition. Error bars specify ±1 SEM.

Reproduced with permission of the copyright owner. Further reproduction prohibited without permission.

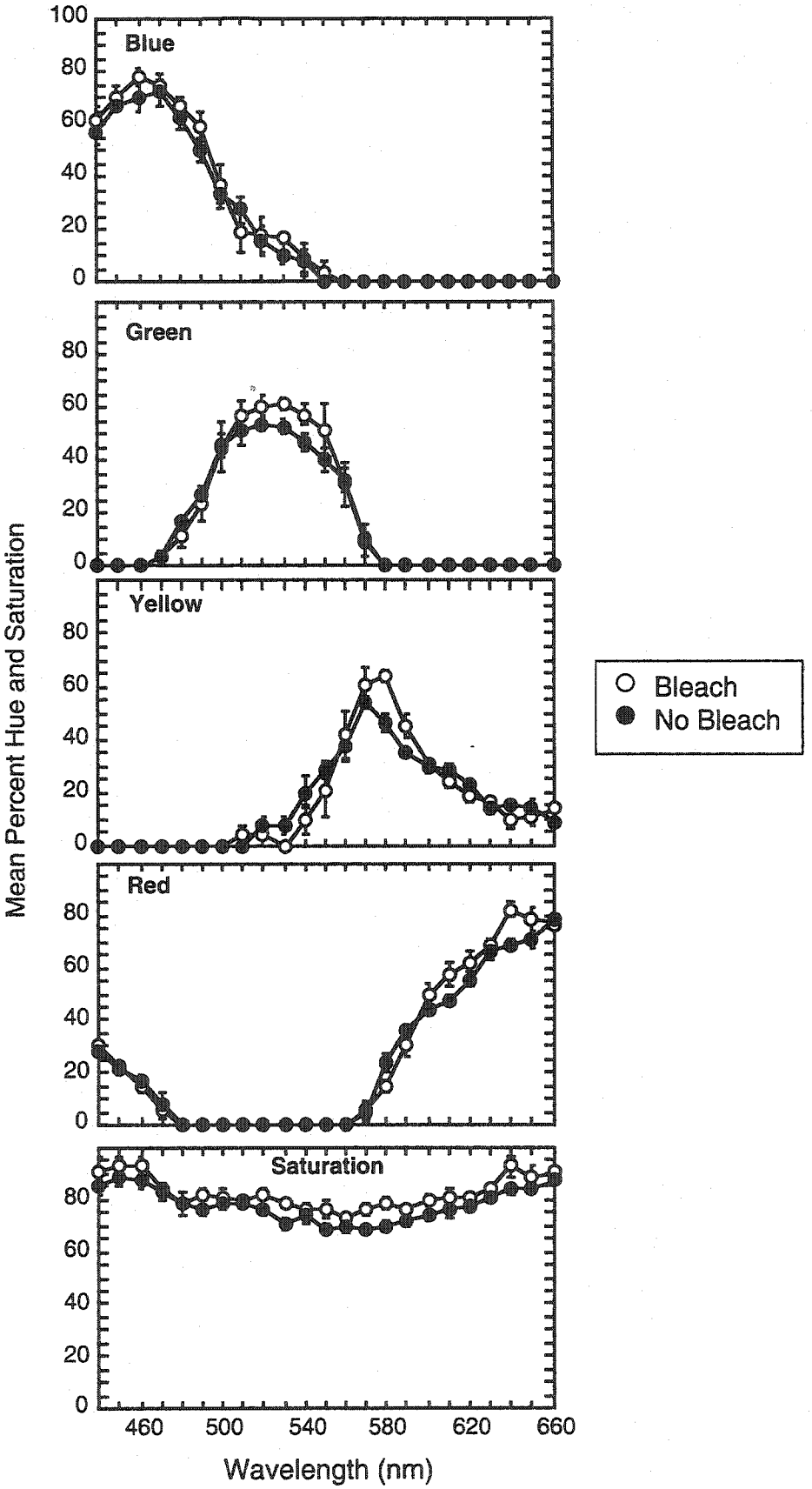

Reproduced with permission of the copyright owner. Further reproduction prohibited without permission.

utilized. The open symbols represent data from the foveal-bleach condition and filled symbols specify data from the foveal no-bleach condition.

As shown in figure 5.4, only small differences exist between the two conditions. Bleaching the fovea may have had a slight effect on green, yellow, and long-wavelengthred. At a few wavelengths for each of these hues, the open symbols are slightly higher than the closed symbols, indicating enhanced responding in the rod-bleach condition. Although it is possible that some rods were being stimulated by the 1° stimulus in the fovea, the effects shown in figure 5.4 are opposite to what was found in this study.

Differences in Macular Pigmentation

Measurements were made to investigate potential differences between the fovea and 10° peripheral retina due to differences in macular pigmentation densities. Since monochromatic stimuli were used in this study, the macular pigment acted only as a neutral density filter and would not have caused any variation in the chromatic content of the test stimulus. The lack of macular pigment at 10° would, however, cause an overall increase in the intensity of light at shorter wavelengths compared to the fovea. To investigate the potential impact of this intensity difference, stimuli below 540 nm were increased in intensity by the density of the macular pigment in the fovea. Figure 5.5 plots scaled mean percent hue and saturation responses as a function of wavelength for each hue term and saturation. The filled symbols represent data from the fovea, which were increased in intensity by the density of the macular pigment below 540 nm. Open symbols represent data from the fovea using the original intensity calculations.

Reproduced with permission of the copyright owner. Further reproduction prohibited without permission.

Figure 5.5. Scaled mean percent hue and saturation responses as a function of wavelength for each hue term and saturation. Filled symbols represent data from the fovea, which were increased in intensity by the density of the macular pigment below 540 nm. Open symbols represent data from the fovea using the original intensity calculations. Error bars specify ±1 SEM.

Reproduced with permission of the copyright owner. Further reproduction prohibited without permission.

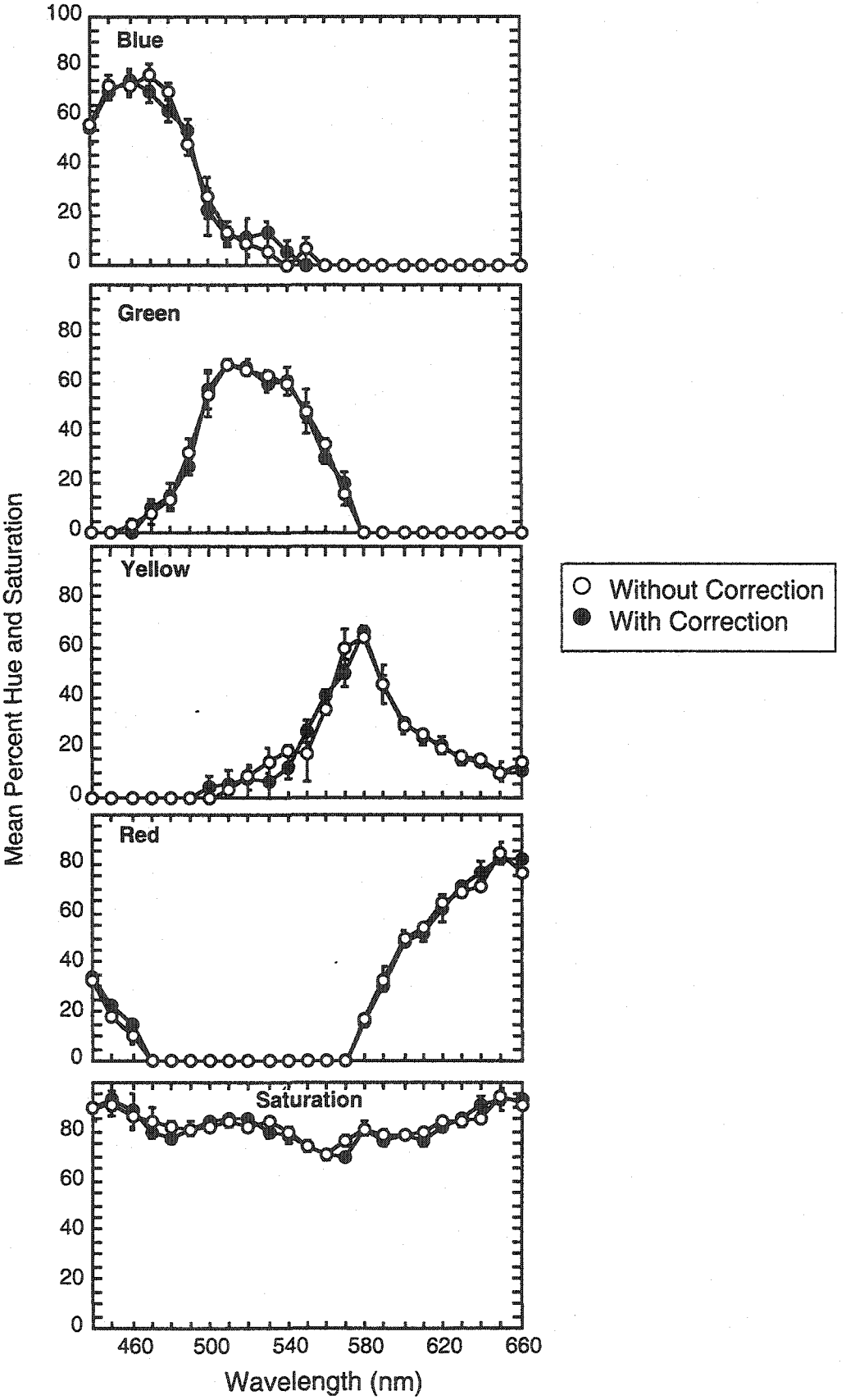

Reproduced with permission of the copyright owner. Further reproduction prohibited without permission.

As expected, for all hue terms and saturation, there are no differences between the two functions.

Effects of the Point-Spread Function

If light from a small, self-luminous stimulus enters the eye, its retinal image will be degraded in sharpness and appear larger than the actual stimulus, resulting in a smooth, Gaussian-shaped luminance distribution, termed the point-spread function (Campbell & Gubish, 1966). Since small stimuli were used in this study, such an effect may need to be considered. That is, the smaller test sizes may have been physically larger on the retinal surface than when estimated using visual-angle calculations external to the eye. Based on Gubisch's (1967) foveal point-spread functions for a 2.4 mm pupil size, corrections are only necessary for stimulus diameters less than 17.5'. When this factor is taken into account, the diameters of the three smallest stimulus sizes used in the present study (0.098°, 0.125°, and 0.25°), may have been increased on the retinal surface by as much as 0.5' when presented to the fovea (Gubish, 1967). These stimuli were not presented to the fovea, however, so any variations in the point-spread function that occur with eccentricity need to be considered.

While the point-spread function has been found to be independent of wavelength (Charman & Jennings, 1976), it does, indeed, vary with retinal eccentricity (Jennings & Charman, 1978). Consistent with arguments made in Volbrecht et al. (2000b), it is assumed that at 10° retinal eccentricity, the stimuli may have been as much as 1.0' larger in diameter. This means that stimuli smaller than 1° in diameter could have been as much as 0.017° larger on the retinal surface at 10° eccentricity. This size difference

Reproduced with permission of the copyright owner. Further reproduction prohibited without permission.

would have had a negligible effect on the shape and position of the growth functions. Thus, it is concluded that optical spreading did not effect the calculations of perceptive field sizes obtained in this study.

Conclusion

This research on the effect of rods on the sizes of perceptive fields at 10° retinal eccentricity indicates that under dark-adapted conditions, stimuli for some colors need to be made larger to obtain foveal-like hue perception than they do under light-adapted conditions. Rods desaturated peripherally-viewed stimuli at shorter wavelengths and affected green perception the most among the four basic hues. Not surprisingly, perceptive field sizes were largest for the color green in the area of the spectrum where rods are maximally sensitive.

The results from this study indicate that cone mechanisms in the periphery may be functioning differently from those in the fovea. Many of the same effects observed under conditions where rod signals were maximized (no-bleach condition) persisted in peripheral conditions where rod signals were minimized (rod-bleach condition). These differences are best accounted for at the level of neural connectivity rather than with photopigment variations.

Hue responses grew to asymptotic values for most colors under both dark-adapted and light-adapted conditions, indicating that perceptive fields were being filled as stimulus size increased. As expected, no indication of an inhibitory surround was observed in the shapes of these functions. Differences in perceptive field sizes were revealed both among hue terms and across the retinal quadrants. Through an analysis of cell densities and distributions, it was concluded that perceptive field sizes did not

Reproduced with permission of the copyright owner. Further reproduction prohibited without permission.

correspond with differences in cone densities, ganglion cell densities, or spatial summation at the retinal level. Perceptive fields are therefore implicated to be cortical in origin, as several other researchers have indicated (Abramov et al., 1991; DeValois, Switkes, & Mahon, 1997).

Reproduced with permission of the copyright owner. Further reproduction prohibited without permission.

References

Abramov, I., & Gordon, J. (1977). Color vision in the peripheral retina. I. *Spectral sensitivity. Journal of the Optical Society of America, 67,* 195-202.

Abramov, I., Gordon, J., & Chan, H. (1991). Color appearance in the peripheral retina: Effects of stimulus size. *Journal of the Optical Society of America, 8,* 404-414.

Ahnelt, P., Keri, C., & Kolb, H. (1990). Identification of pedicles of putative blue-sensitive cones in the human retina. *The Journal of Comparative Neurology, 293,* 39-53.

Ahnelt, P., Kolb, H., & Pflug, R. (1987). Identification of a subtype of cone photoreceptor, likely to be blue sensitive, in the human retina. *The Journal of Comparative Neurology, 255,* 18-34.

Alpern M. (1971). Rhodopsin kinetics in the human eye. *Journal of Physiology (London), 217,* 447-471.

Ambler, B. (1974). Hue discrimination in peripheral vision under conditions of dark and light adaptation. *Perception and Psychophysics, 15,* 586-590.

Ambler, B. & Proctor, R. (1976). Rod involvement in peripheral color processing. *Scandinavian Journal or Psychology, 17,* 142-148.

Angel, C., Volbrecht, V., & Nerger, J. (submitted). The effects of rods on the scalar invariance of unique hues. *Journal of the Optical Society of America.*

Barlow, H.B. (1953). Summation and inhibition in the frog's retina. *Journal of Physiology, 119,* 69-88.

Barlow, H.B. (1957). Increment thresholds at low intensities considered as signal/noise discriminations. *Journal of Physiology, 136,* 69469-488.

Barlow, H.B., Fitzhugh, R., & Kuffler, S.W. (1957). Change of organization in the receptive fields of the cat's retina during dark adaptation. *Journal of Physiology, 137,* 338-354.

Reproduced with permission of the copyright owner. Further reproduction prohibited without permission.

Benimoff, N., Schneider, S., & Hood, D. (1982). Interactions between rod and cone channels above threshold: A test of various models. *Vision Research, 22,* 1133-1140.

Boynton, R.M., Schafer, W., & Neun, M.E. (1964). Hue-wavelength relation measured by color-naming method for three retinal locations. *Science, 146,* 666-668.

Buck, S. (1997). Influence of rod signals on hue perception: Evidence from successive scotopic contrast. *Vision Research, 37,* 1295-1301.

Buck, S. & Knight, R. (1994). Partial additivity of rod signals with M- and L-cone signals in increment detection. *Vision Research, 34,* 2537-2545.

Buck, S., Knight, R., & Bechtold, J. (2000). Opponent-color models and the influence of rod signals on the loci of unique hues. *Vision Research, 40,* 3333-3344.

Buck, S., Knight, R., Fowler, G., & Hunt, D. (1998). Rod influence on hue-scaling function. *Vision Research, 38,* 3259-3263.

Buck, S. & Makous, W. (1981). Rod-cone interaction on large and small backgrounds. *Vision Research, 21,* 1181-1187.

Buck, S., Peeples, D., Makous, W. (1979). Spatial patterns of rod-cone interaction. *Vision Research, 19,* 775-782.

Campbell, F.W. & Gubisch, R.W. (1966). Optical quality of the human eye. *Journal of Physiology (London), 186,* 558-578.

Charman, W.N. & Jennings, J.A.M. (1976). The optical quality of the monochromatic retinal image as a function of focus. *British Journal of Physiological Optics, 31,* 119-134.

Connors, M.M. & Kelsey, P.A. (1961). Shape of the red and green color zone gradients. *Journal of the Optical Society of America, 51,* 874-877.

Connors, M.M. & Kinney, J.A.S. (1962). Relative red-green sensitivity as a function of retinal position. *Journal of the Optical Society of America, 52,* 81-84.

Cornsweet, T. (1970). *Visual Perception.* Academic Press: New York.

Curcio, C. and Allen, K. (1990a). Topography of ganglion cells in human retina. *Journal of Comparative Neurology, 300,* 5-25.

Curcio, C., Allen, K., Sloan, K., Lerea, C., Hurley, J., Klock, I., & Milam, A. (1991). Distribution and morphology of human cone photoreceptors stained with anti-blue opsin. *Journal of Comparative Neurology, 312,* 610-624.

Reproduced with permission of the copyright owner. Further reproduction prohibited without permission.

Curcio, C., Sloan, K., Kalina, R., & Hendrickson, A. (1990b). Human photoreceptor topography. *Journal of Comparative Neurology, 292,* 497-523.

Curcio, C., Sloan, K., Packer, O., Hendrickson, A., & Kalina, R. (1987). Distribution of cones in human and monkey retina: Individual variability and radial asymmetry. *Science, 236,* 579-581.

Daw, N., Jensen., R., & Brunken, W. (1990). Rod pathways in mammalian retinae. *Trends in Neuroscience, 13,* 110-115.

DeValois, R. & DeValois, K. (1993). A multi-stage color model. *Vision Research, 33,* 1053-1065.

DeValois, R. & DeValois, K. (1975). The neural coding of color. In *Handbook of Perception.* E.C. Carterette & M.P. Friedman (Eds). New York: Academic Press.

DeValois, R., DeValois, K., Switkes, E., & Mahon, L. (1997). Hue scaling of isoluminant and cone-specific lights. *Vision Research, 37,* 885-897.

Donner, O. & Rushton, W. (1959). Rod-cone interaction in the frog's retina analysed by the Stiles-Crawford effect and by dark adaptation. *Journal of Physiology, 149,* 303-317.

D'Zmura, M. & Lennie, P. (1986). Shared pathways for rod and cone vision. *Vision Research, 26,* 1273-1280.

van Esch, J.A., Koldenhof, E.E., van Doorn, A.J., & Koenderink, J.J. (1984). Spectral sensitivity and wavelength discrimination of the human peripheral visual field. *Journal of the Optical Society of America A, 1,* 443-450.

Ferree, C. & Rand, G. (1919). Chromatic thresholds of sensation from center to periphery of the retina and the bearing on color theory part I. *Psychological Review, 26,* 16-41.

Frumkes, T.E., Sekuler, M.C., Barris, M.C., Reiss, E.H., & Chalupa, L.M. (1973). Rod-cone interaction in human scotopic vision - I. Temporal analysis. *Vision Research, 13,* 1269-1282.

Frumkes, T., Sekuler, M., & Reiss, E. (1972). Rod-cone interaction in human scotopic vision. *Science, 175,* 913-914.

Goldberg, S., Frumkes, T., & Nygaard, R. (1983). Inhibitory influence of unstimulated rods in the human retina: Evidence provided by examining cone flicker. *Science, 221,* 180-182.

Reproduced with permission of the copyright owner. Further reproduction prohibited without permission.

Gordon, J. & Abramov, I. (1977). Color vision in the peripheral retina. II. Hue and saturation. *Journal of the Optical Society of America, 67,* 202-207.

Gordon, J. & Abramov, I. (1988). Scaling procedures for specifying color appearance. *Color Research and Application, 13,* 146-152.

Gordon, J., Abramov, I., & Chan, H. (1994). Describing color appearance: Hue and saturation scaling. *Perception and Psychophysics, 56,* 27-41.

Gouras, P. (1965). Primate retina: Duplex function of dark-adapted ganglion cells. *Science, 147,* 1593-1594.

Gouras, P. & Link, K. (1966). Rod and cone interaction in dark-adapted monkey ganglion cells. *Journal of Physiology, 184,* 499-510.

Granit, R. (1943). The spectral properties of the visual receptors of the cat. *Acta Physiology Scand., 5,* 219-229.

Granit, R. (1944). The dark-adaptation of mammalian visual receptors. *Acta Physiology Scand., 7,* 216-220.

Gubisch, R.W. (1967). Optical performance of the human eye. *Journal of the Optical Society of America, 57,* 407-415.

Hartline, H.K. (1940). The receptive fields of optic nerve fibers. *American Journal of Physiology, 130,* 690-699.

Hubel, D.H. & Wiesel, T.N. (1960). Receptive fields of optic nerve fibres in the spider monkey. *Journal of Physiology, 154,* 572-580.

Hubel, D.H. & Wiesel, T.N. (1965). Receptive fields and functional architecture in the two nonstriate visual areas (18 and 19) of the cat. *Journal of Neurophysiology, 28,* 229-289.

Hunt, R.W.G. (1952). Light and dark adaptation and the perception of color. *Journal of the Optical Society of America, 42,* 190-199.

Hurvich, L.M. & Jameson, D. (1957). An opponent-process theory of color vision. *Psychological Review, 64,* 384-404.

Ingling, C., Lewis, A., & Loose, D. (1977). Cones change rod sensitivity. *Vision Research, 17,* 555-563.

Jacobs, R. (1979). Visual resolution and contour interaction in the fovea and periphery. *Vision Research, 19,* 1187-1195.

Reproduced with permission of the copyright owner. Further reproduction prohibited without permission.

Jameson, D. & Hurvich L.M. (1967). Fixation-light bias: an unwanted by-product of fixation control. *Vision Research, 7,* 805-809.

Jennings, J.A.M. & Charman, W.N. (1978). Optical image quality in the peripheral retina. *American Journal of Optometry and Physiological Optics, 55,* 582-590.

Johnson, M. (1986). Color vision in the peripheral retina. *American Journal of Optometry and Physiological Optics, 63,* 97-103.

Jung, R. & Spillmann, L. (1970). Receptive field estimation and perceptual integration in human vision. In *Early Experience and Visual Information Processing in Perceptual and Reading Disorders* (Edited by Young, F.A. and Lindsley, D.B.), pp. 181-197. National Academy of Science, Washington D.C.

Knau, H. & Werner, J. (2002). Senescent changes in parafoveal color appearance: Saturation as a function of stimulus area. *Journal of the Optical Society of America, 19,* 208-214.

Koenderink, J., Bouman, M., Bueno de Mesquita, A., & Slappendel, S. (1978a). Perimetry of contrast detection thresholds of moving spatial sine wave patterns I: The near peripheral visual field (eccentricity 0°-8°). *Journal of the Optical Society of America, 68,* 845-849.

Koenderink, J., Bouman, M., Bueno de Mesquita, A., & Slappendel, S. (1978b). Perimetry of contrast detection thresholds of moving spatial sine wave patterns II: The far peripheral visual field (eccentricity 0°-50°). *Journal of the Optical Society of America, 68,* 850-854.

von Kries, J. (1905). Die Gesichtsempfindungen. In W. Nagel (ed.), *Handbuch der Physiologie des Menschen, Vol. 3.* Vieweg: Braunschweig.

Kuffler, S.W. (1953). Discharge patterns and functional organization of mammalian retina. *Journal of Neurophysiology, 16,* 37-68.

Kuyk, T. (1982). Spectral sensitivity of the peripheral retina to large and small stimuli. *Vision Research, 22,* 1293-1297.

Lee, B., Smith, V., Pokorny., J., & Kremers, J. (1997). Rod inputs to macaque ganglion cells. *Vision Research, 37,* 2813-2828.

Lie, I. (1963). Dark adaptation and the photochromatic interval. *Documnta Ophthalmologica, 17,* 411-510.

MacLeod, D. (1972). Rods cancels cones in flicker. *Nature, 235,* 173-174.

Reproduced with permission of the copyright owner. Further reproduction prohibited without permission.

Makous, W., & Boothe, R. (1974). Cones block signals from rods. *Vision Research, 14,* 285-294.

McCann, J. & Benton, J. (1969). Interaction of the long-wave cones and the rods to produce color sensations. *Journal of the Optical Society of America, 59,* 103-107.

Moreland, J.D. (1972). Peripheral colour vision. In *Handbook of Sensory Physiology, Vol. VII/4. Visual Psychophysics* (edited by Jameson, D. and Hurvich, L.M.), pp. 517-536. Springer, Berlin.

Naarendorp, F., Rice, K., & Sieving, P. (1996). Summation of rod and S cone signals at threshold in human observers. *Vision Research, 36,* 2681-2688.

Nagy, A. & Doyal, J. (1993). Red-green color discrimination as a function of stimulus field size in peripheral vision. *Journal of the Optical Society of America A, 10,* 1147-1156.

Nerger, J. & Cicerone, C. (1992). The ratio of L cones to M cones in the human parafoveal retina. *Vision Research, 32,* 879-888.

Nerger, J., Volbrecht, V., & Ayde, C. (1995). Unique hue judgments as a function of test size in the fovea and at 20-deg temporal eccentricity, *Journal of the Optical Society of America A, 12,* 1225-1232.

Nerger, J., Volbrecht., V., Ayde, C., & Imhoff, S. (1998). Effect of the s-cone mosaic and rods on red/green equilibria. *Journal of the Optical Society of America, 15,* 2816-2826.

Noorlander, C., Koenderink, J., den Ouden, R., & Edens, B. (1983). Sensitivity to spatiotemporal colour contrast in the peripheral visual field. *Vision Research, 23,* 1-11.

Oehler, R. (1985). Spatial interactions in the rhesus monkey retina: A behavioural study using the Westheimer paradigm. *Experimental Brain Research, 59,* 217-225.

Østerberg, G. (1935). Topography of the layer of rods and cones in the human retina. *Acta Ophthalmologica, 6,* 76-102.

Otake, S. & Cicerone, C. (2000). L and M cone relative numerosity and red-green opponency from fovea to midperiphery in the human retina. *Journal of the Optical Society of America, 17,* 615-625.

Ransom-Hogg, A., & Spillmann, L. (1980). Perceptive field size in fovea and periphery of the light- and dark-adapted retina. *Vision Research, 20,* 221-228.

Reproduced with permission of the copyright owner. Further reproduction prohibited without permission.

Raviola, E. & Gilula, N. (1973). Gap junctions between photoreceptor cells in the vertebrate retina. *Proceedings of the National Academy of Science, 70,* 1677-1681.

Richards, W. & Luria, S.M. (1964). Color-mixture functions at low luminance levels. *Vision Research, 4,* 281-313.

Ronchi, L. & Fidanzati, G. (1972). Changes in psychophysical organization across the light-adapted retina. *Journal of the Optical Society of America, 62,* 912-915.

Rovamo, J. & Virsu, V. (1979). An estimation and application of the human cortical magnification factor. *Experimental Brain Research, 37,* 495-510.

Rovamo, J., Virsu, V., & Nasanen, R. (1978). Cortical magnification factor predicts the photopic sensitivity of peripheral retina. *Nature, 271,* 54-56.

Rushton, W. & Powell, D. (1972). The rhodopsin content and the visual threshold of human rods. *Vision Research, 12,* 1073-1081.

Schneeweis, D. & Schnapf, J. (1995). Photovoltage of rods and cones in the macaque retina. *Science, 268,* 1053-1056.

Scholtes, A.M.W. & Bouman, M.A. (1977). Psychophysical experiments on spatial summation at threshold level of the human peripheral retina. *Vision Research, 17,* 867-873.

Schultze, M. (1866). Zur Anatomie und Physiologie der Retina. *Arch. Mikrosk. Anat., 2,* 176-286.

Shapley, R. & Perry, V.H. (1986). Cat and monkey retinal ganglion cells and their visual functional roles. *Trends in Neuroscience, 9,* 229-235.

Spillmann, L., Ransom-Hogg, A., & Oehler, R. (1987). A comparison of perceptive and receptive fields in man and monkey. *Human Neurobiology, 6,* 51-62.

Stabell, B. & Stabell, U. (1976a). Rod and cone contributions to peripheral colour vision. *Vision Research, 16,* 1099-1104.

Stabell, B. & Stabell, U. (1979). Rod and cone contributions to change in hue with eccentricity. *Vision Research, 19,* 1121-1125.

Stabell, B. & Stabell, U. (1980). Peripheral color vision: Effects of rod intrusion at different eccentricities. *Vision Research, 36,* 3407-3414.

Stabell, B. & Stabell, U. (1990). Rod suppression of cone-mediated information about colour and form during dark aaptation. *Vision Research, 36,* 3407-3414.

Reproduced with permission of the copyright owner. Further reproduction prohibited without permission.

Stabell, B. & Stabell, U. (1996). Peripheral color vision: Effects of rod intrusion at different eccentricities. *Scandinavian Journal of Psychology, 31,* 139-148.

Stabell, U. & Stabell, B. (1975). The effect of rod activity on colour matching functions. *Vision Research, 15,* 1119-1123.

Stabell, U. & Stabell, B. (1976b). Absence of rod activity from peripheral vision. *Vision Research, 16,* 1433-1437.

Stabell, U. & Stabell, B. (1977). Wavelength discrimination of peripheral cones and its change with rod intrusion. *Vision Research, 17,* 423-426.

Stabell, U. & Stabell, B. (1994). Mechanisms of chromatic rod vision in scotopic illumination. *Vision Research, 34,* 1019-1027.

Stockman, A., Sharpe, L., Zrenner, E., & Nordby, K. (1991). Slow and fast pathways in the human rod visual system: electrophysiology and psychophysics. *Journal of the Optical Society of America A., 8,* 1657-1665.

Sugita, Y., Suzuki, H., & Tasaki, K. (1989). Human rods are acting in the light and cones are inhibited in the dark. *Tohoku Journal of Experimental Medicine, 157,* 365-372.

Sugita, Y. & Tasaki, K. (1988a). Rods also participate in human color vision. *Tohoku Journal of Experimental Medicine, 154,* 57-62.

Sugita, Y. & Tasaki, K. (1988b). The activation of cones in scotopic and rods in photopic vision. *Tohoku Journal of Experimental Medicine, 156,* 311-317.

Tootell, R.B.H., Switkes, E., Silverman, M.S., & Hamilton, S.L. (1988). Functional anatomy of macaque striate cortex. II. Retinotopic organization. *Journal of Neuroscience, 8,* 1531-1568.

Trezona, P. (1970). Rod participation in the 'blue' mechanism and its effects on colour matching. *Vision Research, 10,* 317-332.

Troscianko, T. (1982). A given visual field location has a wide range of perceptive field sizes. *Vision Research, 22,* 1363-1369.

Uchikawa, H., Kaiser, P.K., & Uchikawa, K. (1982). Color discrimination perimetry. *Color Research and Application, 7,* 264-272.

Volbrecht, V., Nerger, J., Imhoff, S., & Ayde, C. (2000a). Effect of the short-wavelength-sensitive-cone mosaic and rods on the locus of unique green. *Journal of the Optical Society of AmericaA,* 17, 628-634.

Reproduced with permission of the copyright owner. Further reproduction prohibited without permission.

Volbrecht, V., Shrago, E., Schefrin, B., & Werner, J. (2000b). Spatial summation in human cone mechanisms from 0° to 20° in the superior retina. *Journal of the Optical Society of America, 17,* 641-650.

Vos, J.J. (1972). Literature review of human macular absorption in the visible and its consequences for the cone receptor primaries. Technical report of the Institute for Perception - TNO No. IZF1972-17.

Vos, J. & Walraven, P. (1971). On the derivation of the foveal receptor primaries. *Vision Rsearch, 11,* 799-818.

Wässle, H., Yamashita, M., Greferath, U., Grünert, U., & Müller, F. (1991). The rod bipolar cell of the mammalian retina. *Neuroscience, 7,* 99-112.

Wässle, H., Grunert, U., Rohrenbeck, J., & Boycott, B. (1989). Cortical magnification factor and the ganglion cell density of the primate retina. *Nature, 341,* 643-646.

Weale, R.A. (1953). Spectral sensitivity and wave-length discrimination of the peripheral retina. *Journal of Physiology, London, 119,* 170-190.

Weitzman, D.O. & Kinney, J.S. (1969). Effect of stimulus size, duration, and retinal location upon the appearance of color. *Journal of the Optical Society of America, 59,* 640-643.

Westheimer, G. (1965). Spatial interaction in the human retina during scotopic vision. *Journal of Physiology (London), 181,* 881-894.

Westheimer, G. (1966). The Maxwellian view. *Vision Research, 6,* 669-682.

Wilson, M.E. (1970). Invariant features of spatial summation with changing locus in the visual field. *Journal of Physiology, 207,* 611-622.

Winer, B., Brown, D., & Michels, K. (1991). *Statistical Principles in Experimental Design, 3rd Ed.* McGraw-Hill, Inc.: New York.

Wooten, B.R. & Wald, G. (1973). Color-vision mechanisms in the peripheral retinas of normal and dichromatic observers. *Journal of General Physiology, 61,* 125-145.

Wyszecki, G., & Stiles, W. (1982). *Color Science: Concepts, and Methods, Quantitative Data and Formulae.* Wiley: New York.

Reproduced with permission of the copyright owner. Further reproduction prohibited without permission.

Appendix A

Mean Foveal Data

Reproduced with permission of the copyright owner. Further reproduction prohibited without permission.

Reproduced with permission of the copyright owner. Further reproduction prohibited without permission.

Fovea

1.00° Stimulus

Mean

λ	Blue	Green	Yellow	Red	Sat
440	73.57	0.00	0.00	26.43	93.57
450	85.71	0.00	0.00	14.29	95.71
460	88.57	0.00	0.00	11.43	94.29
470	92.14	1.43	0.00	6.43	91.43
480	88.57	11.43	0.00	0.00	87.14
490	72.14	27.86	0.00	0.00	86.43
500	38.57	61.43	0.00	0.00	88.57
510	30.00	70.00	0.00	0.00	89.29
520	16.43	78.57	5.00	0.00	86.43
530	9.29	82.14	5.71	0.00	82.14
540	7.14	69.29	23.57	0.00	83.57
550	0.00	61.43	38.57	0.00	77.86
560	0.00	46.43	53.57	0.00	78.57
570	0.00	7.14	88.57	4.29	77.86
580	0.00	0.00	72.14	27.86	79.29
590	0.00	0.00	48.57	51.43	81.43
600	0.00	0.00	35.71	64.29	83.57
610	0.00	0.00	31.43	70.00	85.00
620	0.00	0.00	20.00	80.00	87.86
630	0.00	0.00	9.29	90.71	91.43
640	0.00	0.00	7.86	92.14	93.57
650	0.00	0.00	8.57	91.43	94.29
660	0.00	0.00	3.57	96.43	95.00

Standard Error of the Mean

Blue	Green	Yellow	Red	Sat
4.97	0.00	0.00	4.97	1.43
1.70	0.00	0.00	1.70	1.30
3.73	0.00	0.00	3.73	2.54
3.06	1.43	0.00	3.22	2.37
2.61	2.61	0.00	0.00	3.06
6.25	6.25	0.00	0.00	2.83
5.85	5.85	0.00	0.00	2.61
8.66	8.66	0.00	0.00	1.30
6.24	4.19	2.44	0.00	1.80
3.85	3.06	2.97	0.00	2.40
5.65	6.21	7.92	0.00	3.22
0.00	8.78	8.78	0.00	2.14
0.00	10.28	10.28	0.00	3.03
0.00	2.86	2.61	2.97	1.49
0.00	0.00	5.76	5.76	2.54
0.00	0.00	2.37	2.37	2.10
0.00	0.00	1.70	1.70	2.10
0.00	0.00	3.22	2.44	2.89
0.00	0.00	2.44	2.44	2.14
0.00	0.00	2.30	2.30	0.92
0.00	0.00	1.01	1.01	1.43
0.00	0.00	2.37	2.37	0.71
0.00	0.00	0.92	0.92	1.54

Appendix B

Mean Data from the No-Bleach Condition

Reproduced with permission of the copyright owner. Further reproduction prohibited without permission.

Reproduced with permission of the copyright owner. Further reproduction prohibited without permission.

No-Bleach Condition
10° Temporal

0.25° Stimulus

Mean

λ	Blue	Green	Yellow	Red	Sat
440	86.67	2.22	0.00	11.11	50.00
450	88.89	1.11	0.00	10.00	53.33
460	78.33	2.22	11.11	8.33	40.00
470	62.33	26.11	11.11	0.44	31.11
480	54.44	21.11	24.44	0.00	30.56
490	42.22	21.67	32.78	3.33	33.33
500	17.78	28.89	48.89	4.44	34.44
510	11.11	30.00	57.78	1.11	36.11
520	28.89	14.44	50.00	6.67	29.44
530	20.00	19.44	60.56	0.00	30.56
540	5.56	25.56	60.00	8.89	32.22
550	5.56	30.56	53.89	10.00	37.22
560	10.56	31.11	49.44	8.89	52.22
570	2.22	11.11	58.33	28.33	41.67
580	0.00	33.33	46.67	20.00	45.00
590	0.00	5.56	52.78	41.67	62.22
600	0.00	2.22	56.67	41.11	68.89
610	0.00	0.00	35.56	64.44	70.56
620	0.00	0.00	30.00	70.00	77.22
630	0.00	0.00	22.22	77.78	78.33
640	0.00	0.00	8.89	91.11	83.33
650	0.00	0.00	7.22	92.78	82.22
660	0.00	0.00	15.00	85.00	81.67

Standard Error of the Mean

Blue	Green	Yellow	Red	Sat
4.41	2.22	0.00	4.55	6.92
2.74	1.11	0.00	3.00	5.71
10.17	2.22	11.11	3.00	8.33
14.37	10.73	8.89	0.44	4.31
14.73	9.64	14.44	0.00	6.79
13.82	7.55	14.12	2.36	5.34
11.88	12.41	14.28	2.42	7.09
11.11	12.13	13.31	1.11	6.96
14.67	8.84	15.18	5.53	5.17
12.02	9.22	15.60	0.00	6.37
3.77	12.81	14.81	6.55	6.83
5.56	9.52	11.66	8.82	7.55
10.56	10.86	11.26	7.67	7.73
2.22	8.73	14.95	14.09	8.42
0.00	12.80	10.27	10.41	6.35
0.00	3.67	9.06	11.24	4.34
0.00	2.22	10.03	10.89	3.31
0.00	0.00	11.71	11.71	4.75
0.00	0.00	10.57	10.57	3.13
0.00	0.00	9.13	9.13	4.41
0.00	0.00	4.15	4.15	2.36
0.00	0.00	2.65	2.65	4.26
0.00	0.00	2.64	2.64	4.17

0.5° Stimulus

Mean

Blue	Green	Yellow	Red	Sat
83.00	0.00	0.00	17.00	70.50
88.00	2.00	0.00	10.00	69.00
90.50	7.00	0.00	2.50	62.50
83.00	15.00	0.00	2.00	63.00
59.50	39.50	1.00	0.00	52.50
10.00	51.00	39.00	0.00	62.00
0.00	53.00	47.00	0.00	56.50
2.00	56.00	42.00	0.00	58.50
0.00	53.50	46.50	0.00	60.00
0.00	21.50	70.50	8.00	64.00
1.00	36.50	62.50	0.00	59.50
0.00	16.00	78.00	6.00	70.50
0.00	17.50	78.00	4.50	67.00
0.00	4.00	74.00	22.00	74.50
0.00	13.50	69.00	17.50	67.00
0.00	6.00	63.00	31.00	75.00
0.00	0.00	46.50	53.50	78.00
0.00	0.00	25.50	74.50	82.00
0.00	0.00	20.00	80.00	85.50
0.00	0.00	17.50	82.50	83.50
0.00	0.00	13.00	87.00	87.50
0.00	0.00	11.00	89.00	87.00
0.00	0.00	12.00	88.00	87.00

Standard Error of the Mean

Blue	Green	Yellow	Red	Sat
2.49	0.00	0.00	2.49	3.91
2.00	2.00	0.00	2.11	4.20
1.74	2.00	0.00	1.71	6.07
3.27	3.65	0.00	2.00	4.90
10.18	9.56	1.00	0.00	5.93
8.03	9.71	10.80	0.00	3.82
0.00	12.02	12.02	0.00	4.95
2.00	10.35	11.04	0.00	3.34
0.00	9.49	9.49	0.00	5.43
0.00	11.01	10.42	5.07	4.76
1.00	10.00	10.63	0.00	5.80
0.00	6.00	6.29	4.99	4.50
0.00	8.00	7.46	3.02	4.78
0.00	2.21	7.48	8.41	3.61
0.00	8.43	8.06	6.80	1.70
0.00	4.99	6.84	7.95	2.58
0.00	0.00	8.43	8.43	2.38
0.00	0.00	4.97	4.97	3.09
0.00	0.00	4.41	4.41	1.38
0.00	0.00	2.61	2.61	2.24
0.00	0.00	3.51	3.51	2.50
0.00	0.00	1.80	1.80	2.60
0.00	0.00	2.91	2.91	2.26

Reproduced with permission of the copyright owner. Further reproduction prohibited without permission.

No-Bleach Condition
10° Temporal

1.00° Stimulus

Mean

λ	Blue	Green	Yellow	Red	Sat
440	76.00	0.00	0.00	24.00	80.00
450	87.50	0.00	0.00	12.50	83.50
460	93.00	5.00	0.00	2.00	79.50
470	90.00	10.00	0.00	0.00	78.50
480	55.00	40.50	3.50	1.00	71.50
490	13.50	71.50	15.00	0.00	76.50
500	6.00	75.50	18.50	0.00	75.00
510	6.50	74.50	19.00	0.00	78.00
520	4.00	59.50	36.50	0.00	75.00
530	0.00	52.00	48.00	0.00	73.00
540	0.00	36.00	64.00	0.00	76.00
550	0.00	40.00	60.00	0.00	72.00
560	0.00	9.00	84.00	7.00	81.50
570	0.00	2.50	84.00	13.50	80.00
580	0.00	0.00	70.50	29.50	81.00
590	0.00	0.00	50.00	50.00	80.00
600	0.00	0.00	36.00	65.00	83.50
610	0.00	0.00	23.00	77.00	82.50
620	0.00	0.00	23.50	76.50	87.00
630	0.00	0.00	14.50	85.50	88.50
640	0.00	0.00	12.50	87.50	88.00
650	0.00	0.00	7.50	92.50	90.50
660	0.00	0.00	8.00	92.00	90.50

Standard Error of the Mean

Blue	Green	Yellow	Red	Sat
4.27	0.00	0.00	4.27	3.16
2.71	0.00	0.00	2.71	3.50
2.49	2.69	0.00	1.11	3.45
2.47	2.47	0.00	0.00	3.88
10.98	9.56	2.36	1.00	3.50
5.58	5.63	6.75	0.00	3.42
4.27	4.80	5.43	0.00	4.22
3.50	2.83	4.82	0.00	4.36
4.00	7.69	8.69	0.00	3.50
0.00	10.03	10.03	0.00	3.51
0.00	7.99	7.99	0.00	4.00
0.00	8.13	8.13	0.00	3.74
0.00	3.14	3.32	3.89	2.79
0.00	1.34	5.15	5.68	3.65
0.00	0.00	7.09	7.09	2.67
0.00	0.00	8.66	8.66	2.47
0.00	0.00	2.56	2.36	2.24
0.00	0.00	2.91	2.91	3.18
0.00	0.00	4.66	4.66	2.71
0.00	0.00	1.74	1.74	2.11
0.00	0.00	2.01	2.01	2.26
0.00	0.00	1.54	1.54	2.93
0.00	0.00	1.11	1.11	2.41

2.00° Stimulus

Mean

Blue	Green	Yellow	Red	Sat
75.00	0.00	0.00	25.00	87.00
89.00	1.00	0.00	9.00	91.00
94.50	3.00	0.00	2.50	88.50
91.50	6.50	0.00	2.00	88.50
58.50	41.50	0.00	0.00	79.00
16.00	70.50	13.50	0.00	83.00
7.00	73.50	19.50	0.00	81.50
6.50	76.00	17.50	0.00	84.50
5.00	79.00	16.00	0.00	81.50
0.00	75.50	24.50	0.00	83.00
0.00	49.00	51.00	0.00	75.00
0.00	32.00	68.00	0.00	76.50
0.00	15.00	84.00	1.00	76.00
0.00	0.00	83.50	16.50	84.00
0.00	0.00	58.00	42.00	80.00
0.00	0.00	44.50	55.50	84.00
0.00	0.00	31.00	69.00	85.00
0.00	0.00	22.00	78.00	89.50
0.00	0.00	20.00	80.00	88.50
0.00	0.00	11.50	88.50	91.00
0.00	0.00	12.50	87.50	90.00
0.00	0.00	6.00	94.00	93.00
0.00	0.00	6.50	93.50	94.40

Standard Error of the Mean

Blue	Green	Yellow	Red	Sat
3.42	0.00	0.00	3.42	2.13
1.80	1.00	0.00	1.80	2.67
1.57	1.70	0.00	1.12	2.99
2.69	3.08	0.00	0.82	2.36
7.34	7.34	0.00	0.00	3.32
5.21	3.98	6.06	0.00	3.59
3.59	5.73	7.09	0.00	3.66
4.48	4.33	4.90	0.00	1.89
3.42	3.93	4.64	0.00	3.73
0.00	4.62	4.62	0.00	2.71
0.00	8.62	8.62	0.00	3.65
0.00	8.44	8.44	0.00	2.59
0.00	6.45	6.27	1.00	3.40
0.00	0.00	3.66	3.66	2.56
0.00	0.00	6.84	6.84	2.11
0.00	0.00	4.11	4.11	1.94
0.00	0.00	3.40	3.40	2.36
0.00	0.00	2.91	2.91	1.38
0.00	0.00	2.98	2.98	1.07
0.00	0.00	3.17	3.17	2.08
0.00	0.00	2.61	2.61	1.97
0.00	0.00	1.25	1.25	1.53
0.00	0.00	1.98	1.98	1.34

Reproduced with permission of the copyright owner. Further reproduction prohibited without permission.

No-Bleach Condition
10° Temporal

3.00° Stimulus

Mean

λ	Blue	Green	Yellow	Red	Sat
440	77.00	0.00	0.00	23.00	86.50
450	87.00	2.00	0.00	11.00	92.00
460	94.50	2.50	0.00	3.00	90.50
470	92.00	5.50	0.00	2.50	90.50
480	73.50	26.50	0.00	0.00	84.00
490	29.50	67.50	3.00	0.00	88.00
500	3.50	76.00	20.50	0.00	89.50
510	3.00	79.00	18.00	0.00	88.50
520	0.00	70.00	30.00	0.00	87.50
530	0.00	67.00	33.00	0.00	84.00
540	0.00	58.50	41.50	0.00	81.00
550	0.00	36.50	63.50	0.00	78.00
560	0.00	21.00	79.00	0.00	76.50
570	0.00	0.00	86.00	14.00	84.50
580	0.00	0.00	69.50	30.50	84.00
590	0.00	0.00	44.00	56.00	84.50
600	0.00	0.00	30.50	69.50	85.00
610	0.00	0.00	24.00	76.00	86.50
620	0.00	0.00	18.00	82.00	86.50
630	0.00	0.00	13.00	87.00	91.00
640	0.00	0.00	9.00	91.00	94.00
650	0.00	0.00	5.50	94.50	96.00
660	0.00	0.00	6.00	94.00	93.50

Standard Error of the Mean

Blue	Green	Yellow	Red	Sat
4.36	0.00	0.00	4.36	2.48
1.70	2.00	0.00	1.94	2.49
1.57	1.71	0.00	1.11	1.74
2.38	2.73	0.00	1.12	1.74
2.89	2.89	0.00	0.00	2.87
7.32	6.20	2.13	0.00	1.86
3.50	4.46	4.86	0.00	2.03
3.00	4.82	5.12	0.00	1.98
0.00	4.41	4.41	0.00	2.50
0.00	4.90	4.90	0.00	2.67
0.00	7.78	7.78	0.00	2.33
0.00	8.50	8.50	0.00	2.71
0.00	7.48	7.48	0.00	1.83
0.00	0.00	4.14	4.14	1.74
0.00	0.00	6.26	6.26	2.21
0.00	0.00	1.94	1.94	2.52
0.00	0.00	3.20	3.20	2.24
0.00	0.00	4.14	4.14	2.11
0.00	0.00	2.38	2.38	1.67
0.00	0.00	2.00	2.00	2.08
0.00	0.00	2.56	2.56	1.25
0.00	0.00	1.89	1.89	1.45
0.00	0.00	1.25	1.25	1.50

5.00° Stimulus

Mean

Blue	Green	Yellow	Red	Sat
75.00	0.00	0.00	25.00	96.25
92.50	0.00	0.00	7.50	97.50
95.00	1.25	0.00	3.75	97.50
93.75	6.25	0.00	0.00	95.00
61.25	38.75	0.00	0.00	92.50
17.50	78.75	3.75	0.00	93.75
0.00	90.00	10.00	0.00	95.00
0.00	83.75	16.25	0.00	90.00
0.00	83.75	16.25	0.00	88.75
0.00	67.50	32.50	0.00	86.25
0.00	50.00	50.00	0.00	83.75
0.00	30.00	70.00	0.00	83.75
0.00	7.50	92.50	0.00	78.75
0.00	0.00	92.50	7.50	85.00
0.00	0.00	76.25	23.75	85.00
0.00	0.00	42.50	57.50	88.75
0.00	0.00	33.75	66.25	88.75
0.00	0.00	18.75	81.25	90.00
0.00	0.00	13.75	86.25	92.50
0.00	0.00	6.25	93.75	96.00
0.00	0.00	5.00	95.00	97.50
0.00	0.00	3.75	96.25	98.50
0.00	0.00	5.00	95.00	96.00

Standard Error of the Mean

Blue	Green	Yellow	Red	Sat
6.12	0.00	0.00	6.12	2.39
2.50	0.00	0.00	2.50	1.44
2.04	1.25	0.00	2.39	1.44
2.39	2.39	0.00	0.00	2.04
17.12	17.12	0.00	0.00	1.44
10.31	8.26	2.39	0.00	1.25
0.00	2.04	2.04	0.00	2.89
0.00	3.75	3.75	0.00	3.54
0.00	5.54	5.54	0.00	2.39
0.00	2.50	2.50	0.00	1.25
0.00	10.80	10.80	0.00	2.39
0.00	12.25	12.25	0.00	2.39
0.00	3.23	3.23	0.00	1.25
0.00	0.00	1.44	1.44	2.04
0.00	0.00	6.88	6.88	2.89
0.00	0.00	2.50	2.50	1.25
0.00	0.00	2.39	2.39	1.25
0.00	0.00	2.39	2.39	0.00
0.00	0.00	2.39	2.39	1.44
0.00	0.00	2.39	2.39	1.00
0.00	0.00	0.00	0.00	1.44
0.00	0.00	1.25	1.25	1.19
0.00	0.00	2.04	2.04	1.00

Reproduced with permission of the copyright owner. Further reproduction prohibited without permission.

No-Bleach Condition
10° Nasal

0.25° Stimulus

Mean

λ	Blue	Green	Yellow	Red	Sat
440	91.67	3.33	0.00	5.00	27.50
450	92.50	0.83	0.00	6.67	30.00
460	90.00	4.17	0.00	5.83	20.00
470	45.00	8.33	28.33	1.67	19.17
480	59.17	25.83	13.33	1.67	23.33
490	44.17	14.17	25.00	0.00	22.50
500	15.00	7.50	75.83	1.67	30.00
510	32.50	8.33	57.50	1.67	20.00
520	0.00	8.33	55.00	20.00	24.17
530	45.00	33.33	5.00	0.00	13.33
540	4.17	29.17	48.33	1.67	25.00
550	33.33	11.67	37.50	17.50	21.67
560	3.33	36.67	42.50	17.50	27.50
570	15.83	20.83	45.83	17.50	29.17
580	8.33	10.00	78.33	3.33	38.33
590	0.00	29.17	70.00	0.83	35.00
600	0.00	1.67	69.17	29.17	42.50
610	0.00	0.00	50.83	49.17	41.67
620	0.00	0.00	40.00	60.00	47.50
630	0.00	0.00	16.67	83.33	49.17
640	0.00	0.00	37.50	62.50	48.33
650	0.00	0.00	31.67	68.33	50.83
660	0.00	0.00	7.50	92.50	54.17

Standard Error of the Mean

Blue	Green	Yellow	Red	Sat
1.05	2.11	0.00	1.83	10.06
1.12	0.83	0.00	1.67	11.25
4.28	4.17	0.00	3.27	7.19
20.12	4.77	18.33	1.67	7.46
18.99	15.41	13.33	1.67	8.72
20.02	8.21	17.08	0.00	9.90
15.00	3.10	15.41	1.67	11.25
20.56	8.33	19.74	1.05	8.16
0.00	8.33	18.93	16.33	12.54
19.10	15.63	5.00	0.00	6.01
4.17	18.73	21.63	1.05	10.49
21.08	8.33	17.78	16.52	10.85
3.33	16.67	18.43	16.52	11.46
10.52	10.99	20.67	16.52	9.70
8.33	8.16	16.00	3.33	13.46
0.00	17.72	17.46	0.83	13.10
0.00	1.67	12.00	12.68	14.59
0.00	0.00	16.70	16.70	12.82
0.00	0.00	14.55	14.55	16.82
0.00	0.00	1.67	1.67	13.25
0.00	0.00	15.15	15.15	13.70
0.00	0.00	12.89	12.89	12.41
0.00	0.00	3.82	3.82	15.35

0.5° Stimulus

Mean

Blue	Green	Yellow	Red	Sat
91.11	0.00	0.00	8.89	40.00
90.56	0.00	0.00	9.44	42.78
92.22	5.00	0.00	2.78	37.22
78.89	10.00	11.11	0.00	28.33
46.11	28.33	3.33	0.00	24.44
11.11	24.44	53.33	0.00	33.33
1.11	36.67	51.11	0.00	38.89
2.22	32.22	65.56	0.00	38.89
5.56	29.44	64.44	0.56	31.67
0.00	38.89	48.89	1.11	32.22
11.11	16.67	72.22	0.00	42.22
0.00	18.89	79.44	1.67	40.56
0.00	8.89	77.78	2.22	40.56
0.00	2.22	67.78	7.78	36.67
11.11	5.56	78.33	5.00	43.33
0.00	2.22	82.22	15.56	52.78
0.00	0.00	51.88	48.13	56.88
0.00	0.00	44.44	55.56	59.44
0.00	0.56	41.67	57.78	62.78
0.00	0.00	30.56	69.44	63.33
0.00	0.00	35.00	65.00	66.11
0.00	0.00	23.89	76.11	62.78
0.00	0.00	22.22	77.78	66.67

Standard Error of the Mean

Blue	Green	Yellow	Red	Sat
2.74	0.00	0.00	2.74	7.22
2.69	0.00	0.00	2.69	7.69
2.52	2.89	0.00	1.21	8.00
10.73	4.41	11.11	0.00	7.02
14.38	10.99	3.33	0.00	7.29
11.11	12.71	15.55	0.00	8.33
1.11	11.79	13.17	0.00	8.89
2.22	12.11	13.34	0.00	9.23
5.56	11.38	13.58	0.56	6.56
0.00	13.89	13.99	1.11	6.30
11.11	8.33	12.11	0.00	9.40
0.00	8.73	8.35	1.18	9.30
0.00	8.89	12.97	1.21	11.19
0.00	1.69	14.82	7.78	10.10
11.11	5.56	11.15	2.50	9.32
0.00	2.22	4.57	4.96	7.46
0.00	0.00	10.56	10.56	7.50
0.00	0.00	9.11	9.11	6.79
0.00	0.56	10.41	10.77	7.13
0.00	0.00	8.52	8.52	7.31
0.00	0.00	9.01	9.01	7.30
0.00	0.00	9.23	9.23	6.57
0.00	0.00	8.70	8.70	7.31

Reproduced with permission of the copyright owner. Further reproduction prohibited without permission.

No-Bleach Condition
10° Nasal

1.00° Stimulus

Mean

λ	Blue	Green	Yellow	Red	Sat
440	82.78	0.00	0.00	17.22	70.00
450	89.44	1.11	0.00	9.44	71.11
460	89.38	8.75	0.00	1.88	70.63
470	80.00	20.00	0.00	0.00	65.56
480	45.56	50.00	4.44	0.00	64.44
490	14.44	68.33	17.22	0.00	67.22
500	8.33	47.78	43.89	0.00	63.89
510	0.00	63.33	36.11	0.56	65.56
520	11.67	42.78	45.56	0.00	66.67
530	0.00	41.11	58.33	0.56	64.44
540	0.00	26.11	73.89	0.00	62.78
550	6.67	33.89	58.89	0.56	64.44
560	0.00	8.89	90.00	1.11	68.33
570	0.00	1.11	93.89	5.00	67.78
580	0.00	0.00	83.33	16.67	74.44
590	0.00	0.00	54.44	45.56	72.78
600	0.00	0.00	56.67	43.33	71.67
610	0.00	0.00	40.00	60.00	71.67
620	0.00	0.00	29.44	70.56	74.44
630	0.00	0.00	23.89	76.11	77.78
640	0.00	0.00	15.00	85.00	79.44
650	0.00	0.00	12.78	87.22	78.89
660	0.00	0.00	13.89	86.11	77.78

Standard Error of the Mean

Blue	Green	Yellow	Red	Sat
2.65	0.00	0.00	2.65	4.25
1.76	1.11	0.00	2.12	4.55
1.99	2.27	0.00	1.88	5.04
4.64	4.64	0.00	0.00	3.86
11.53	9.54	2.94	0.00	4.29
6.48	8.42	9.54	0.00	3.92
6.24	12.34	14.31	0.00	4.91
0.00	12.39	12.04	0.56	5.03
7.73	11.25	14.13	0.00	4.41
0.00	11.20	10.96	0.56	4.12
0.00	10.10	10.10	0.00	4.34
6.67	9.49	11.81	0.56	6.21
0.00	3.41	3.12	0.73	5.46
0.00	0.73	1.11	1.44	4.09
0.00	0.00	4.71	4.71	4.37
0.00	0.00	6.84	6.84	4.50
0.00	0.00	7.02	7.02	4.41
0.00	0.00	7.91	7.91	4.93
0.00	0.00	4.12	4.12	4.60
0.00	0.00	4.98	4.98	4.87
0.00	0.00	3.73	3.73	5.17
0.00	0.00	2.06	2.06	4.98
0.00	0.00	2.32	2.32	5.28

2.00° Stimulus

Mean

Blue	Green	Yellow	Red	Sat
83.89	0.00	0.00	16.11	80.56
90.00	2.78	0.00	7.22	83.89
90.56	8.33	0.00	1.11	84.44
86.67	13.33	0.00	0.00	81.67
47.22	52.78	0.00	0.00	81.67
20.56	73.89	5.56	0.00	81.11
1.67	67.22	31.11	0.00	83.89
3.33	81.67	15.00	0.00	81.67
2.22	85.00	12.78	0.00	77.22
0.00	62.22	37.78	0.00	77.78
0.00	50.56	49.44	0.00	78.89
0.00	36.67	62.78	0.56	77.22
0.00	17.78	81.67	0.56	79.44
0.00	2.22	94.44	3.33	82.22
0.00	0.00	74.44	25.56	82.22
0.00	0.00	66.67	33.33	84.44
0.00	0.00	48.89	51.11	82.78
0.00	0.00	29.44	70.56	83.33
0.00	0.00	26.11	73.89	85.00
0.00	0.00	21.11	78.89	83.89
0.00	0.00	14.44	85.56	85.00
0.00	0.00	11.67	88.33	86.67
0.00	0.00	11.67	88.33	87.78

Standard Error of the Mean

Blue	Green	Yellow	Red	Sat
2.61	0.00	0.00	2.61	3.67
1.44	1.88	0.00	1.88	3.71
2.27	2.64	0.00	0.73	3.38
3.54	3.54	0.00	0.00	3.33
10.00	10.00	0.00	0.00	2.50
7.70	6.11	2.56	0.00	3.20
1.67	10.28	10.76	0.00	2.74
2.36	6.56	7.07	0.00	2.20
1.69	2.50	3.24	0.00	2.22
0.00	9.17	9.17	0.00	1.69
0.00	8.72	8.72	0.00	2.86
0.00	9.57	9.32	0.56	3.02
0.00	7.64	7.50	0.56	2.94
0.00	1.21	0.56	0.83	2.37
0.00	0.00	5.56	5.56	2.22
0.00	0.00	6.07	6.07	2.27
0.00	0.00	5.82	5.82	1.88
0.00	0.00	3.77	3.77	2.76
0.00	0.00	4.31	4.31	2.36
0.00	0.00	3.71	3.71	3.20
0.00	0.00	2.56	2.56	2.89
0.00	0.00	2.64	2.64	2.89
0.00	0.00	3.00	3.00	2.78

Reproduced with permission of the copyright owner. Further reproduction prohibited without permission.

No-Bleach Condition
10° Nasal

3.00° Stimulus

Mean

λ	Blue	Green	Yellow	Red	Sat
440	83.89	0.00	0.00	16.11	90.56
450	91.67	3.33	0.00	5.00	91.67
460	91.67	5.56	0.00	2.78	90.56
470	85.00	15.00	0.00	0.00	90.00
480	58.33	41.67	0.00	0.00	87.22
490	27.78	71.11	1.11	0.00	89.44
500	11.11	83.33	5.56	0.00	89.44
510	6.11	87.22	6.67	0.00	86.67
520	1.11	82.78	16.11	0.00	85.00
530	8.89	81.11	10.00	0.00	86.67
540	5.56	55.56	38.89	0.00	79.44
550	0.00	40.00	60.00	0.00	82.22
560	0.00	10.56	87.22	2.22	84.44
570	0.00	2.22	93.33	4.44	86.11
580	0.00	0.00	77.22	22.78	86.11
590	0.00	0.00	56.67	43.33	86.67
600	0.00	0.00	38.33	61.67	87.78
610	0.00	0.00	26.67	73.33	87.78
620	0.00	0.00	20.56	79.44	89.44
630	0.00	0.00	18.33	81.67	90.00
640	0.00	0.00	11.67	88.33	92.78
650	0.00	0.00	7.78	92.22	95.44
660	0.00	0.00	10.56	89.44	91.67

Standard Error of the Mean

Blue	Green	Yellow	Red	Sat
1.62	0.00	0.00	1.62	2.42
1.67	1.44	0.00	2.20	2.20
2.20	2.56	0.00	1.47	2.27
3.73	3.73	0.00	0.00	1.18
7.17	7.17	0.00	0.00	1.47
8.13	7.72	1.11	0.00	2.12
6.39	5.65	2.56	0.00	1.55
3.51	2.37	1.86	0.00	2.50
1.11	2.78	3.31	0.00	1.18
5.45	4.39	3.44	0.00	1.86
5.56	6.99	8.49	0.00	2.27
0.00	7.99	7.99	0.00	2.06
0.00	4.29	3.83	1.47	2.12
0.00	1.69	1.18	1.00	1.11
0.00	0.00	7.37	7.37	1.39
0.00	0.00	5.40	5.40	1.18
0.00	0.00	3.33	3.33	1.47
0.00	0.00	4.08	4.08	1.21
0.00	0.00	3.06	3.06	1.30
0.00	0.00	3.63	3.63	1.67
0.00	0.00	2.76	2.76	1.21
0.00	0.00	2.06	2.06	1.72
0.00	0.00	2.82	2.82	1.18

5.00° Stimulus

Mean

Blue	Green	Yellow	Red	Sat
75.00	0.00	0.00	25.00	95.00
92.50	1.25	0.00	6.25	97.50
96.25	2.50	0.00	1.25	96.25
87.50	12.50	0.00	0.00	93.75
43.75	56.25	0.00	0.00	92.50
8.75	88.75	2.50	0.00	95.00
1.25	95.00	3.75	0.00	97.50
1.25	93.75	5.00	0.00	93.75
0.00	83.75	16.25	0.00	90.00
0.00	80.00	20.00	0.00	83.75
0.00	43.75	56.25	0.00	82.50
0.00	33.75	66.25	0.00	80.00
0.00	6.25	93.75	0.00	78.75
0.00	0.00	93.75	6.25	85.00
0.00	0.00	81.25	18.75	86.25
0.00	0.00	50.00	50.00	86.25
0.00	0.00	33.75	66.25	85.00
0.00	0.00	28.75	71.25	90.00
0.00	0.00	20.00	80.00	92.50
0.00	0.00	13.75	86.25	92.50
0.00	0.00	8.75	91.25	95.00
0.00	0.00	7.50	92.50	96.00
0.00	0.00	5.00	95.00	97.25

Standard Error of the Mean

Blue	Green	Yellow	Red	Sat
6.45	0.00	0.00	6.45	3.54
2.50	1.25	0.00	3.15	1.44
1.25	1.44	0.00	1.25	1.25
2.50	2.50	0.00	0.00	1.25
19.72	19.72	0.00	0.00	2.50
5.15	3.75	1.44	0.00	2.04
1.25	0.00	1.25	0.00	1.44
1.25	1.25	2.04	0.00	2.39
0.00	4.73	4.73	0.00	2.04
0.00	3.54	3.54	0.00	1.25
0.00	14.34	14.34	0.00	1.44
0.00	14.05	14.05	0.00	3.54
0.00	2.39	2.39	0.00	1.25
0.00	0.00	1.25	1.25	0.00
0.00	0.00	7.47	7.47	3.15
0.00	0.00	4.08	4.08	1.25
0.00	0.00	3.15	3.15	0.00
0.00	0.00	9.66	9.66	0.00
0.00	0.00	3.54	3.54	1.44
0.00	0.00	4.27	4.27	1.44
0.00	0.00	4.27	4.27	0.00
0.00	0.00	1.44	1.44	1.00
0.00	0.00	2.04	2.04	1.31

Reproduced with permission of the copyright owner. Further reproduction prohibited without permission.

No-Bleach Condition
10° Superior

0.5° Stimulus

Mean

λ	Blue	Green	Yellow	Red	Sat
440	94.50	2.00	0.00	3.50	21.00
450	94.50	2.00	0.00	3.50	23.00
460	70.00	10.00	10.00	0.00	24.00
470	63.00	16.00	0.00	1.00	15.00
480	2.00	28.00	50.00	0.00	29.00
490	9.00	16.50	63.50	1.00	36.00
500	5.00	26.50	58.50	0.00	37.00
510	5.00	17.50	76.00	1.50	39.00
520	8.00	16.00	75.50	0.50	37.50
530	0.00	19.50	79.00	1.50	45.50
540	0.00	20.00	66.50	3.50	41.50
550	0.00	14.50	84.50	1.00	39.50
560	0.00	21.50	77.00	1.50	44.50
570	5.00	20.00	72.50	2.50	45.50
580	0.00	12.50	80.00	7.50	52.00
590	0.00	12.50	82.50	5.00	54.00
600	0.00	5.00	70.00	25.00	59.50
610	0.00	5.00	73.00	22.00	62.00
620	0.00	0.00	56.00	44.00	62.50
630	0.00	0.50	48.50	51.00	64.50
640	0.00	0.00	56.50	43.50	66.50
650	0.00	0.00	38.00	62.00	67.50
660	0.00	0.00	37.50	62.50	67.00

Standard Error of the Mean

Blue	Green	Yellow	Red	Sat
2.52	2.00	0.00	1.98	4.27
2.17	1.33	0.00	2.11	4.42
12.11	3.65	10.00	0.00	6.74
13.91	9.68	0.00	1.00	5.11
2.00	12.98	15.49	0.00	8.97
6.05	6.91	14.02	1.00	9.54
5.00	11.74	14.80	0.00	8.27
5.00	7.57	10.59	1.07	6.36
8.00	8.19	11.65	0.50	7.12
0.00	12.62	12.40	1.07	8.64
0.00	13.33	14.80	2.99	9.49
0.00	6.26	6.03	0.67	7.65
0.00	10.80	10.52	1.07	7.05
5.00	7.75	10.31	1.34	7.83
0.00	6.02	6.67	5.39	5.88
0.00	7.86	7.54	2.98	4.99
0.00	5.00	7.03	7.23	3.91
0.00	3.42	6.20	7.16	3.67
0.00	0.00	8.19	8.19	3.82
0.00	0.50	8.73	9.03	3.61
0.00	0.00	9.81	9.81	3.80
0.00	0.00	6.84	6.84	4.61
0.00	0.00	6.92	6.92	3.74

1.0° Stimulus

Mean

Blue	Green	Yellow	Red	Sat
89.50	0.00	0.00	10.50	59.00
92.00	3.00	0.00	5.00	58.00
89.50	8.50	0.00	2.00	47.50
90.00	10.00	0.00	0.00	52.50
50.50	22.50	27.00	0.00	40.50
20.00	30.00	49.00	1.00	52.50
14.50	37.00	48.50	0.00	51.50
6.00	35.50	57.50	1.00	52.00
4.00	38.00	58.00	0.00	51.00
0.00	42.00	58.00	0.00	52.50
2.50	35.00	62.50	0.00	54.00
0.00	16.00	83.00	1.00	58.00
0.00	11.00	86.50	2.50	63.50
0.00	1.00	93.50	5.50	60.50
0.00	1.50	80.50	18.00	65.50
0.00	0.00	74.50	25.50	69.00
0.00	0.00	62.50	37.50	68.00
0.00	0.00	55.50	44.50	73.50
0.00	0.00	48.00	52.00	76.50
0.00	0.00	38.00	62.00	75.50
0.00	0.00	26.00	74.00	76.50
0.00	0.00	23.50	76.50	76.00
0.00	0.00	24.00	76.00	78.00

Standard Error of the Mean

Blue	Green	Yellow	Red	Sat
3.61	0.00	0.00	3.61	3.86
2.38	2.13	0.00	2.11	4.10
3.98	4.28	0.00	1.11	6.02
2.69	2.69	0.00	0.00	5.59
11.56	4.43	13.75	0.00	4.74
9.31	8.16	13.86	1.00	4.61
8.90	10.98	14.06	0.00	5.43
4.27	10.29	12.54	1.00	4.90
2.67	11.31	13.13	0.00	5.67
0.00	8.54	8.54	0.00	5.79
2.50	9.13	10.57	0.00	5.76
0.00	7.63	7.46	1.00	4.29
0.00	5.67	5.48	2.01	4.28
0.00	0.67	1.98	2.17	6.64
0.00	1.50	4.25	4.67	3.53
0.00	0.00	5.98	5.98	3.93
0.00	0.00	8.67	8.67	2.38
0.00	0.00	8.38	8.38	3.34
0.00	0.00	5.83	5.83	3.17
0.00	0.00	5.49	5.49	3.61
0.00	0.00	3.93	3.93	3.73
0.00	0.00	2.36	2.36	4.07
0.00	0.00	2.96	2.96	4.36

Reproduced with permission of the copyright owner. Further reproduction prohibited without permission.

No-Bleach Condition
10° Superior

2.00° Stimulus

Mean

λ	Blue	Green	Yellow	Red	Sat
440	81.00	0.00	0.00	19.00	82.50
450	89.50	4.00	0.00	6.50	81.00
460	92.50	7.00	0.00	0.50	84.00
470	84.00	16.00	0.00	0.00	80.00
480	59.00	41.00	0.00	0.00	77.00
490	16.50	76.50	7.00	0.00	80.00
500	5.00	84.00	11.00	0.00	84.00
510	2.50	64.50	33.00	0.00	80.00
520	4.00	62.00	34.00	0.00	80.00
530	1.00	47.00	52.00	0.00	74.00
540	2.00	32.00	65.50	0.50	76.00
550	0.00	27.00	72.50	0.50	74.50
560	0.00	4.00	94.00	2.00	78.00
570	0.00	1.00	88.50	10.50	78.50
580	0.00	0.00	77.00	23.00	80.50
590	0.00	0.00	69.00	31.00	80.50
600	0.00	0.00	43.00	57.00	84.00
610	0.00	0.00	32.50	67.50	84.00
620	0.00	0.00	24.00	76.00	88.00
630	0.00	0.00	15.50	84.50	87.50
640	0.00	0.00	14.00	86.00	87.00
650	0.00	0.00	8.50	91.50	89.00
660	0.00	0.00	11.00	89.00	90.00

Standard Error of the Mean

Blue	Green	Yellow	Red	Sat
3.23	0.00	0.00	3.23	3.18
1.38	1.63	0.00	2.24	3.14
1.71	1.86	0.00	0.50	2.56
3.93	3.93	0.00	0.00	2.24
5.31	5.31	0.00	0.00	3.09
7.15	5.68	2.60	0.00	2.58
3.42	2.45	2.56	0.00	1.45
2.50	7.87	8.60	0.00	1.83
2.77	7.00	8.46	0.00	1.97
1.00	9.55	10.09	0.00	2.67
2.00	11.01	11.96	0.50	2.21
0.00	9.67	9.52	0.50	2.52
0.00	1.80	1.63	1.11	2.60
0.00	1.00	3.66	3.83	1.98
0.00	0.00	7.46	7.46	2.29
0.00	0.00	7.56	7.56	2.29
0.00	0.00	5.44	5.44	2.21
0.00	0.00	3.00	3.00	2.45
0.00	0.00	1.63	1.63	2.13
0.00	0.00	1.57	1.57	2.14
0.00	0.00	2.21	2.21	3.35
0.00	0.00	1.30	1.30	2.56
0.00	0.00	2.08	2.08	1.97

3.00° Stimulus

Mean

Blue	Green	Yellow	Red	Sat
85.00	0.00	0.00	15.00	88.50
90.00	2.50	0.00	7.50	92.50
91.00	7.00	0.00	2.00	90.00
86.00	14.00	0.00	0.00	87.00
56.50	43.50	0.00	0.00	86.00
22.00	77.00	1.00	0.00	87.50
3.50	83.00	13.50	0.00	88.00
0.00	76.00	24.00	0.00	88.00
7.00	77.00	16.00	0.00	85.00
2.50	54.50	43.00	0.00	80.50
2.50	41.50	56.00	0.00	79.00
0.00	21.50	78.50	0.00	80.00
0.00	9.50	87.50	3.00	82.50
0.00	1.00	84.00	15.00	84.50
0.00	0.00	74.50	25.50	83.50
0.00	0.00	46.00	54.00	83.50
0.00	0.00	41.50	58.50	87.00
0.00	0.00	26.00	74.00	89.00
0.00	0.00	20.00	80.00	88.50
0.00	0.00	15.50	84.50	90.00
0.00	0.00	11.00	89.00	90.50
0.00	0.00	11.00	89.00	93.00
0.00	0.00	9.00	91.00	94.80

Standard Error of the Mean

Blue	Green	Yellow	Red	Sat
1.49	0.00	0.00	1.49	2.79
1.49	1.71	0.00	1.86	1.71
1.80	2.26	0.00	1.11	1.67
1.63	1.63	0.00	0.00	1.53
4.02	4.02	0.00	0.00	2.87
7.23	6.96	1.00	0.00	2.27
2.36	2.26	3.17	0.00	2.00
0.00	4.99	4.99	0.00	2.00
3.59	4.42	5.62	0.00	2.58
2.50	8.83	9.78	0.00	3.20
2.50	10.22	11.37	0.00	2.67
0.00	7.82	7.82	0.00	3.57
0.00	4.04	3.44	1.33	2.14
0.00	1.00	5.15	5.37	2.83
0.00	0.00	7.76	7.76	1.67
0.00	0.00	5.21	5.21	1.67
0.00	0.00	3.50	3.50	1.53
0.00	0.00	1.94	1.94	1.94
0.00	0.00	2.89	2.89	2.36
0.00	0.00	2.73	2.73	2.11
0.00	0.00	2.08	2.08	2.73
0.00	0.00	1.94	1.94	1.53
0.00	0.00	1.45	1.45	1.42

Reproduced with permission of the copyright owner. Further reproduction prohibited without permission.

No-Bleach Condition
10° Superior

5.00° Stimulus

	Mean					Standard Error of the Mean				
λ	Blue	Green	Yellow	Red	Sat	Blue	Green	Yellow	Red	Sat
440	76.25	0.00	0.00	23.75	93.75	5.91	0.00	0.00	5.91	3.75
450	92.50	0.00	0.00	7.50	95.00	1.44	0.00	0.00	1.44	2.89
460	95.00	3.75	0.00	1.25	95.00	2.04	2.39	0.00	1.25	2.04
470	95.00	3.75	0.00	1.25	93.75	2.04	2.39	0.00	1.25	2.39
480	66.25	33.75	0.00	0.00	90.00	6.88	6.88	0.00	0.00	2.04
490	21.25	76.25	2.50	0.00	92.50	14.77	13.75	2.50	0.00	1.44
500	0.00	92.50	7.50	0.00	95.00	0.00	1.44	1.44	0.00	2.04
510	0.00	80.00	20.00	0.00	93.75	0.00	6.12	6.12	0.00	1.25
520	0.00	81.25	18.75	0.00	90.00	0.00	1.25	1.25	0.00	0.00
530	0.00	75.00	25.00	0.00	90.00	0.00	6.45	6.45	0.00	2.04
540	0.00	45.00	55.00	0.00	82.50	0.00	9.57	9.57	0.00	1.44
550	0.00	23.75	76.25	0.00	81.25	0.00	7.47	7.47	0.00	2.39
560	0.00	6.25	93.75	0.00	80.00	0.00	1.25	1.25	0.00	2.04
570	0.00	2.50	93.75	3.75	80.00	0.00	2.50	2.39	2.39	2.04
580	0.00	0.00	91.25	8.75	81.25	0.00	0.00	1.25	1.25	3.75
590	0.00	0.00	71.25	28.75	87.50	0.00	0.00	10.48	10.48	1.44
600	0.00	0.00	37.50	62.50	88.75	0.00	0.00	2.50	2.50	1.25
610	0.00	0.00	21.25	78.75	90.00	0.00	0.00	3.75	3.75	0.00
620	0.00	0.00	15.00	85.00	92.50	0.00	0.00	2.89	2.89	1.44
630	0.00	0.00	8.75	91.25	96.25	0.00	0.00	2.39	2.39	1.25
640	0.00	0.00	6.25	93.75	96.25	0.00	0.00	1.25	1.25	1.25
650	0.00	0.00	3.75	96.25	96.25	0.00	0.00	2.39	2.39	1.25
660	0.00	0.00	6.25	93.75	96.25	0.00	0.00	1.25	1.25	1.25

Reproduced with permission of the copyright owner. Further reproduction prohibited without permission.

No-Bleach Condition
10° Inferior

0.5° Stimulus

Mean

λ	Blue	Green	Yellow	Red	Sat
440	92.78	1.11	0.00	6.11	35.00
450	68.89	2.22	0.00	6.67	25.00
460	91.11	8.89	0.00	0.00	28.89
470	62.22	14.44	11.11	1.11	25.56
480	64.44	1.11	10.56	1.67	10.56
490	8.89	22.22	46.67	0.00	15.56
500	22.22	22.78	43.89	0.00	17.22
510	12.22	15.56	58.89	2.22	21.11
520	11.11	22.22	32.22	1.11	13.33
530	33.33	0.00	55.00	0.56	21.67
540	24.44	11.67	63.89	0.00	25.00
550	11.11	16.11	60.56	1.11	22.22
560	8.89	15.56	62.22	2.22	32.78
570	33.33	1.67	62.22	2.78	31.11
580	0.00	11.11	56.67	32.22	42.22
590	11.11	0.00	60.00	28.89	40.00
600	0.00	0.00	75.56	24.44	41.11
610	0.00	0.00	38.33	61.67	53.33
620	0.00	8.89	33.89	57.22	49.44
630	0.00	0.00	28.89	71.11	54.44
640	0.00	0.00	20.00	80.00	65.56
650	0.00	0.00	16.25	83.75	55.63
660	0.00	0.00	21.67	78.33	53.89

Standard Error of the Mean

Blue	Green	Yellow	Red	Sat
3.13	1.11	0.00	3.20	6.18
13.17	2.22	0.00	2.36	6.67
3.09	3.09	0.00	0.00	6.50
13.10	6.69	11.11	1.11	6.94
16.17	1.11	10.56	1.18	5.30
6.76	11.76	17.00	0.00	5.49
14.70	11.99	15.22	0.00	4.26
8.13	7.84	15.56	1.21	6.71
11.11	14.70	16.14	1.11	5.20
16.67	0.00	17.40	0.56	8.70
14.44	8.66	16.02	0.00	6.29
11.11	10.73	15.22	0.73	8.17
6.11	8.64	15.59	1.47	9.02
16.67	1.18	15.59	1.47	8.53
0.00	9.89	11.27	10.90	7.27
11.11	0.00	10.17	7.76	7.91
0.00	0.00	7.43	7.43	6.17
0.00	0.00	9.68	9.68	7.82
0.00	8.89	8.16	10.71	8.23
0.00	0.00	5.88	5.88	9.15
0.00	0.00	9.24	9.24	6.74
0.00	0.00	3.37	3.37	9.28
0.00	0.00	9.20	9.20	8.28

1.00° Stimulus

Mean

Blue	Green	Yellow	Red	Sat
84.00	1.00	0.00	15.00	67.00
90.50	4.50	0.00	5.00	66.50
93.50	2.50	0.00	4.00	68.00
90.00	7.00	0.00	3.00	49.00
46.00	24.00	30.00	0.00	40.50
11.00	41.00	44.00	4.00	56.00
7.50	39.00	52.50	1.00	60.50
3.50	22.00	72.50	2.00	57.00
4.00	22.50	71.00	2.50	55.50
0.00	20.50	79.00	0.50	64.00
0.00	23.00	76.00	1.00	57.00
0.00	1.50	94.50	4.00	65.50
5.00	7.00	79.00	9.00	66.00
0.00	13.50	82.50	4.00	65.50
0.00	6.00	87.50	6.50	68.50
0.00	5.00	67.00	28.00	69.50
0.00	0.00	59.00	41.00	71.50
0.00	0.00	45.50	54.50	77.50
0.00	0.00	27.50	72.50	75.50
0.00	0.00	23.00	77.00	79.00
0.00	0.00	15.00	85.00	79.00
0.00	0.00	17.50	82.50	77.50
0.00	0.00	15.50	84.50	80.50

Standard Error of the Mean

Blue	Green	Yellow	Red	Sat
2.45	1.00	0.00	2.89	6.55
2.03	2.17	0.00	2.11	5.00
1.83	1.71	0.00	1.63	5.44
2.11	2.60	0.00	1.53	5.67
12.13	8.59	15.28	0.00	4.97
6.05	11.13	12.78	2.21	5.47
5.01	12.31	14.36	1.00	6.08
3.50	10.14	11.77	1.11	5.59
4.00	10.14	11.78	1.12	8.18
0.00	9.53	9.42	0.50	4.14
0.00	11.62	11.45	1.00	7.20
0.00	1.07	1.17	1.25	3.83
5.00	5.01	9.42	3.86	5.57
0.00	7.96	7.46	2.08	5.98
0.00	4.00	3.44	2.11	4.48
0.00	5.00	8.70	9.04	3.45
0.00	0.00	6.90	6.90	3.25
0.00	0.00	7.43	7.43	3.35
0.00	0.00	3.96	3.96	3.29
0.00	0.00	4.48	4.48	3.14
0.00	0.00	2.79	2.79	3.56
0.00	0.00	2.61	2.61	3.67
0.00	0.00	4.18	4.18	2.93

Reproduced with permission of the copyright owner. Further reproduction prohibited without permission.

No-Bleach Condition
10° Inferior

2.00° Stimulus

Mean

λ	Blue	Green	Yellow	Red	Sat
440	87.22	0.00	0.00	12.78	84.44
450	89.44	0.00	0.00	10.56	85.56
460	95.56	3.89	0.00	0.56	84.44
470	88.89	10 00	0.00	1.11	82.22
480	58.89	38.89	2.22	0.00	79.44
490	32.78	62.22	5.00	0.00	73.33
500	6.67	82.22	11.11	0.00	78.33
510	6.67	66.11	27.22	0.00	75.56
520	4.44	51.11	44.44	0.00	72.22
530	8.33	53.89	37.78	0.00	72.22
540	0.00	47.22	51.67	1.11	66.11
550	0.00	14.44	82.78	2.78	76.11
560	0.00	6.11	90.00	3.89	76.11
570	0.00	1.67	80.00	18.33	76.67
580	0.00	0.00	77.78	22.22	78.33
590	0.00	0.00	59.44	40.56	78.89
600	0.00	0.00	46.11	53.89	80.00
610	0.00	0.00	35.00	65.00	84.44
620	0.00	0.00	26.67	73.33	83.89
630	0.00	0.00	17.22	82.78	86.67
640	0.00	0.00	13.89	86.11	88.89
650	0.00	0.00	12.78	87.22	87.22
660	0.00	0.00	12.22	87.78	88.33

Standard Error of the Mean

Blue	Green	Yellow	Red	Sat
2.52	0.00	0.00	2.52	3.48
1.30	0.00	0.00	1.30	3.77
1.94	2.00	0.00	0.56	4.29
2.47	2.76	0.00	1.11	4.01
10.37	8.93	2.22	0.00	3.95
10.14	8.54	3.33	0.00	4.86
4.17	3.24	3.41	0.00	2.20
4.71	9.49	10.64	0.00	2.42
4.44	10.16	11.53	0.00	3.13
5.53	10.03	12.19	0.00	3.45
0.00	10.21	9.61	1.11	8.03
0.00	6.32	5.72	1.69	4.06
0.00	2.61	1.86	1.62	3.20
0.00	0.83	7.02	7.50	1.86
0.00	0.00	8.25	8.25	1.18
0.00	0.00	7.97	7.97	3.80
0.00	0.00	5.76	5.76	2.76
0.00	0.00	2.50	2.50	2.12
0.00	0.00	4.41	4.41	2.32
0.00	0.00	2.78	2.78	2.20
0.00	0.00	2.61	2.61	1.82
0.00	0.00	2.52	2.52	2.22
0.00	0.00	3.24	3.24	2.04

3.00° Stimulus

Mean

Blue	Green	Yellow	Red	Sat
82.22	0.00	0.00	17.78	90.56
92.78	3.33	0.00	3.89	90.56
91.67	5.00	0.00	3.33	90.00
90.00	10.00	0.00	0.00	86.11
56.11	43.89	0.00	0.00	87.78
28.33	67.22	4.44	0.00	82.22
5.56	83.89	10.56	0.00	82.22
6.11	78.89	15.00	0.00	81.67
4.44	61.67	33.89	0.00	78.33
8.33	64.44	27.22	0.00	78.33
5.56	49.44	45.00	0.00	72.78
3.33	36.67	60.00	0.00	73.89
0.00	10.00	88.33	1.67	78.89
0.00	5.00	88.89	6.11	77.78
0.00	0.00	78.89	21.11	81.11
0.00	0.00	62.78	37.22	86.11
0.00	0.00	40.00	60.00	85.00
0.00	0.00	32.78	67.22	85.56
0.00	0.00	25.00	75.00	88.89
0.00	0.00	16.67	83.33	88.89
0.00	0.00	12.78	87.22	91.11
0.00	0.00	10.56	89.44	91.11
0.00	0.00	11.67	88.33	92.22

Standard Error of the Mean

Blue	Green	Yellow	Red	Sat
1.69	0.00	0.00	1.69	2.42
1.69	1.67	0.00	1.82	2.82
1.86	2.50	0.00	1.18	2.89
2.36	2.36	0.00	0.00	2.17
12.04	12.04	0.00	0.00	1.88
8.12	6.78	3.38	0.00	2.22
2.94	2.00	3.17	0.00	1.88
3.51	4.31	5.40	0.00	1.44
2.94	8.37	9.96	0.00	2.64
5.14	6.21	8.30	0.00	2.20
5.56	5.49	7.86	0.00	3.02
3.33	10.83	12.50	0.00	2.61
0.00	5.27	4.93	0.83	2.00
0.00	3.33	3.71	3.20	3.13
0.00	0.00	6.60	6.60	1.82
0.00	0.00	6.13	6.13	1.39
0.00	0.00	2.50	2.50	1.67
0.00	0.00	4.34	4.34	1.94
0.00	0.00	4.25	4.25	1.11
0.00	0.00	2.76	2.76	1.62
0.00	0.00	2.65	2.65	1.39
0.00	0.00	2.12	2.12	1.11
0.00	0.00	2.89	2.89	1.69

Reproduced with permission of the copyright owner. Further reproduction prohibited without permission.

No-Bleach Condition
10° Inferior

5.00° Stimulus

Mean

λ	Blue	Green	Yellow	Red	Sat
440	76.25	0.00	0.00	23.75	93.75
450	87.50	0.00	0.00	12.50	97.50
460	95.00	0.00	0.00	5.00	96.25
470	90.00	10.00	0.00	0.00	90.00
480	41.25	57.50	1.25	0.00	93.75
490	22.50	73.75	3.75	0.00	92.50
500	2.50	91.25	6.25	0.00	92.50
510	0.00	53.75	46.25	0.00	87.50
520	0.00	88.75	11.25	0.00	88.75
530	0.00	50.00	50.00	0.00	82.50
540	0.00	27.50	71.25	1.25	76.25
550	0.00	27.50	72.50	0.00	77.50
560	0.00	13.75	86.25	0.00	80.00
570	0.00	0.00	97.50	2.50	81.25
580	0.00	0.00	92.50	7.50	85.00
590	0.00	0.00	67.50	32.50	87.50
600	0.00	0.00	43.75	56.25	87.50
610	0.00	0.00	27.50	72.50	88.75
620	0.00	0.00	15.00	85.00	90.00
630	0.00	0.00	13.75	86.25	93.75
640	0.00	0.00	10.00	90.00	92.50
650	0.00	0.00	7.50	92.50	93.50
660	0.00	0.00	11.25	88.75	94.50

Standard Error of the Mean

Blue	Green	Yellow	Red	Sat
2.39	0.00	0.00	2.39	3.15
3.23	0.00	0.00	3.23	1.44
2.89	0.00	0.00	2.89	1.25
4.08	4.08	0.00	0.00	2.04
22.76	22.03	1.25	0.00	1.25
16.52	14.91	2.39	0.00	1.44
2.50	1.25	2.39	0.00	1.44
0.00	19.93	19.93	0.00	2.50
0.00	1.25	1.25	0.00	2.39
0.00	20.41	20.41	0.00	2.50
0.00	13.77	12.97	1.25	2.39
0.00	7.50	7.50	0.00	1.44
0.00	5.54	5.54	0.00	2.04
0.00	0.00	1.44	1.44	5.15
0.00	0.00	1.44	1.44	2.04
0.00	0.00	11.09	11.09	2.50
0.00	0.00	10.68	10.68	1.44
0.00	0.00	5.20	5.20	1.25
0.00	0.00	5.00	5.00	0.00
0.00	0.00	5.15	5.15	1.25
0.00	0.00	3.54	3.54	1.44
0.00	0.00	4.79	4.79	2.18
0.00	0.00	5.15	5.15	2.60

Appendix C

Mean Data from the Rod-Bleach Condition

Reproduced with permission of the copyright owner. Further reproduction prohibited without permission.

Reproduced with permission of the copyright owner. Further reproduction prohibited without permission.

Rod-Bleach Condition
10° Temporal

0.098° Stimulus

Mean

λ	Blue	Green	Yellow	Red	Sat
440	86.67	0.00	0.00	13.33	85.56
450	94.44	1.67	0.00	3.89	67.78
460	80.56	14.44	0.00	5.00	80.56
470	67.22	13.33	6.11	13.33	67.22
480	70.00	30.00	0.00	0.00	57.78
490	15.56	38.89	38.89	6.67	49.44
500	2.22	46.67	48.33	2.78	57.22
510	0.00	35.00	38.33	26.67	55.56
520	1.11	28.89	58.89	11.11	62.22
530	0.00	20.56	51.67	27.78	54.44
540	5.56	5.56	60.00	28.89	61.11
550	0.00	19.44	54.44	26.11	55.00
560	6.67	10.00	27.22	56.11	61.67
570	0.00	0.00	37.78	62.22	56.67
580	8.89	3.33	27.78	60.00	61.11
590	0.00	0.00	18.33	81.67	78.33
600	0.00	0.00	53.89	46.11	64.44
610	0.00	0.00	20.56	79.44	76.67
620	0.00	0.00	17.78	82.22	77.78
630	0.00	0.00	12.22	87.78	80.56
640	0.00	0.00	21.11	78.89	73.89
650	0.00	0.00	12.78	87.22	70.00
660	0.00	0.00	17.78	82.22	73.33

Standard Error of the Mean

Blue	Green	Yellow	Red	Sat
2.50	0.00	0.00	2.50	2.56
1.30	1.18	0.00	1.39	10.61
8.95	9.73	0.00	1.86	2.27
14.07	7.99	5.51	10.31	7.64
8.98	8.98	0.00	0.00	7.37
9.73	14.67	15.06	4.49	9.18
2.22	13.72	13.51	2.22	5.01
0.00	14.19	9.65	11.18	7.24
1.11	13.69	14.86	9.92	5.01
0.00	12.87	13.44	12.56	5.62
5.56	5.56	13.20	11.45	4.77
0.00	11.97	13.32	12.69	8.16
6.67	6.67	12.99	16.24	8.12
0.00	0.00	11.15	11.15	8.70
8.89	2.36	12.91	15.12	8.11
0.00	0.00	4.33	4.33	4.08
0.00	0.00	12.63	12.63	3.38
0.00	0.00	4.75	4.75	3.73
0.00	0.00	8.00	8.00	4.26
0.00	0.00	3.24	3.24	2.82
0.00	0.00	7.85	7.85	4.91
0.00	0.00	3.92	3.92	8.16
0.00	0.00	4.94	4.94	3.91

0.125° Stimulus

Mean

Blue	Green	Yellow	Red	Sat
84.58	0.00	0.00	15.42	90.83
91.67	0.83	0.00	7.50	91.25
89.58	6.25	0.00	4.17	84.58
84.17	15.00	0.00	0.83	80.00
40.42	35.42	23.33	0.83	70.83
25.00	40.00	32.92	2.08	62.08
10.83	41.25	41.67	6.25	70.42
27.50	24.17	38.75	9.58	73.33
5.00	49.17	33.33	12.50	71.67
5.00	35.83	42.92	17.08	70.42
0.00	43.64	48.18	8.18	67.27
4.17	34.58	35.00	26.25	72.08
0.00	17.50	34.58	47.92	68.75
0.00	30.00	39.17	30.83	73.75
0.00	6.67	35.42	57.92	72.92
0.00	0.00	37.92	62.08	76.67
0.00	0.45	25.00	74.55	79.09
0.00	0.00	35.83	64.17	76.67
0.00	0.00	26.25	73.75	84.58
0.00	0.00	20.42	79.58	81.25
0.00	0.00	17.50	82.50	86.25
0.00	0.00	17.92	82.08	81.25
0.00	0.00	13.33	86.67	83.75

Standard Error of the Mean

Blue	Green	Yellow	Red	Sat
1.79	0.00	0.00	1.79	1.49
1.42	0.83	0.00	1.57	1.75
1.79	2.05	0.00	1.93	2.71
3.13	3.43	0.00	0.56	3.14
8.78	7.70	12.21	0.83	3.30
9.25	10.37	12.68	2.08	8.11
5.83	9.01	10.77	5.81	3.96
11.69	9.81	12.00	5.72	6.16
2.89	12.15	10.61	7.40	5.45
3.37	13.00	12.45	8.56	7.08
0.00	15.15	13.54	5.01	6.85
4.17	12.05	11.66	12.11	6.89
0.00	9.38	9.52	12.45	7.36
0.00	11.55	7.83	9.81	4.53
0.00	6.67	8.76	10.12	5.31
0.00	0.00	8.97	8.97	5.69
0.00	0.45	7.92	8.32	4.85
0.00	0.00	9.37	9.37	4.10
0.00	0.00	7.39	7.39	2.78
0.00	0.00	4.24	4.24	4.57
0.00	0.00	6.89	6.89	2.76
0.00	0.00	6.87	6.87	5.33
0.00	0.00	3.10	3.10	3.85

Reproduced with permission of the copyright owner. Further reproduction prohibited without permission.

Rod-Bleach Condition
10° Temporal

0.25° Stimulus

Mean

λ	Blue	Green	Yellow	Red	Sat
440	83.00	0.00	0.00	17.00	89.50
450	86.50	2.00	0.00	11.50	89.00
460	90.00	6.00	0.00	4.00	88.00
470	86.00	9.00	0.00	5.00	83.00
480	23.50	66.50	10.00	0.00	76.50
490	6.00	80.50	13.50	0.00	81.50
500	6.00	75.00	18.50	0.50	81.50
510	4.00	63.00	32.50	0.50	79.50
520	3.50	45.50	50.00	1.00	80.50
530	11.00	53.50	32.50	3.00	79.00
540	0.00	65.50	33.50	1.00	80.50
550	1.00	33.00	51.00	15.00	81.00
560	3.50	22.50	48.50	25.50	80.50
570	0.00	4.00	59.50	36.50	82.00
580	0.00	0.00	47.50	52.50	85.00
590	0.00	0.00	46.50	53.50	83.00
600	0.00	0.00	13.50	86.50	88.00
610	0.00	0.00	18.00	82.00	89.50
620	0.00	0.00	11.00	89.00	90.00
630	0.00	0.00	9.00	91.00	91.50
640	0.00	0.00	13.00	87.00	92.00
650	0.00	0.00	8.50	91.50	92.00
660	0.00	0.00	6.00	94.00	93.00

Standard Error of the Mean

Blue	Green	Yellow	Red	Sat
2.49	0.00	0.00	2.49	1.57
1.98	1.33	0.00	2.69	1.00
1.49	2.08	0.00	1.80	1.11
3.56	4.14	0.00	2.36	3.27
8.63	7.15	5.37	0.00	5.22
4.00	2.17	2.59	0.00	3.80
4.27	8.82	8.73	0.50	1.83
4.00	8.37	8.73	0.50	2.73
3.50	11.56	12.27	0.67	1.17
7.67	10.11	9.81	3.00	2.77
0.00	9.44	8.69	1.00	1.74
1.00	11.81	10.90	8.88	3.14
3.50	11.04	10.73	9.76	3.69
0.00	2.67	8.61	9.97	2.26
0.00	0.00	9.61	9.61	1.97
0.00	0.00	6.46	6.46	1.53
0.00	0.00	2.89	2.89	1.33
0.00	0.00	3.18	3.18	1.89
0.00	0.00	3.14	3.14	1.67
0.00	0.00	2.45	2.45	1.30
0.00	0.00	3.43	3.43	1.11
0.00	0.00	2.69	2.69	1.70
0.00	0.00	1.25	1.25	1.11

0.5° Stimulus

Mean

Blue	Green	Yellow	Red	Sat
79.50	0.00	0.00	20.50	89.50
88.00	1.50	0.00	10.50	88.00
87.50	12.50	0.00	0.00	84.00
76.50	23.50	0.00	0.00	78.50
49.50	49.50	1.00	0.00	86.00
11.00	73.50	15.50	0.00	86.00
10.00	76.00	14.00	0.00	87.50
7.00	67.50	25.50	0.00	86.00
1.00	77.50	21.50	0.00	87.00
1.00	58.00	41.00	0.00	86.00
0.50	60.00	39.50	0.00	85.00
0.00	31.50	63.00	5.50	82.50
0.00	22.00	70.50	7.50	83.50
0.00	2.50	67.50	30.00	85.00
0.00	0.00	44.00	56.00	81.00
0.00	0.00	29.00	71.00	87.00
0.00	0.00	28.00	72.00	87.50
0.00	0.00	13.00	87.00	91.50
0.00	0.00	9.50	90.50	92.50
0.00	0.00	8.50	91.50	94.50
0.00	0.00	5.50	94.50	94.50
0.00	0.00	6.00	94.00	94.50
0.00	0.00	4.00	96.00	94.00

Standard Error of the Mean

Blue	Green	Yellow	Red	Sat
2.73	0.00	0.00	2.73	1.74
2.49	1.50	0.00	2.73	2.13
3.89	3.89	0.00	0.00	2.45
4.78	4.78	0.00	0.00	4.54
8.64	8.04	1.00	0.00	1.63
4.52	6.01	7.32	0.00	1.80
4.53	3.40	4.70	0.00	1.71
3.67	7.86	9.38	0.00	1.63
1.00	4.17	4.60	0.00	3.00
1.00	9.29	9.71	0.00	2.21
0.50	10.06	10.26	0.00	2.47
0.00	9.22	8.14	4.44	1.71
0.00	9.55	8.08	3.27	2.48
0.00	2.50	6.92	7.64	1.67
0.00	0.00	6.94	6.94	2.96
0.00	0.00	3.71	3.71	2.38
0.00	0.00	6.06	6.06	1.12
0.00	0.00	1.70	1.70	1.30
0.00	0.00	2.41	2.41	0.83
0.00	0.00	2.36	2.36	0.90
0.00	0.00	1.17	1.17	0.90
0.00	0.00	1.25	1.25	0.50
0.00	0.00	1.25	1.25	0.67

Reproduced with permission of the copyright owner. Further reproduction prohibited without permission.

Rod-Bleach Condition
10° Temporal

1.00 Stimulus

Mean

λ	Blue	Green	Yellow	Red	Sat
440	73.00	0.00	0.00	27.00	89.50
450	87.50	1.50	0.00	11.00	90.50
460	91.50	4.00	0.00	4.50	88.50
470	84.50	15.50	0.00	0.00	89.00
480	64.00	36.00	0.00	0.00	82.50
490	20.00	73.50	6.50	0.00	88.00
500	11.00	74.00	15.00	0.00	88.50
510	8.50	81.50	10.00	0.00	90.50
520	1.50	80.00	18.50	0.00	89.50
530	4.50	78.50	17.00	0.00	89.50
540	0.00	60.00	39.50	0.50	85.00
550	0.00	53.50	46.50	0.00	85.50
560	0.00	12.00	85.50	2.50	83.00
570	0.00	2.00	68.50	29.50	86.00
580	0.00	0.00	38.00	62.00	87.00
590	0.00	0.00	24.00	76.00	88.50
600	0.00	0.00	19.00	81.00	90.00
610	0.00	0.00	12.50	87.50	90.50
620	0.00	0.00	8.50	91.50	94.50
630	0.00	0.00	7.50	92.50	93.50
640	0.00	0.00	4.00	96.00	96.00
650	0.00	0.00	2.50	97.50	95.50
660	0.00	0.00	3.00	97.00	96.50

Standard Error of the Mean

Blue	Green	Yellow	Red	Sat
3.96	0.00	0.00	3.96	2.17
2.01	1.07	0.00	2.56	2.17
1.50	1.80	0.00	1.74	2.11
2.03	2.03	0.00	0.00	1.63
2.67	2.67	0.00	0.00	1.54
6.83	5.17	2.99	0.00	1.53
4.99	7.41	8.16	0.00	1.50
3.73	2.89	3.65	0.00	1.57
1.07	3.94	4.54	0.00	1.17
2.41	4.22	5.39	0.00	1.38
0.00	10.03	9.70	0.50	1.29
0.00	9.13	9.13	0.00	1.74
0.00	4.61	4.04	1.34	1.70
0.00	2.00	6.83	7.47	1.45
0.00	0.00	2.91	2.91	1.33
0.00	0.00	2.96	2.96	1.30
0.00	0.00	2.45	2.45	1.67
0.00	0.00	2.50	2.50	0.90
0.00	0.00	1.30	1.30	0.50
0.00	0.00	1.71	1.71	1.30
0.00	0.00	1.00	1.00	0.67
0.00	0.00	0.83	0.83	0.50
0.00	0.00	0.82	0.82	0.76

2.00° Stimulus

Mean

Blue	Green	Yellow	Red	Sat
72.50	0.00	0.00	27.50	90.00
84.50	1.00	0.00	14.50	92.00
94.00	5.00	0.00	1.00	91.50
89.50	9.00	0.00	1.50	87.00
65.00	35.00	0.00	0.00	86.50
18.50	78.50	3.00	0.00	87.50
2.00	84.00	14.00	0.00	92.00
2.50	85.00	12.50	0.00	90.50
2.00	79.00	19.00	0.00	89.00
2.00	70.00	28.00	0.00	88.00
0.00	61.00	39.00	0.00	87.00
0.00	38.50	60.00	1.50	86.00
0.00	6.00	89.00	5.00	88.50
0.00	1.50	71.50	27.00	89.50
0.00	0.00	39.50	60.50	89.00
0.00	0.00	31.50	68.50	89.50
0.00	0.00	25.00	75.00	91.50
0.00	0.00	12.50	87.50	91.50
0.00	0.00	9.50	90.50	94.50
0.00	0.00	7.00	93.00	94.50
0.00	0.00	5.50	94.50	96.50
0.00	0.00	4.00	96.00	97.50
0.00	0.00	4.00	96.00	96.50

Standard Error of the Mean

Blue	Green	Yellow	Red	Sat
4.10	0.00	0.00	4.10	1.83
2.93	1.00	0.00	3.29	2.13
2.45	2.58	0.00	0.67	1.67
3.76	4.00	0.00	1.07	1.53
4.47	4.47	0.00	0.00	1.50
5.87	4.95	1.53	0.00	2.14
2.00	3.23	3.56	0.00	1.70
1.71	2.58	3.27	0.00	1.38
1.53	3.86	4.58	0.00	1.80
2.00	3.73	4.73	0.00	1.70
0.00	6.98	6.98	0.00	1.53
0.00	10.78	10.19	0.76	1.94
0.00	2.56	2.45	2.47	1.50
0.00	1.07	7.68	8.17	1.57
0.00	0.00	5.65	5.65	1.80
0.00	0.00	3.58	3.58	1.17
0.00	0.00	4.47	4.47	1.07
0.00	0.00	2.81	2.81	1.30
0.00	0.00	1.89	1.89	1.17
0.00	0.00	2.13	2.13	1.38
0.00	0.00	1.38	1.38	0.76
0.00	0.00	0.67	0.67	0.83
0.00	0.00	1.45	1.45	1.07

Reproduced with permission of the copyright owner. Further reproduction prohibited without permission.

Rod-Bleach Condition
10° Temporal

3.00° Stimulus

	Mean					Standard Error of the Mean				
λ	Blue	Green	Yellow	Red	Sat	Blue	Green	Yellow	Red	Sat
440	74.00	0.00	0.00	26.00	91.50	3.48	0.00	0.00	3.48	2.36
450	83.50	0.00	0.00	16.50	91.00	3.08	0.00	0.00	3.08	2.21
460	92.50	2.50	0.00	5.00	93.00	1.71	1.71	0.00	1.67	1.53
470	88.00	11.50	0.00	0.50	90.00	2.71	2.89	0.00	0.50	1.67
480	71.00	29.00	0.00	0.00	86.50	4.40	4.40	0.00	0.00	0.76
490	19.50	75.50	5.00	0.00	86.00	6.21	5.13	3.07	0.00	2.08
500	0.00	84.50	15.50	0.00	91.00	0.00	3.20	3.20	0.00	1.45
510	0.00	80.00	20.00	0.00	90.50	0.00	4.47	4.47	0.00	2.03
520	0.00	79.50	20.50	0.00	90.00	0.00	4.04	4.04	0.00	1.29
530	0.00	71.00	29.00	0.00	87.50	0.00	4.64	4.64	0.00	1.71
540	0.00	45.00	55.00	0.00	88.00	0.00	8.56	8.56	0.00	1.86
550	0.00	32.00	67.50	0.50	85.00	0.00	9.84	9.67	0.50	2.11
560	0.00	13.50	80.00	6.50	89.50	0.00	8.73	7.85	2.24	1.74
570	0.00	0.00	74.50	25.50	89.50	0.00	0.00	5.80	5.80	1.57
580	0.00	0.00	44.00	56.00	90.00	0.00	0.00	3.56	3.56	1.29
590	0.00	0.00	38.00	62.00	90.00	0.00	0.00	3.43	3.43	1.49
600	0.00	0.00	24.00	76.00	90.50	0.00	0.00	3.48	3.48	1.17
610	0.00	0.00	12.50	87.50	93.00	0.00	0.00	2.71	2.71	1.53
620	0.00	0.00	8.50	91.50	95.40	0.00	0.00	2.48	2.48	1.35
630	0.00	0.00	8.00	92.00	95.50	0.00	0.00	2.26	2.26	1.17
640	0.00	0.00	5.50	94.50	96.80	0.00	0.00	1.74	1.74	0.76
650	0.00	0.00	4.50	95.50	97.00	0.00	0.00	1.57	1.57	0.82
660	0.00	0.00	7.50	92.50	94.50	0.00	0.00	2.39	2.39	1.38

Reproduced with permission of the copyright owner. Further reproduction prohibited without permission.

Rod-Bleach Condition
10° Nasal

0.125° Stimulus

Mean

λ	Blue	Green	Yellow	Red	Sat
440	88.00	2.00	0.00	10.00	80.50
450	89.00	7.50	0.00	3.50	81.50
460	87.00	10.00	0.00	3.00	79.00
470	75.50	15.00	9.50	0.00	74.00
480	40.00	59.50	0.50	0.00	70.00
490	12.00	45.50	42.50	0.00	67.50
500	14.00	50.00	35.00	1.00	70.50
510	18.50	45.50	35.00	1.00	70.00
520	13.50	50.00	17.50	19.00	70.00
530	15.00	60.50	21.00	3.50	70.50
540	7.50	62.50	20.00	10.00	70.50
550	5.00	38.00	46.00	11.00	67.00
560	3.00	25.00	27.00	45.00	73.50
570	10.00	17.00	45.50	27.50	68.00
580	0.00	31.00	37.50	31.50	71.50
590	4.00	14.00	50.00	32.00	68.00
600	0.00	9.00	43.00	48.00	72.00
610	0.00	0.00	46.11	53.89	80.56
620	0.00	0.00	26.50	73.50	75.00
630	0.00	0.00	44.00	56.00	75.50
640	0.00	0.00	39.00	61.00	74.00
650	0.00	0.50	31.00	68.50	77.50
660	0.00	0.00	31.50	68.50	74.00

Standard Error of the Mean

Blue	Green	Yellow	Red	Sat
2.13	1.53	0.00	2.58	3.02
1.45	2.27	0.00	1.67	2.89
4.03	4.53	0.00	1.53	4.52
9.20	3.94	9.50	0.00	4.40
10.41	10.20	0.50	0.00	6.75
6.63	10.66	13.52	0.00	6.11
8.06	11.62	12.97	0.67	6.21
6.83	9.96	13.68	1.00	7.23
9.89	13.19	8.83	12.67	7.15
6.24	11.63	11.18	2.36	6.97
3.89	11.09	8.16	8.03	6.21
3.42	12.18	13.92	9.94	5.83
3.00	12.85	9.72	13.06	6.19
10.00	8.44	10.76	12.14	7.90
0.00	13.94	11.09	12.07	6.83
4.00	9.45	12.02	11.23	6.16
0.00	7.95	10.73	12.16	7.57
0.00	0.00	11.27	11.27	2.94
0.00	0.00	8.17	8.17	4.83
0.00	0.00	12.69	12.69	4.74
0.00	0.00	9.30	9.30	6.05
0.00	0.50	9.74	10.11	4.36
0.00	0.00	9.22	9.22	6.36

0.25° Stimulus

Mean

Blue	Green	Yellow	Red	Sat
87.73	4.55	0.00	7.73	86.36
87.73	6.36	0.00	5.91	82.73
91.82	5.91	0.00	2.27	82.73
75.91	14.09	9.09	0.91	75.45
50.00	41.82	8.18	0.00	71.82
30.91	58.18	10.91	0.00	70.91
12.27	55.91	31.82	0.00	78.64
11.82	82.73	5.45	0.00	77.73
10.45	71.36	18.18	0.00	75.91
4.55	33.64	58.18	3.64	72.27
10.91	35.45	52.27	1.36	75.45
9.55	35.91	51.36	3.18	75.91
0.00	29.55	57.73	12.73	72.73
0.00	35.45	45.45	19.09	77.27
0.00	5.45	58.18	36.36	74.09
0.00	1.82	50.91	47.27	79.09
0.00	0.00	31.36	68.64	80.45
0.00	0.00	27.27	72.73	81.36
0.00	0.00	27.27	72.73	83.18
0.00	0.00	24.55	75.45	83.64
0.00	0.00	15.45	84.55	83.64
0.00	0.00	16.36	83.64	83.09
0.00	0.00	14.09	85.91	84.55

Standard Error of the Mean

Blue	Green	Yellow	Red	Sat
1.56	1.84	0.00	2.46	2.14
1.41	2.03	0.00	2.32	2.89
2.05	2.32	0.00	1.24	2.81
8.97	5.17	9.09	0.91	2.73
6.94	5.77	8.18	0.00	4.97
11.32	8.82	4.15	0.00	4.20
5.97	9.41	11.45	0.00	2.70
5.19	4.28	2.07	0.00	2.97
4.98	8.15	8.93	0.00	3.49
4.55	11.28	11.78	1.92	3.12
6.77	11.78	14.08	0.97	2.73
5.74	11.46	13.32	1.94	3.74
0.00	12.24	10.30	5.62	4.74
0.00	11.63	10.01	10.02	3.26
0.00	5.45	9.61	10.12	4.03
0.00	1.82	8.14	8.95	3.15
0.00	0.00	6.43	6.43	3.33
0.00	0.00	5.77	5.77	3.88
0.00	0.00	7.82	7.82	3.18
0.00	0.00	8.32	8.32	2.87
0.00	0.00	5.24	5.24	3.82
0.00	0.00	4.16	4.16	2.91
0.00	0.00	3.56	3.56	3.05

Reproduced with permission of the copyright owner. Further reproduction prohibited without permission.

Rod-Bleach Condition
10° Nasal

0.5 Stimulus

Mean

λ	Blue	Green	Yellow	Red	Sat
440	82.22	0.00	0.00	17.78	84.44
450	89.44	1.67	0.00	8.89	83.33
460	87.78	10.56	0.00	1.67	78.33
470	73.33	26.67	0.00	0.00	79.44
480	44.44	55.56	0.00	0.00	78.33
490	19.44	73.89	6.67	0.00	80.56
500	23.33	62.22	14.44	0.00	82.22
510	4.44	79.44	16.11	0.00	82.78
520	11.11	67.22	21.67	0.00	82.22
530	11.11	77.22	11.67	0.00	81.67
540	8.33	46.11	45.56	0.00	78.89
550	8.89	42.78	46.67	1.67	78.89
560	2.22	51.67	45.00	1.11	77.78
570	0.00	19.44	77.78	2.78	78.33
580	0.00	4.44	74.44	21.11	78.89
590	0.00	0.00	52.22	47.78	78.33
600	0.00	0.00	33.33	66.67	79.44
610	0.00	0.00	20.00	80.00	83.33
620	0.00	0.00	17.22	82.78	83.89
630	0.00	0.00	13.33	86.67	85.89
640	0.00	0.00	13.89	86.11	86.00
650	0.00	0.00	11.67	88.33	87.11
660	0.00	0.00	10.00	90.00	86.67

Standard Error of the Mean

Blue	Green	Yellow	Red	Sat
3.02	0.00	0.00	3.02	3.17
1.94	1.18	0.00	2.47	3.00
1.47	2.27	0.00	1.18	2.76
3.12	3.12	0.00	0.00	2.42
7.47	7.47	0.00	0.00	3.00
8.99	7.40	2.50	0.00	3.06
8.21	9.97	10.78	0.00	3.24
3.38	3.17	4.06	0.00	3.55
5.39	10.48	11.87	0.00	2.65
5.64	4.01	4.08	0.00	3.00
5.53	11.87	14.32	0.00	2.61
4.84	11.52	14.02	1.18	3.80
2.22	12.25	12.50	0.73	3.45
0.00	6.53	5.66	1.69	4.49
0.00	4.44	8.18	8.41	4.15
0.00	0.00	9.36	9.36	3.33
0.00	0.00	7.07	7.07	3.06
0.00	0.00	3.91	3.91	3.73
0.00	0.00	3.13	3.13	3.31
0.00	0.00	3.44	3.44	3.70
0.00	0.00	3.41	3.41	3.36
0.00	0.00	3.73	3.73	2.96
0.00	0.00	3.12	3.12	2.76

1.00° Stimulus

Mean

Blue	Green	Yellow	Red	Sat
78.33	0.00	0.00	21.67	87.78
89.44	0.00	0.00	10.56	88.89
85.56	12.22	0.00	2.22	86.67
77.78	22.22	0.00	0.00	81.67
56.11	43.89	0.00	0.00	85.00
17.78	78.33	3.89	0.00	88.89
11.11	80.00	8.89	0.00	88.89
12.78	83.89	3.33	0.00	90.00
8.89	83.33	7.78	0.00	90.56
5.56	77.22	17.22	0.00	88.33
1.11	66.67	32.22	0.00	87.78
1.11	44.44	53.89	0.56	83.89
0.00	33.33	65.00	1.67	86.11
0.00	10.00	73.89	16.11	85.00
0.00	0.00	51.11	48.89	85.56
0.00	0.00	36.67	63.33	87.22
0.00	0.00	22.78	77.22	88.89
0.00	0.00	16.67	83.33	90.00
0.00	0.00	11.67	88.33	93.33
0.00	0.00	8.33	91.67	92.67
0.00	0.00	7.78	92.22	92.67
0.00	0.00	8.89	91.11	94.33
0.00	0.00	7.78	92.22	94.33

Standard Error of the Mean

Blue	Green	Yellow	Red	Sat
2.76	0.00	0.00	2.76	1.69
1.94	0.00	0.00	1.94	1.82
4.89	5.41	0.00	1.21	1.44
5.01	5.01	0.00	0.00	1.67
6.50	6.50	0.00	0.00	2.50
6.24	5.07	2.00	0.00	1.39
5.94	4.49	3.09	0.00	2.00
5.47	4.55	1.18	0.00	1.67
5.39	4.79	3.34	0.00	1.76
4.44	3.64	4.18	0.00	1.67
1.11	11.79	12.11	0.00	2.06
1.11	11.23	11.57	0.56	2.00
0.00	11.02	10.41	0.83	2.47
0.00	6.18	7.40	7.54	3.12
0.00	0.00	2.47	2.47	1.94
0.00	0.00	5.00	5.00	2.65
0.00	0.00	4.57	4.57	1.82
0.00	0.00	3.33	3.33	1.44
0.00	0.00	2.89	2.89	1.18
0.00	0.00	2.64	2.64	1.40
0.00	0.00	1.69	1.69	2.33
0.00	0.00	2.98	2.98	1.25
0.00	0.00	2.06	2.06	1.25

Reproduced with permission of the copyright owner. Further reproduction prohibited without permission.

Rod-Bleach Condition
10° Nasal

2.00 Stimulus

Mean

λ	Blue	Green	Yellow	Red	Sat
440	73.89	0.00	0.00	26.11	91.67
450	85.00	2.22	0.00	12.78	92.78
460	93.33	3.33	0.00	3.33	91.67
470	84.44	15.56	0.00	0.00	88.33
480	58.33	41.67	0.00	0.00	85.56
490	23.33	74.44	2.22	0.00	89.44
500	6.67	83.89	9.44	0.00	91.11
510	1.11	85.00	13.89	0.00	90.56
520	2.78	85.56	11.67	0.00	90.56
530	0.00	80.56	19.44	0.00	88.89
540	0.00	49.44	50.56	0.00	87.78
550	0.00	42.22	57.78	0.00	86.67
560	0.00	18.89	79.44	1.67	86.67
570	0.00	1.11	89.44	9.44	87.22
580	0.00	0.00	47.22	52.78	86.67
590	0.00	0.00	37.22	62.78	88.33
600	0.00	0.00	24.44	75.56	90.56
610	0.00	0.00	17.78	82.22	91.67
620	0.00	0.00	12.22	87.78	92.78
630	0.00	0.00	9.44	90.56	94.78
640	0.00	0.00	7.78	92.22	95.89
650	0.00	0.00	9.44	90.56	96.56
660	0.00	0.00	8.89	91.11	96.00

Standard Error of the Mean

Blue	Green	Yellow	Red	Sat
3.09	0.00	0.00	3.09	1.67
2.20	2.22	0.00	2.65	1.88
1.44	1.44	0.00	1.67	1.86
2.69	2.69	0.00	0.00	1.44
5.53	5.53	0.00	0.00	1.30
6.72	5.86	1.47	0.00	1.30
4.17	2.98	2.69	0.00	1.11
1.11	2.04	2.61	0.00	1.00
1.47	2.56	3.54	0.00	1.30
0.00	6.79	6.79	0.00	1.82
0.00	9.66	9.66	0.00	1.47
0.00	10.28	10.28	0.00	1.67
0.00	7.11	6.59	0.83	2.36
0.00	1.11	1.55	1.94	1.69
0.00	0.00	6.78	6.78	1.67
0.00	0.00	4.80	4.80	1.86
0.00	0.00	5.36	5.36	1.00
0.00	0.00	3.64	3.64	0.83
0.00	0.00	3.34	3.34	1.47
0.00	0.00	2.94	2.94	1.06
0.00	0.00	3.02	3.02	1.32
0.00	0.00	2.69	2.69	0.78
0.00	0.00	3.41	3.41	1.07

3.00° Stimulus

Mean

Blue	Green	Yellow	Red	Sat
74.44	0.00	0.00	25.56	91.67
87.22	0.00	0.00	12.78	93.89
92.22	3.33	0.00	4.44	93.33
89.44	10.00	0.00	0.56	88.33
61.67	38.33	0.00	0.00	88.33
21.11	74.44	4.44	0.00	89.44
2.78	90.56	6.67	0.00	92.22
1.11	88.33	10.56	0.00	91.67
0.56	90.56	8.89	0.00	91.67
1.11	86.67	12.22	0.00	90.00
0.00	71.67	28.33	0.00	89.44
0.00	32.22	67.78	0.00	86.67
0.00	20.56	78.89	0.56	86.67
0.00	4.44	82.78	12.78	88.89
0.00	0.00	51.11	48.89	88.89
0.00	0.00	33.33	66.67	90.56
0.00	0.00	25.56	74.44	92.78
0.00	0.00	14.44	85.56	93.33
0.00	0.00	13.33	86.67	94.44
0.00	0.00	7.78	92.22	97.11
0.00	0.00	10.00	90.00	96.44
0.00	0.00	8.33	91.67	97.00
0.00	0.00	7.78	92.22	97.11

Standard Error of the Mean

Blue	Green	Yellow	Red	Sat
2.94	0.00	0.00	2.94	0.83
2.06	0.00	0.00	2.06	2.00
1.88	1.44	0.00	2.27	1.67
2.42	2.64	0.00	0.56	1.67
7.02	7.02	0.00	0.00	1.18
8.85	7.79	2.42	0.00	1.00
1.88	1.30	1.67	0.00	1.21
1.11	1.86	2.27	0.00	1.18
0.56	1.30	1.62	0.00	1.18
1.11	1.86	2.37	0.00	1.67
0.00	7.12	7.12	0.00	1.30
0.00	9.83	9.83	0.00	1.67
0.00	8.10	7.94	0.56	1.18
0.00	3.86	6.88	6.83	1.62
0.00	0.00	2.86	2.86	2.00
0.00	0.00	4.33	4.33	1.30
0.00	0.00	4.52	4.52	0.88
0.00	0.00	3.17	3.17	0.83
0.00	0.00	3.54	3.54	1.30
0.00	0.00	2.06	2.06	0.84
0.00	0.00	3.12	3.12	0.73
0.00	0.00	2.76	2.76	1.15
0.00	0.00	2.06	2.06	0.84

Reproduced with permission of the copyright owner. Further reproduction prohibited without permission.

Rod-Bleach Condition
10° Superior

0.125° Stimulus

Mean

λ	Blue	Green	Yellow	Red	Sat
440	86.25	1.25	0.00	12.50	85.83
450	87.50	0.83	0.00	11.67	84.17
460	89.58	5.42	0.00	5.00	81.25
470	87.92	11.67	0.00	0.42	76.67
480	61.67	37.08	0.00	1.25	73.33
490	31.25	42.50	25.42	0.83	68.33
500	41.25	48.75	10.00	0.00	67.50
510	20.83	58.33	15.83	5.00	70.42
520	28.75	45.83	25.42	0.00	73.33
530	0.83	28.33	50.83	20.00	68.33
540	35.83	22.50	30.83	10.83	68.33
550	10.83	27.92	43.75	17.50	70.83
560	15.00	17.50	51.25	16.25	70.42
570	0.00	27.08	38.33	35.42	75.42
580	0.00	20.83	57.92	21.25	68.75
590	0.00	7.50	41.67	50.83	77.08
600	0.00	0.42	32.08	67.50	75.83
610	0.00	0.83	40.83	58.33	77.50
620	0.00	6.67	51.25	42.08	68.33
630	0.00	0.00	60.00	40.00	73.75
640	0.00	0.00	37.50	62.50	75.83
650	0.00	0.00	44.17	55.83	72.92
660	0.00	0.00	35.83	64.17	76.25

Standard Error of the Mean

Blue	Green	Yellow	Red	Sat
1.96	1.25	0.00	2.26	3.13
2.50	0.83	0.00	2.71	3.30
1.44	1.89	0.00	1.85	3.08
2.71	2.84	0.00	0.42	4.37
9.09	9.46	0.00	1.25	4.94
9.81	10.07	11.99	0.83	5.82
10.87	8.03	4.61	0.00	5.31
7.12	9.83	8.59	4.56	4.62
10.77	10.24	11.03	0.00	5.12
0.83	11.42	10.13	8.26	4.82
12.88	9.88	12.04	7.53	6.04
7.93	11.37	11.10	7.70	4.64
10.19	10.60	13.34	9.03	5.69
0.00	11.85	10.21	11.42	5.31
0.00	10.28	9.05	7.54	6.13
0.00	7.50	10.06	10.69	5.02
0.00	0.42	8.84	9.12	4.30
0.00	0.83	9.45	9.87	5.38
0.00	5.82	9.13	10.03	5.45
0.00	0.00	10.44	10.44	6.88
0.00	0.00	9.40	9.40	4.88
0.00	0.00	10.92	10.92	5.17
0.00	0.00	9.37	9.37	4.81

0.25° Stimulus

Mean

Blue	Green	Yellow	Red	Sat
85.50	1.00	0.00	13.50	85.50
90.50	2.00	0.00	7.50	88.00
90.00	7.50	0.00	2.50	85.00
84.00	16.00	0.00	0.00	77.00
43.50	45.50	11.00	0.00	75.50
9.00	57.50	33.50	0.00	79.00
6.00	49.00	45.00	0.00	77.00
4.50	41.00	45.50	9.00	73.50
8.00	36.50	51.50	4.00	79.00
6.00	70.50	23.50	0.00	77.00
4.00	60.00	36.00	0.00	77.50
0.00	37.50	56.50	6.00	73.00
0.00	31.00	58.50	10.50	76.00
0.00	23.00	68.50	8.50	76.50
0.00	0.00	74.00	26.00	79.00
0.00	3.00	64.50	32.50	79.00
0.00	0.00	58.00	42.00	76.50
0.00	0.00	37.22	62.78	81.11
0.00	0.00	32.50	67.50	82.50
0.00	0.00	35.50	64.50	79.50
0.00	0.00	39.50	60.50	81.00
0.00	0.00	28.00	72.00	81.00
0.00	0.00	18.50	81.50	85.00

Standard Error of the Mean

Blue	Green	Yellow	Red	Sat
2.29	1.00	0.00	2.69	2.17
1.74	1.11	0.00	2.27	2.38
2.24	2.71	0.00	1.34	2.47
2.56	2.56	0.00	0.00	3.00
11.40	10.12	8.88	0.00	4.11
6.05	9.70	11.16	0.00	3.86
4.27	8.62	10.78	0.00	3.82
2.41	12.58	12.35	6.05	3.80
6.96	11.95	12.76	3.06	4.14
4.99	8.25	8.63	0.00	4.67
2.67	12.56	13.52	0.00	3.59
0.00	10.49	9.81	6.00	4.10
0.00	12.86	10.22	3.37	3.06
0.00	11.77	10.19	2.99	3.80
0.00	0.00	6.49	6.49	3.06
0.00	3.00	8.64	9.35	3.32
0.00	0.00	9.32	9.32	3.58
0.00	0.00	10.11	10.11	4.06
0.00	0.00	9.52	9.52	4.30
0.00	0.00	9.65	9.65	3.20
0.00	0.00	10.66	10.66	3.40
0.00	0.00	7.23	7.23	4.52
0.00	0.00	6.06	6.06	2.58

Reproduced with permission of the copyright owner. Further reproduction prohibited without permission.

Rod-Bleach Condition
10° Superior

0.5° Stimulus

Mean

λ	Blue	Green	Yellow	Red	Sat
440	85.00	0.00	0.00	15.00	88.00
450	89.50	7.00	0.00	3.50	88.50
460	88.00	10.00	0.00	2.00	84.50
470	78.50	20.50	0.00	1.00	78.50
480	54.50	37.50	8.00	0.00	79.00
490	14.00	69.00	17.00	0.00	85.50
500	6.50	80.50	13.00	0.00	83.50
510	13.50	74.50	12.00	0.00	84.00
520	2.00	67.50	30.50	0.00	84.50
530	1.00	52.50	46.00	0.50	83.00
540	0.00	39.50	56.00	4.50	82.00
550	0.00	34.50	59.50	6.00	81.00
560	0.00	11.50	83.00	5.50	82.50
570	0.00	15.50	69.50	15.00	81.50
580	0.00	0.50	69.00	30.50	82.00
590	0.00	0.00	56.00	44.00	83.00
600	0.00	0.00	34.00	66.00	85.50
610	0.00	0.00	19.50	80.50	88.00
620	0.00	0.00	19.50	80.50	87.00
630	0.00	0.00	13.50	86.50	87.00
640	0.00	0.00	8.50	91.50	90.50
650	0.00	0.00	10.50	89.50	90.00
660	0.00	0.00	13.00	87.00	90.00

Standard Error of the Mean

Blue	Green	Yellow	Red	Sat
2.58	0.00	0.00	2.58	1.70
1.57	2.49	0.00	1.30	1.50
2.13	2.58	0.00	1.53	2.03
3.50	3.98	0.00	1.00	2.48
9.23	7.24	8.00	0.00	3.79
5.57	8.59	9.78	0.00	2.83
3.66	2.52	3.43	0.00	2.24
6.41	4.80	4.23	0.00	2.87
2.00	8.64	9.17	0.00	2.41
1.00	11.14	11.30	0.50	3.35
0.00	11.17	10.05	3.98	3.00
0.00	11.24	9.79	3.93	2.87
0.00	5.38	5.23	3.53	2.71
0.00	9.56	8.67	5.96	2.69
0.00	0.50	9.21	9.38	2.38
0.00	0.00	8.23	8.23	2.38
0.00	0.00	6.86	6.86	2.52
0.00	0.00	2.17	2.17	2.38
0.00	0.00	4.91	4.91	2.00
0.00	0.00	2.99	2.99	2.49
0.00	0.00	2.11	2.11	2.03
0.00	0.00	2.41	2.41	2.11
0.00	0.00	4.10	4.10	2.11

1.00° Stimulus

Mean

Blue	Green	Yellow	Red	Sat
75.00	0.00	0.00	25.00	91.00
88.50	3.50	0.00	8.00	87.00
87.50	12.00	0.00	0.50	86.00
81.50	18.50	0.00	0.00	83.00
60.50	39.50	0.00	0.00	82.50
11.50	82.50	6.00	0.00	89.00
4.00	79.00	17.00	0.00	86.50
4.50	80.00	15.50	0.00	87.50
5.00	73.00	22.00	0.00	88.00
2.00	57.50	40.50	0.00	88.00
0.00	46.00	54.00	0.00	88.00
0.00	30.50	69.50	0.00	85.00
0.00	10.50	79.00	10.50	87.00
0.00	1.50	87.00	11.50	89.00
0.00	0.00	47.50	52.50	86.00
0.00	0.00	46.50	53.50	85.50
0.00	0.00	25.50	74.50	87.00
0.00	0.00	15.00	85.00	91.00
0.00	0.00	11.50	88.50	92.40
0.00	0.00	9.50	90.50	94.20
0.00	0.00	7.50	92.50	95.20
0.00	0.00	5.00	95.00	96.20
0.00	0.00	8.50	91.50	94.30

Standard Error of the Mean

Blue	Green	Yellow	Red	Sat
2.69	0.00	0.00	2.69	1.45
1.98	2.36	0.00	2.13	1.70
3.52	3.67	0.00	0.50	1.94
3.58	3.58	0.00	0.00	1.86
5.65	5.65	0.00	0.00	1.34
5.11	3.89	2.08	0.00	1.00
3.06	3.23	4.03	0.00	2.11
3.20	2.89	3.69	0.00	0.83
3.33	8.10	8.89	0.00	1.53
2.00	8.41	9.20	0.00	1.70
0.00	7.85	7.85	0.00	2.00
0.00	8.58	8.58	0.00	2.11
0.00	6.77	7.45	5.84	1.86
0.00	1.50	5.33	5.48	1.45
0.00	0.00	6.02	6.02	1.25
0.00	0.00	7.11	7.11	1.17
0.00	0.00	1.74	1.74	1.11
0.00	0.00	2.11	2.11	0.67
0.00	0.00	2.69	2.69	1.28
0.00	0.00	2.03	2.03	1.46
0.00	0.00	2.27	2.27	1.04
0.00	0.00	1.67	1.67	0.61
0.00	0.00	2.48	2.48	1.07

Reproduced with permission of the copyright owner. Further reproduction prohibited without permission.

Rod-Bleach Condition
10° Superior

2.00 Stimulus

Mean

λ	Blue	Green	Yellow	Red	Sat
440	75.00	0.00	0.00	25.00	90.00
450	87.50	1.25	0.00	11.25	92.50
460	93.13	5.63	0.00	1.25	88.75
470	81.25	18.75	0.00	0.00	86.88
480	60.63	39.38	0.00	0.00	84.38
490	0.63	86.88	12.50	0.00	90.00
500	0.00	83.13	16.88	0.00	90.63
510	0.00	78.13	21.88	0.00	90.63
520	0.00	78.75	21.25	0.00	91.88
530	0.63	74.38	25.00	0.00	88.13
540	0.00	41.25	58.75	0.00	85.63
550	0.00	19.38	80.63	0.00	85.63
560	0.00	5.00	91.88	3.13	87.50
570	0.00	0.00	78.13	21.88	90.00
580	0.00	0.00	51.88	48.13	87.50
590	0.00	0.00	31.88	68.13	89.38
600	0.00	0.00	21.25	78.75	90.63
610	0.00	0.00	13.13	86.88	91.75
620	0.00	0.00	12.50	87.50	93.00
630	0.00	0.00	9.38	90.63	94.75
640	0.00	0.00	8.75	91.25	94.25
650	0.00	0.00	10.00	90.00	94.38
660	0.00	0.00	11.25	88.75	95.38

Standard Error of the Mean

Blue	Green	Yellow	Red	Sat
3.54	0.00	0.00	3.54	1.64
1.64	1.25	0.00	2.27	1.89
1.62	1.99	0.00	0.82	1.57
4.70	4.70	0.00	0.00	1.88
3.71	3.71	0.00	0.00	1.48
0.63	4.53	4.72	0.00	1.89
0.00	2.30	2.30	0.00	1.48
0.00	3.77	3.77	0.00	1.48
0.00	6.03	6.03	0.00	0.91
0.63	4.57	5.00	0.00	1.62
0.00	7.78	7.78	0.00	1.48
0.00	2.20	2.20	0.00	1.75
0.00	2.99	2.49	1.32	1.89
0.00	0.00	6.05	6.05	1.64
0.00	0.00	7.90	7.90	1.64
0.00	0.00	3.40	3.40	1.13
0.00	0.00	2.80	2.80	1.13
0.00	0.00	3.40	3.40	1.80
0.00	0.00	3.41	3.41	1.55
0.00	0.00	3.59	3.59	1.21
0.00	0.00	2.27	2.27	1.41
0.00	0.00	2.11	2.11	0.63
0.00	0.00	3.63	3.63	1.38

3.00° Stimulus

Mean

Blue	Green	Yellow	Red	Sat
76.50	0.00	0.00	23.50	91.00
88.50	4.50	0.00	7.00	91.50
92.00	5.50	0.00	2.50	91.00
84.50	15.50	0.00	0.00	87.00
54.00	46.00	0.00	0.00	87.50
11.50	82.50	6.00	0.00	90.00
2.00	84.50	13.50	0.00	92.50
2.00	82.50	15.50	0.00	92.50
1.00	86.00	13.00	0.00	91.00
0.50	74.00	25.50	0.00	89.50
0.00	50.00	50.00	0.00	88.00
0.00	28.00	71.50	0.50	88.00
0.00	4.50	91.00	4.50	89.00
0.00	0.00	85.50	14.50	90.50
0.00	0.00	47.00	53.00	89.00
0.00	0.00	33.50	66.50	90.50
0.00	0.00	23.33	76.67	92.67
0.00	0.00	15.50	84.50	93.00
0.00	0.00	12.00	88.00	95.90
0.00	0.00	12.00	88.00	94.50
0.00	0.00	9.50	90.50	94.90
0.00	0.00	11.00	89.00	94.30
0.00	0.00	11.50	88.50	95.30

Standard Error of the Mean

Blue	Green	Yellow	Red	Sat
2.79	0.00	0.00	2.79	1.94
1.50	1.57	0.00	2.60	2.11
2.00	1.74	0.00	2.01	1.25
1.74	1.74	0.00	0.00	0.82
5.21	5.21	0.00	0.00	1.12
4.78	3.52	2.21	0.00	1.05
2.00	2.41	2.79	0.00	1.12
2.00	3.00	3.45	0.00	1.12
1.00	1.00	1.70	0.00	1.25
0.50	4.00	4.31	0.00	1.38
0.00	8.43	8.43	0.00	1.70
0.00	7.57	7.38	0.50	1.33
0.00	2.73	2.21	1.38	1.45
0.00	0.00	2.83	2.83	1.17
0.00	0.00	4.55	4.55	1.25
0.00	0.00	2.48	2.48	1.17
0.00	0.00	3.54	3.54	1.13
0.00	0.00	2.73	2.73	1.11
0.00	0.00	2.38	2.38	0.96
0.00	0.00	2.00	2.00	0.50
0.00	0.00	1.89	1.89	1.00
0.00	0.00	2.21	2.21	1.30
0.00	0.00	2.36	2.36	0.79

Reproduced with permission of the copyright owner. Further reproduction prohibited without permission.

Rod-Bleach Condition
10° Inferior

0.25° Stimulus

Mean

λ	Blue	Green	Yellow	Red	Sat
440	84.55	4.09	0.00	11.36	71.82
450	84.55	10.91	0.00	4.55	70.91
460	82.73	11.36	0.00	5.91	72.73
470	78.64	17.27	2.27	1.82	68.64
480	42.73	36.36	12.27	8.64	57.73
490	42.00	41.50	16.50	0.00	55.50
500	3.64	33.64	46.36	16.36	57.27
510	21.36	23.64	38.18	7.73	54.55
520	10.91	23.64	51.82	13.64	55.45
530	14.55	26.82	35.00	23.64	60.45
540	1.82	17.73	52.73	27.73	60.45
550	7.27	20.91	45.45	26.36	62.27
560	2.73	16.36	61.82	19.09	55.45
570	4.55	4.55	40.45	50.45	62.73
580	0.00	6.36	57.27	36.36	62.73
590	0.00	0.00	43.64	56.36	66.36
600	0.00	0.00	50.45	49.55	65.45
610	0.00	4.55	30.45	65.00	66.36
620	0.00	0.00	25.45	74.55	72.27
630	0.00	0.00	21.82	78.18	68.64
640	0.00	0.00	24.09	75.91	71.82
650	0.00	0.00	46.36	53.64	64.55
660	0.00	0.00	29.55	70.45	70.91

Standard Error of the Mean

Blue	Green	Yellow	Red	Sat
2.90	2.92	0.00	3.02	6.48
4.13	4.99	0.00	1.42	5.55
2.17	3.44	0.00	2.51	4.39
8.29	6.55	2.27	1.22	4.96
12.51	10.98	8.07	7.69	6.04
14.05	11.50	9.43	0.00	4.74
3.64	10.47	11.22	10.29	3.53
11.44	9.54	12.36	6.37	7.31
7.32	10.98	13.18	7.63	3.60
9.28	11.27	11.81	11.12	6.05
1.82	10.17	11.78	10.86	4.23
7.27	9.55	11.94	12.17	4.23
2.73	8.12	10.83	9.36	6.48
4.55	4.55	9.92	10.37	6.01
0.00	6.36	9.08	9.39	4.78
0.00	0.00	10.09	10.09	3.99
0.00	0.00	10.90	10.90	5.33
0.00	4.55	9.13	11.04	4.63
0.00	0.00	7.02	7.02	5.24
0.00	0.00	5.19	5.19	6.40
0.00	0.00	5.59	5.59	4.54
0.00	0.00	11.20	11.20	6.01
0.00	0.00	10.86	10.86	5.71

0.5° Stimulus

Mean

Blue	Green	Yellow	Red	Sat
83.64	0.00	0.00	16.36	79.55
88.64	2.73	0.00	8.64	78.64
88.18	6.82	0.00	5.00	79.09
80.45	19.55	0.00	0.00	75.91
44.09	53.64	2.27	0.00	69.55
24.55	67.27	8.18	0.00	75.45
9.55	61.82	27.27	1.36	72.73
9.09	70.00	20.91	0.00	75.45
13.00	52.50	30.50	4.00	76.00
3.64	27.73	51.82	16.82	74.09
0.00	24.55	58.18	17.27	72.73
6.36	25.91	47.73	20.00	75.00
5.00	14.55	57.27	23.18	75.00
0.00	14.55	50.45	35.00	74.55
0.00	0.00	50.91	49.09	77.73
0.00	1.82	43.64	54.55	75.91
0.00	0.00	29.09	70.91	78.18
0.00	0.00	25.00	75.00	82.73
0.00	0.00	25.91	74.09	80.91
0.00	0.00	12.27	87.73	82.73
0.00	0.00	12.73	87.27	83.64
0.00	0.00	10.00	90.00	82.18
0.00	0.00	15.00	85.00	82.64

Standard Error of the Mean

Blue	Green	Yellow	Red	Sat
1.92	0.00	0.00	1.92	4.88
1.52	1.56	0.00	2.14	4.91
1.82	2.36	0.00	2.13	4.25
4.60	4.60	0.00	0.00	4.03
9.36	8.37	1.56	0.00	6.62
9.26	7.82	3.95	0.00	4.84
6.41	7.67	7.40	1.36	4.28
4.99	7.39	8.22	0.00	4.13
8.41	13.46	12.55	2.33	5.04
3.64	10.56	10.36	8.04	4.66
0.00	10.67	9.08	7.30	4.18
4.72	9.67	11.09	9.72	4.16
5.00	7.99	9.78	8.18	3.81
0.00	8.38	11.35	12.67	3.78
0.00	0.00	10.80	10.80	4.18
0.00	1.82	8.09	9.06	4.31
0.00	0.00	7.74	7.74	4.49
0.00	0.00	7.07	7.07	4.12
0.00	0.00	7.65	7.65	4.85
0.00	0.00	2.97	2.97	4.54
0.00	0.00	3.12	3.12	4.32
0.00	0.00	3.02	3.02	5.03
0.00	0.00	3.09	3.09	4.61

Reproduced with permission of the copyright owner. Further reproduction prohibited without permission.

Rod-Bleach Condition
10° Inferior

1.00° Stimulus

Mean

λ	Blue	Green	Yellow	Red	Sat
440	80.56	0.00	0.00	19.44	85.56
450	89.44	3.33	0.00	7.22	87.78
460	90.00	5.00	0.00	5.00	84.44
470	67.22	31.11	0.00	1.67	78.89
480	28.33	70.56	1.11	0.00	83.33
490	20.56	72.78	6.67	0.00	82.78
500	7.22	73.33	19.44	0.00	80.00
510	9.44	70.56	20.00	0.00	80.00
520	0.00	63.89	36.11	0.00	80.56
530	4.44	70.56	25.00	0.00	80.56
540	0.00	56.67	43.33	0.00	76.67
550	0.00	50.56	49.44	0.00	77.78
560	0.00	4.44	87.78	7.78	80.00
570	0.00	4.44	72.22	23.33	77.78
580	0.00	0.00	57.22	42.78	80.00
590	0.00	0.00	30.00	70.00	85.56
600	0.00	0.00	18.89	81.11	85.00
610	0.00	0.00	16.11	83.89	88.33
620	0.00	0.00	13.89	86.11	88.33
630	0.00	0.00	12.22	87.78	88.89
640	0.00	0.00	11.11	88.89	88.89
650	0.00	0.00	7.78	92.22	90.00
660	0.00	0.00	8.89	91.11	90.56

Standard Error of the Mean

Blue	Green	Yellow	Red	Sat
3.95	0.00	0.00	3.95	2.69
2.12	2.36	0.00	2.22	3.13
2.36	1.86	0.00	2.89	3.38
5.96	6.76	0.00	1.67	4.23
8.12	7.70	1.11	0.00	2.36
7.52	6.67	4.71	0.00	3.02
4.94	7.07	7.79	0.00	4.25
6.26	4.37	5.20	0.00	3.33
0.00	8.81	8.81	0.00	3.06
3.38	4.60	6.12	0.00	2.42
0.00	7.77	7.77	0.00	2.89
0.00	10.82	10.82	0.00	2.65
0.00	1.94	3.13	3.83	3.73
0.00	2.42	8.30	9.43	3.34
0.00	0.00	8.21	8.21	2.76
0.00	0.00	3.44	3.44	2.12
0.00	0.00	3.61	3.61	1.86
0.00	0.00	3.41	3.41	2.50
0.00	0.00	2.86	2.86	2.20
0.00	0.00	3.02	3.02	2.17
0.00	0.00	3.20	3.20	2.17
0.00	0.00	1.47	1.47	1.86
0.00	0.00	2.47	2.47	2.27

2.00° Stimulus

Mean

Blue	Green	Yellow	Red	Sat
77.78	0.00	0.00	22.22	89.44
89.44	2.78	0.00	7.78	91.67
92.78	5.56	0.00	1.67	90.00
89.44	10.00	0.00	0.56	90.00
52.78	47.22	0.00	0.00	83.89
14.44	78.89	5.56	0.00	87.78
8.89	85.56	5.56	0.00	87.22
7.22	85.00	7.78	0.00	85.56
0.00	75.56	24.44	0.00	84.44
0.00	78.89	21.11	0.00	85.56
0.56	70.00	29.44	0.00	81.11
0.00	53.89	46.11	0.00	80.56
0.00	23.89	75.56	0.56	80.56
0.00	1.11	84.44	14.44	82.78
0.00	0.00	54.44	45.56	82.78
0.00	0.00	35.00	65.00	86.11
0.00	0.00	25.56	74.44	87.78
0.00	0.00	16.67	83.33	91.11
0.00	0.00	11.67	88.33	91.11
0.00	0.00	12.22	87.78	92.22
0.00	0.00	8.89	91.11	93.67
0.00	0.00	10.00	90.00	92.67
0.00	0.00	9.44	90.56	93.78

Standard Error of the Mean

Blue	Green	Yellow	Red	Sat
2.78	0.00	0.00	2.78	2.12
1.94	1.47	0.00	2.65	2.04
2.37	2.56	0.00	1.18	1.86
2.12	2.36	0.00	0.56	2.04
6.41	6.41	0.00	0.00	2.17
5.80	4.70	3.38	0.00	1.88
4.31	3.38	2.27	0.00	1.69
4.01	3.00	2.65	0.00	1.55
0.00	4.20	4.20	0.00	1.55
0.00	3.41	3.41	0.00	1.55
0.56	7.45	7.70	0.00	2.17
0.00	8.45	8.45	0.00	2.12
0.00	5.58	5.30	0.56	2.27
0.00	1.11	3.38	3.77	1.47
0.00	0.00	3.77	3.77	1.47
0.00	0.00	3.73	3.73	1.82
0.00	0.00	3.67	3.67	1.69
0.00	0.00	3.63	3.63	1.82
0.00	0.00	2.50	2.50	1.11
0.00	0.00	2.90	2.90	1.21
0.00	0.00	2.00	2.00	1.52
0.00	0.00	2.04	2.04	1.40
0.00	0.00	2.94	2.94	1.33

Reproduced with permission of the copyright owner. Further reproduction prohibited without permission.

Rod-Bleach Condition
10° Inferior

3.00 Stimulus

	Mean					Standard Error of the Mean				
λ	Blue	Green	Yellow	Red	Sat	Blue	Green	Yellow	Red	Sat
440	81.67	0.00	0.00	18.33	92.78	2.50	0.00	0.00	2.50	1.47
450	86.67	0.00	0.00	13.33	93.89	2.76	0.00	0.00	2.76	1.39
460	92.22	3.89	0.00	3.89	93.89	1.21	2.00	0.00	1.11	1.62
470	87.78	12.22	0.00	0.00	91.67	1.69	1.69	0.00	0.00	1.18
480	52.78	47.22	0.00	0.00	86.67	5.84	5.84	0.00	0.00	1.86
490	19.44	79.44	1.11	0.00	90.56	6.59	6.21	0.73	0.00	1.00
500	5.00	86.11	8.89	0.00	91.67	4.41	4.06	2.86	0.00	0.83
510	2.78	85.56	11.67	0.00	90.56	1.88	3.58	4.17	0.00	1.30
520	1.67	82.22	16.11	0.00	88.33	1.18	5.01	5.51	0.00	1.18
530	1.11	83.33	15.56	0.00	87.22	0.73	3.00	3.58	0.00	1.47
540	0.00	68.33	31.67	0.00	85.56	0.00	4.08	4.08	0.00	1.30
550	0.00	37.22	62.78	0.00	83.33	0.00	8.90	8.90	0.00	2.04
560	0.00	15.00	83.33	1.67	85.56	0.00	5.46	5.00	1.18	1.55
570	0.00	0.00	87.22	12.78	87.22	0.00	0.00	1.88	1.88	1.21
580	0.00	0.00	47.22	52.78	88.89	0.00	0.00	2.90	2.90	1.11
590	0.00	0.00	34.44	65.56	88.89	0.00	0.00	4.29	4.29	2.00
600	0.00	0.00	23.89	76.11	89.44	0.00	0.00	4.62	4.62	1.30
610	0.00	0.00	16.11	83.89	92.22	0.00	0.00	2.98	2.98	1.21
620	0.00	0.00	12.78	87.22	93.33	0.00	0.00	3.24	3.24	1.18
630	0.00	0.00	10.56	89.44	95.00	0.00	0.00	3.17	3.17	1.18
640	0.00	0.00	12.22	87.78	93.89	0.00	0.00	2.22	2.22	0.73
650	0.00	0.00	8.33	91.67	95.00	0.00	0.00	1.86	1.86	0.83
660	0.00	0.00	8.33	91.67	95.00	0.00	0.00	1.86	1.86	0.83